國立勤益科技大學
資訊工程系研究所碩士班

碩 士 論 文

改良式生物智能演算法應用在
影像切割之研究

The study on modified biological intelligent algorithms for image segmentation

研 究 生： 巫守竑

指導教授： 林灶生　教授

中 華 民 國　101 年 7 月

國立勤益科技大學

研究所碩士班

論文口試委員會審定書

本校 資訊工程系研究所 碩士班 巫守竑 君

所提論文 改良式生物智能演算法應用在影像切割之研究

合於碩士資格水準，業經本委員會評審認可。

論文口試委員會：

召 集 人：鄭國順

委　　員：張嘉真

指導教授：

所　　長：王圳木

中　華　民　國　[0]1　年　9　月

改良式生物智能演算法應用在影像切割之研究

研究生： 巫守竑　　指導教授： 林灶生 博士

國立勤益科技大學　資訊工程系研究所

摘要

當處理彩色影像時因為不同光源之色溫導致影像產生色偏時，白平衡即是改善這問題很重要的步驟，因此對影像先進行前處理做色偏判斷，並以分區曝光系統結合白平衡來解決色偏區域，再利用仿生物演算，如人工蜂群方法結合 C-mean、FCM，利用空間上的資訊進行蜜蜂的食物採集與分析；粒子群搭配 entropy 門檻法，找出最恰當的門檻值完成影像分群。最後透過影像門檻值或是群集中心，計算其他像素點的歐式距離來進行分類，實驗結果顯示所提之演算法可以獲得不錯之結果。

關鍵字：色偏、白平衡、影像分割、仿生物演算法

The study on modified biological intelligent algorithms for image segmentation

Student: Shou-hung Wu Advisor: Dr. Jzau-Sheng Lin

Institute of Computer Science and Information Engineering

National Chin-Yi University of Technology

ABSTRACT

White balancing is an important step to correct the color value of pixels under varied color temperature of illuminations for color image processing. We have to do the image preprocessing of the color cast, and use the zone system with the white balance to solve this problem. Then we implement the biological intelligent algorithms for images segmentation, such as Artificial Bee Colony (ABC) and Particle Swarm Optimization (PSO). We embed fuzzy inference strategies into the artificial bee colony system to construct a segmentation approach. It is to found the cluster centers with local spatial information in stead of global pixels' intensities as well as we also used the PSO algorithm with maximum entropy thresholding and uniformity as the main structure to find the optimization threshold. The experimental results have shown that promising performance can be obtained.

Keywords： Color cast, White balance, Image segment, Imitation of biological algorithms

誌　謝

在念碩士的路程上，很感謝許多人的幫忙，首先我要感謝的是我的指導教授 林灶生教授，不論是在理論基礎或是研究層面，都讓學生受教許多，同時在演算法開發中，有了很大的突破。感謝林學儀老師與游正義老師平時對我的照顧與教導。在口試期間，感謝鄭國順 教授與張葳英 教授，對學生的論文給予寶貴的建議與指導，使論文更加完善。

研究所期間承蒙楊文鎮與呂彥甫學長，在學習上給了我許多建議與幫忙，感謝實驗室夥伴家祥與上銘，在修課方面能夠互相討論與幫助，並一同度過這充滿歡笑與挑戰的兩年，感謝學弟宇揚與倍瑜在研究上的協助，特別感謝時常與我一起討論與協助的劉秉叡同學與廖又儀學姐，讓我能夠突破難關。

感謝我的女友曹嫻恩，在碩士生涯中不斷的給我打氣與關懷，感謝在這一路上曾幫助過我的師長、朋友與學弟妹們，謝謝你們的照顧，最後我要感謝我的家人，讓我能夠無憂慮的專心讀書，並時常給我鼓勵與支持，以順利完成論文，由衷的感謝你們。

巫守竑

2012 年 7 月

勤益資工所

目 錄

表 目 錄

圖 目 錄

第一章　緒論

1.1 研究背景

在拍攝一張影像的同時，極可能因為色溫的影響，導致拍出的影像與當時我們肉眼所看到的環境色彩有所不同，亦即產生色偏問題，如此也會造成日後在影像處理上會有所誤差。因此，在分類前先將影像進行一個過濾調整、補強的動作，稱之為影像前處理。

在一張影像中，若只想針對某一重要部份或輪廓做進一步觀察研究，則必須由經驗、技術熟練的專家以人工圈選的方式來做，如果有無數張影像都要做分析，將會非常消耗時間，因此若有一個好的分類方法，能夠自動偵測分析，便可以省下人工圈選時間，更可以防止因為經驗不足而造成的誤判。舉例來說，醫院通常會對患者(中樞神經系統病變)進行核磁共振掃瞄，由這些拍出來的 MRI(Magnetic Resonance Imaging)進行分析，並圈選出有病變的部分來做切除，或是進一步觀察等；又如中醫望眼辨症診斷，從眼睛內的部位檢測是否出現異常，可相對應到五臟六腑發生病變的判斷，因此若可以從影像切割出眼睛

來辨識，也可以省下很多人力及時間。

傳統影像分群方法中，可分為二種：監督式分類法與非監督式分類法，監督式分類必須決定分群數目及目標，找出各具代表性的區域後，再去分類，此方法比較耗時，容易有偏見產生；而非監督式分類是指在分群過程中不代入一些經驗的觀念認知，透過不斷疊代修正群集中心或門檻值，最後達到收斂條件才完成分類。

影像分群最主要面臨如何分割出正確的特徵輪廓，以及越快越好的速度效率。常見的分類方法透過歐式距離、影像直方圖，如 Hard C-Mean(HCM) [1][18]、Fuzzy C-Mean(FCM) [2]-[7]、門檻值分割法[1][8][9]、Mena Shift [2]。如果搭配仿生物演算法，如蜂群、螞蟻、粒子群、基因或是細菌演算法等，將會優化效能，並且提升速度。

1.2 研究動機與目的

隨著目前社會高科技發達，人手一台智慧型照相手機已很普遍，走到哪拍到哪，非常便利，可是當拍攝情景太亮或太暗，或受到色溫的影響，導致所拍出來的影像不盡理想，就只能考慮選擇刪除。但若

能透過影像處理的技術來修正，就可以保存這些值得回憶的照片。

近年來超啟發式演算法在應用面越來越廣，主要用來求解最佳化問題，不再需要依賴經驗、手動調整參數設定值，透過客觀的模仿生物行為模式之演算法來找出最佳解，搜尋較佳的門檻值或是群集中心以提升效能。在求解過程也有跳脫陷入區域最佳解(Local Optimal Solustion)機制，並加強區域跟全域的搜尋，進而達到找出全域最佳解(Global Optimal Solustion)或近似全域最佳解(Near-Global Optimal Solustion)。

本論文所開發之演算法，係利用蜂群演算法搭配 FCM 在空間域上做醫學影像分群，並以粒子群搭配熵(entropy) 與均勻度(uniformity)做眼球部分切割，運用這些具智能演算法的架構來找出最好的分群效果。

1.3 論文架構

本論文主體架構由五個章節所組成，各章節的概要說明如下：

第一章　緒論：描述研究背景、研究動機及研究目的。

第二章　影像的前處理：本章節描述在進行影像處理前，先加強或刪除一些資訊，過濾影像使其回復當時拍攝情境。

第三章　演算法之影像分群切割：本章節介紹演算法架構流程，並以生物智能演算法進行影像分群。

第四章　實驗結果：此章節呈現本論文實作的方法與實驗的結果之效能。

第五章　結論與未來期望：此章節將對研究內容做一個總結論，並描述未來可以更進一步改良之地方。

第二章　影像前處理

2.1 色溫

在拍攝一張影像，環境下的光源及色溫是很重要的因素，因為光源與色彩有很大的密切關係，也是造成可見顏色的主要來源，如人的眼球內部有錐狀細胞，能夠感受紅光、藍光及綠光，也就是因為有光，才能去分辨物體的顏色，這些可見光的波長範圍在 4000 到 7000 埃(埃為波長長度的單位)的電磁波，低於 4000 稱作紫外線，高於 7000 稱作紅外線。

色溫是一種物理現象，指的是光波在不同的能量下，人的肉眼所感受到顏色的變異，如同顏色的溫度，計算單位是以 Kelvin 為單位，以度 K 表示，舉例來說，在 2800°K 時，發出的色光和燈泡相同，就可以說燈泡的色溫是 2800°K。當色溫較低的時候，影像顏色偏紅(暖色調)；而色溫較高，影像則偏藍(冷色調)，影響色溫的因素包括：高緯度、高海拔地區色溫會比較高，反之低緯度、低海拔色溫較低。此外，時間、季節、氣候和室內外或是空氣中的塵粒之反射，也會造

成色溫的差異，如圖 2.1 所示，色溫在 3300° K 以下色溫偏紅，屬於低色溫；色溫在 3000° K 到 6000° K 顏色比較中性，屬於中色溫；色溫在 6000° K 以上，顏色偏藍，屬於高色溫。因此，拍攝後的照片無法呈現當時環境之真正的色彩，就是色彩偏差所引起。因此，我們實作白平衡[10]-[13]來解決色偏問題，作為影像的前處理。

圖 2.1 色溫表示圖

2.2 白平衡

人類的視覺感知具有色彩恆常性，能夠自動調節修正不同光照所產生的顏色偏差，我們所看到的白色是將所有顏色反光，也就是人的眼睛中看到所有色彩的組合，而黑色則是吸收所有色彩，沒有將顏色反光出來。在照相設備之感光元件中並沒有此功能，但為了讓拍攝的影像貼近人眼之視覺，必須模仿人類大腦對於光線變化調整色彩，因此加入白平衡演算法在硬體上，讓器材恢復對於白色的認知，也就是在任何光源下，能讓白色的物體恢復白色，舉例來說，自訂白平衡模式，拍攝灰卡之白面，數位相機會就知道在這樣的光線下，什麼才是白色。

市面上具有照相功能的產品，都具備白平衡，可以手動調整，也可以自動調整，前者需具對攝影技巧有一定的認知，因此大部分的人都會採取自動白平衡，可是在各種環境下，以自動的白平衡在拍攝照片上還是會有所偏差，因此，本篇論文在前處理的步驟上，以白平衡加上分區曝光系統(zone system)的概念去做改進。

2.3 分區曝光系統

一般拍攝影像時，決定如何曝光是很重要的一點，如果曝光過多，影像某些地方變成全白，功能再強大的軟體也無法把細節恢復：若是曝光太少，較暗的地方就會變成全黑，也容易產生雜訊，因此曝光程度會嚴重影響影像品質。

分區曝光系統先由 Ansel Adarms [14]提出，Zone 並不是真的存在，而是客觀的對景物的色彩之預估，存在攝影者腦中，從最暗到最亮分成 11 個區域，即第 0 區到 X 區，其中第 V 區最為重要，如同 18% 反射灰卡，代表該顏色的曝光量為其他色彩曝光量的平均值，做為平均測光的參考依據，此外分區曝光相對應到光圈值，每轉動一格光圈以 2 的冪次方倍增或遞減。如圖 2.2 所示，第 0 區完全都是黑色，沒有任何細節；第 X 區完全都是白色，沒有任何細節；有較多的紋理、細節是在第 III 到第 VII 區間。

Zone	Description
0	Total black
I	Near black, with slight tonality but no texture
II	Dark gray-lack. textured black; the darkest part of the image in which slight detail is recorded
III	Very dark gray, average dark materials and low values showing adequate texture. This is where you will want to place shadow details.
IV	Medium-dark gray, average dark foliage, dark stone, or landscape shadows
V	Middle gray; Standard Kodak 18% gray reflectance card, clear north sky; dark skin, average weathered wood
VI	Rich mid-tone gray, average Caucasian skin; light stone; shadows on snow in sunlit landscapes
VII	Off white or bright light gray, very light skin; shadows in snow with acute side lighting, highest zone that will still hold good details.
VIII	Lightest tone with texture; textured snow
IX	Slight tone without texture; glaring snow
X	Pure white; light sources and specular reflections

圖 2.2　Zone system

2.4 白平衡搭配分區曝光系統演算法

首先讀取影像，再透過公式(2-1) 將 RGB 轉換成 YCbCr 之色彩空間上，Y 代表亮度，Cb、Cr 代表彩度，分別為綠色到藍色；黃色到紅色。透過 Cb 與 Cr 的平均值差異，判斷這張影像是否有色偏，若存在色偏的情況，必須找出要調整的候選像素值做一個平均處理計算，集中在 Zone system 的第 III 區到第 VII 區間。

公式(2-1) 為將 RGB 轉成 YCbCr 色彩空間：

$$\begin{aligned} Y &= 0.299 \times R + 0.587 \times G + 0.114 \times B \\ Cb &= -0.1687 \times R - 0.3313 \times G + 0.5 \times B + 128 \\ Cr &= 0.5 \times R - 0.4187 \times G - 0.0813 \times B + 128 \end{aligned} \tag{2-1}$$

公式(2-2) 為將 YCbCr 轉回 RGB 色彩空間：

$$\begin{aligned} R &= Y + 1.402 \times (Cr - 128) \\ G &= Y - 0.34414 \times (Cb - 128) - 0.71414 \times (Cr - 128) \\ B &= Y + 1.772 \times (Cb - 128) \end{aligned} \tag{2-2}$$

公式(2-3) 為計算亮度及彩度的平均值，從算出來的 Cb 與 Cr 做一個相減的動作，所得的值若結果大於設定的門檻值，且 Cb 比較大代表影像有藍色偏，反之若 Cr 較大，則代表為紅色偏。此門檻值是由 Zone system 概念的 11 個區間算出來的，如圖 2.3，若影像為 8 bits 代表 256 色去除上 11；若為 16 bits 則以 65536 除上 11。

$$
\begin{aligned}
Avg_{Y} &= \frac{1}{M \times N} \times \sum_{x=1}^{M} \sum_{y=1}^{N} I_{y}(x,y) \\
Avg_{Cb} &= \frac{1}{M \times N} \times \sum_{x=1}^{M} \sum_{y=1}^{N} I_{Cb}(x,y) \\
Avg_{Cr} &= \frac{1}{M \times N} \times \sum_{x=1}^{M} \sum_{y=1}^{N} I_{Cr}(x,y)
\end{aligned}
\tag{2-3}
$$

MN 分別代表影像的長及寬， I 代表像素灰階值

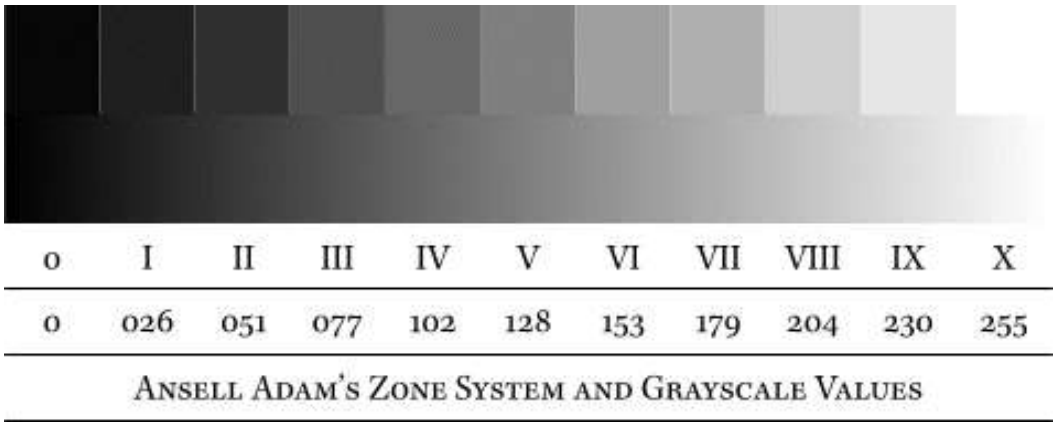

圖 2.3 把灰階值分成 zone system 的區域

接著分別去尋找 Cb 與 Cr 落在第 III 區域至第 VII 區域，具有紋理與細節的地方，如公式(2-4)所式。透過平均值與標準差可以把較亮的部份捨去，得到候選像素值 I_{Cb} 與 I_{Cr}，再由交集處中過濾較暗的區域，如公式(2-5) 與公式(2-6)所示 ，最後的候選像素應該落在圖 2.4 中紅色線條內。

$$I_{Cb\_Cand} = \{I_{Cb} \mid (I_{Cb} - (Avg_{Cb} + Sd_{Cb})) < (\theta \times Sd_{Cb})\}$$
$$I_{Cr\_Cand} = \{I_{Cr} \mid (I_{Cr} - (Avg_{Cr} + Sd_{Cr})) < (\theta \times Sd_{Cr})\} \quad (2\text{-}4)$$

其中，Sd_{Cb} 與 Sd_{Cr} 分別代表 Cb 與 Cr 的標準差，θ 代表門檻值，此門檻值取決於 zone system 的亮區且為細節部分，以第 VI 第 VII 區較為合適，因此 θ 值在 1.5 倍或 2 倍之標準差下，效果較佳。

$$I_{cand} = I_{Cb\_Cand} \cap I_{Cr\_cand} \tag{2-5}$$

$$I_{adj} = \{I_{Cand} \mid I_{Cand} > D_{20}\} \tag{2-6}$$

D20 代表暗部區域的一個程度，也就是濾除以 zone system 概念黑色完全沒細節的部份。

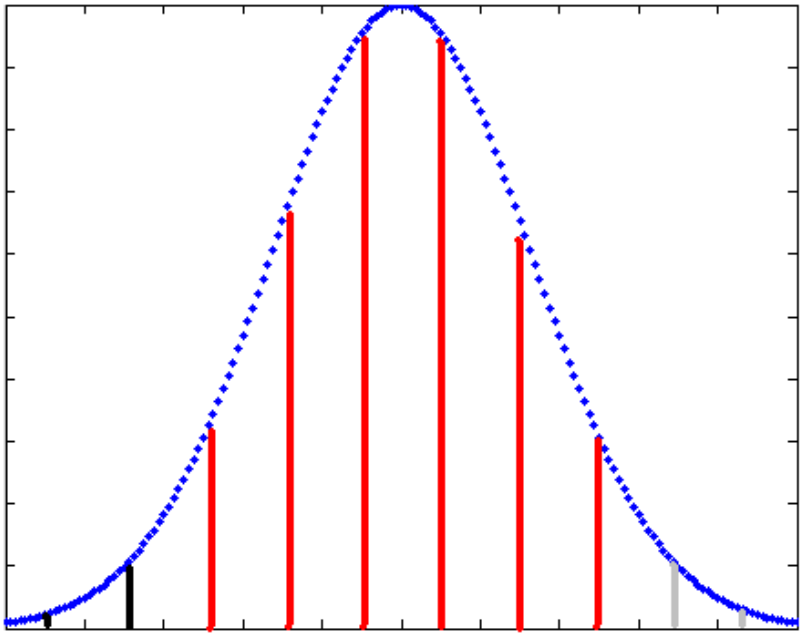

圖 2.4 zone system 的候選像素值區域分佈

接著把找到的候選像素值，分別對應到 RGB 色彩空間下的像素值做處理，由公式(2-7) 算出 RGB 的增益，再由原先的 RGB 值分別乘

上本身的增益，即可搭配分區曝光系統完成白平衡演算法，圖 2.5 為演算法流程圖。

$$I_{R\_new} = I_R \times \frac{\min\left(I_y\right)}{\left(mean\left(I_{adj\_R}\right) + \min\left(I_{adj\_R}\right)\right)/2}$$
$$I_{G\_new} = I_G \times \frac{\min\left(I_y\right)}{\left(mean\left(I_{adj\_G}\right) + \min\left(I_{adj\_G}\right)\right)/2} \quad (2\text{-}7)$$
$$I_{B\_new} = I_R \times \frac{\min\left(I_y\right)}{\left(mean\left(I_{adj\_B}\right) + \min\left(I_{adj\_B}\right)\right)/2}$$

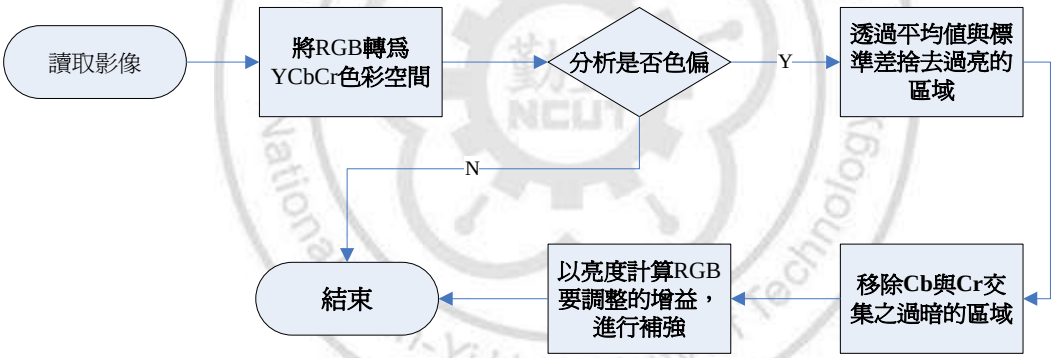

圖 2.5 白平衡搭配 zone system 之流程圖

在影像的前處理部份，本論文以白平衡結合分區曝光系統概念來解決色偏問題，與其他如 Gray world assumption [11][15]和 Retinex theory[11][16][17]等方法做比較，在處理色彩偏差上，可得到較佳的影像品質效果。

2.5 色差評估方法

CIELAB 色彩空間為 CIE 協會所認可的標準色差公式，即在相同環境下，人眼對於兩種顏色的視覺差異，L 代表亮度，a 和 b 代表色度，a 分量代表顏色從綠色到紅色的變化，若為正數，則代表偏紅色，為負數代表顏色偏綠色；b 分量代表由藍色到黃色，b 為正數代表顏色偏黃色，負數為偏藍色。

在同一環境下，拍攝正常的影像與產生色彩偏差的影像，以各種演算法來處理色偏的影像，與正常的影象比較，評估方法主要是計算 2 個影像之間的平均距離，透過 CIELAB 色彩空間去計算正常的影像 L_1, a_1, b_1 和演算法做完色偏影像的結果 L_2, a_2, b_{21}，取平均值後做相減，算出來的值越小代表該演算法較佳，其公式如(2-8)所示。

$$\Delta E = \sqrt{(L_2 - L_1)^2 + (a_2 - a_1)^2 + (b_2 - b_1)^2} \tag{2-8}$$

2.6 影像色偏處理之實驗結果

在實驗結果之統計數據中，圖 2.6 為 Lena 影像，從統計數據可以得知，Cr 的平均值為 163 高於 Cb 平均值 102，且明顯的超過 threshold，因此為紅色偏；圖 2.7 中 Cb 的平均值 38304 大於 Cr 平均值 31358，且高於 threshold，為藍色偏；圖 2.8 的 Cr 平均值 129 大於 Cb 平均值 122，因為較 threshold 值為低，因此判定為正常沒有色偏影像。

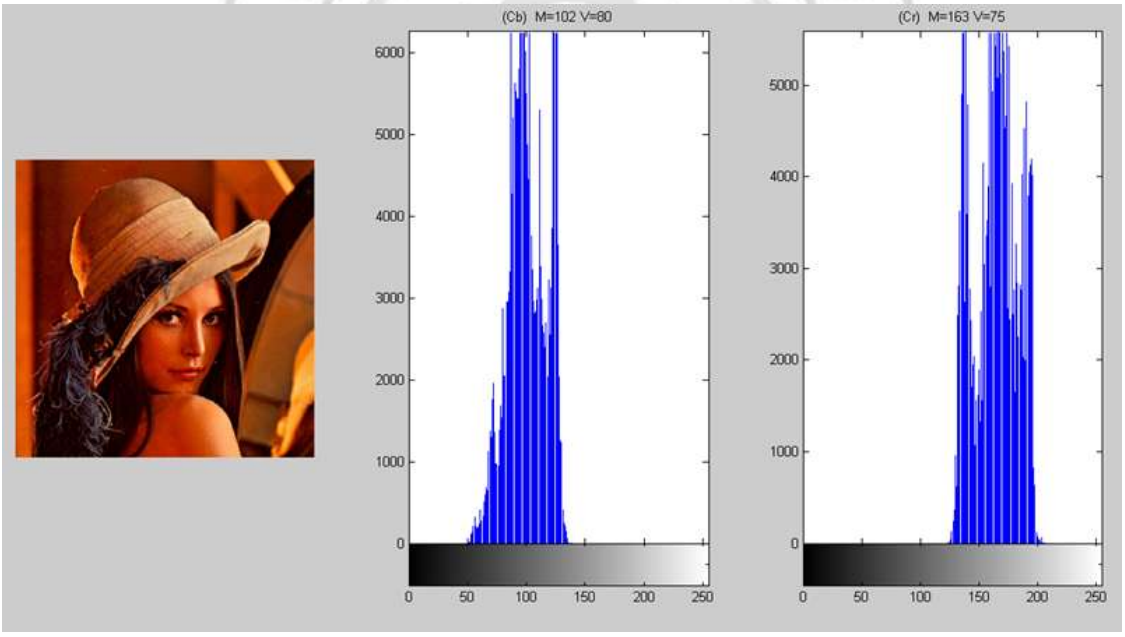

圖 2.6　Lena 圖與統計 Cb 及 Cr 值

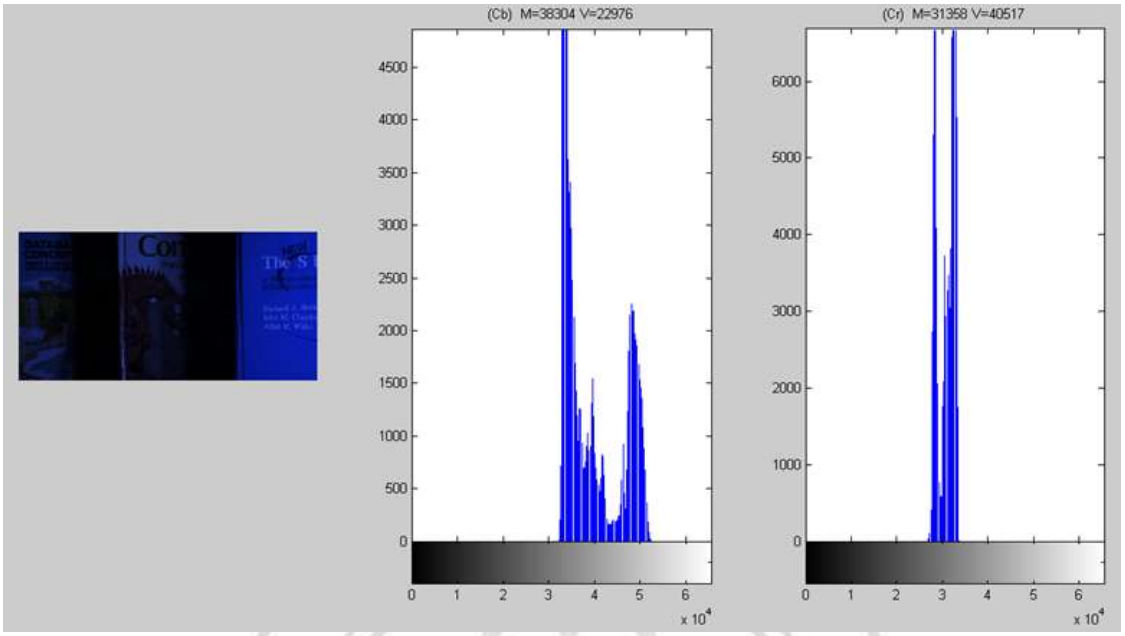

圖 2.7　Book 圖與統計 Cb 及 Cr 值

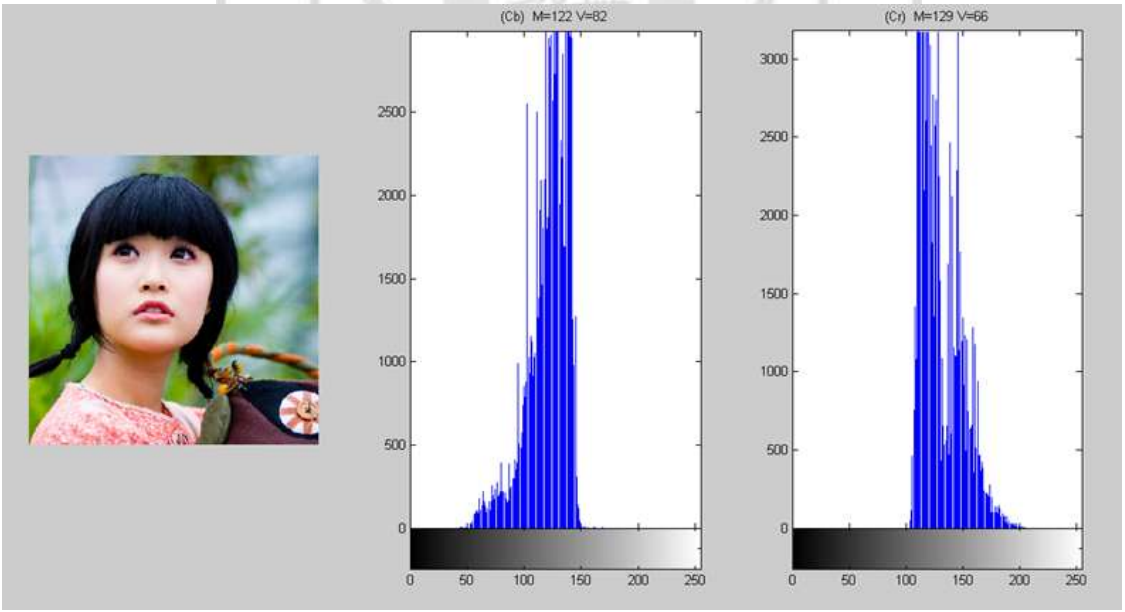

圖 2.8　女孩圖與統計 Cb 及 Cr 值

圖 2.9 與圖 2 .10 呈現θ值為 1.5 倍與 2 倍之白平衡結果，都介於 zone system 的第 VI 區與第 VII 內，若以結構相似性指標檢測，θ值為 2 倍有較佳的相似性。

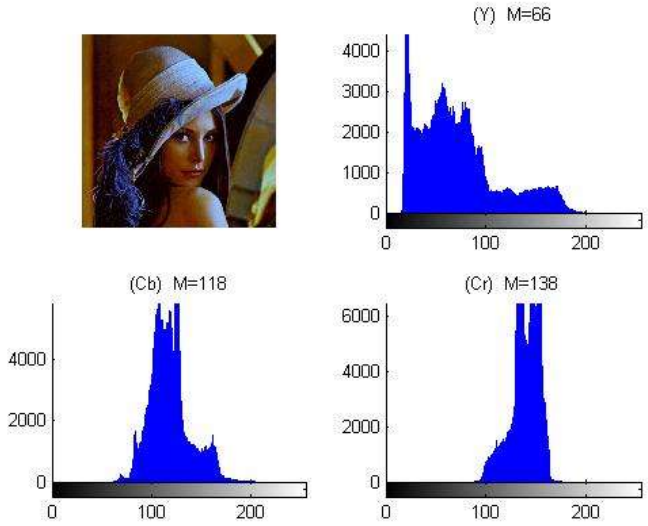

圖 2.9　Lena 白平衡處理結果，θ值為 1.5 倍

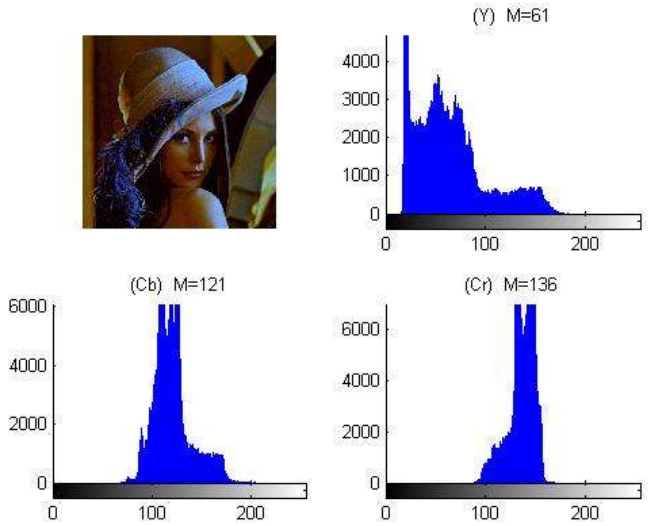

圖 2.10　Lena 白平衡處理結果，θ值為 2 倍

本論文在前處理之處理色偏影像的特色，透過簡單的統計分析出色偏，利用攝影技巧的分區曝光系統概念，找出具有細節的部分。在 zone system 中，介於第 III 區到第 VII 區並具有黑色、白色可以接受範圍內，避免全黑與全白，找出這些候選像素做調整。在整體速度與效能上均可得到較好的結果，也不需要做疊代的處理。圖 2.11(a)為原始色偏影像，與其他如 Gray world assumption 和 Retinex theory 解決色偏方法做比較，呈現結果在圖 2.11(b)到圖 2.11(d)，最後實驗結果顯示各種不同的色偏影像，並以色差評估模式來分析，如表 2.1 所示。展示以白平衡搭配分區曝光系統解決色偏影像，如圖 2.12 到圖 2.17 所示。

(a)原始影像 (b) Gray world assumption (c) Retinex theory (d)本論文提出之方法

圖 2.11 影像色偏圖與 3 種方法之結果

	Gray_World			Retinex			Propose White Balance		
CIELAB	Δa	Δb	ΔE	Δa	Δb	ΔE	Δa	Δb	ΔE
圖 2.12	3.8002	-8.5820	**22.8536**	4.9304	-13.9662	**28.1767**	-0.4462	-7.4080	**7.4421**
圖 2.13	-3.9461	-15.6397	**21.4403**	-6.7571	-25.4131	**53.2280**	-5.8138	-13.9104	**18.4167**
圖 2.14	0.8394	0.6282	**1.0937**	5.9046	-17.2331	**42.9331**	-0.0704	-0.4949	**0.9006**
圖 2.15	-2.0360	-13.2131	**19.2679**	-1.2437	-11.9530	**27.4549**	-3.1814	-10.4520	**13.8134**
圖 2.16	0.7213	-20.4692	**27.9775**	4.8939	-31.8153	**42.2472**	1.0793	-22.7709	**24.0115**
圖 2.17	-42.8303	-42.1660	**62.4120**	-36.7598	-41.8418	**60.0404**	-38.9730	-33.9708	**51.7811**

表 2.1 CIELAB 色差評估表

圖 2.12 影像色偏與白平衡處理

圖 2.13 影像色偏與白平衡處理

圖 2.14 影像色偏與白平衡處理

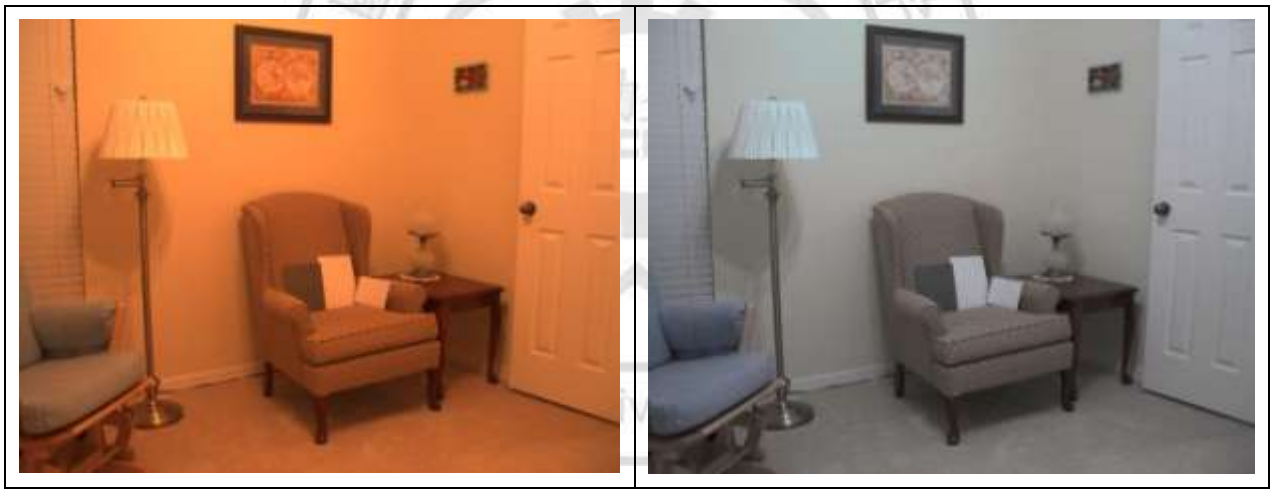

圖 2.15 影像色偏與白平衡處理

圖 2.16 影像色偏與白平衡處理

圖 2.17 影像色偏與白平衡處理

第三章 生物智能演算法進行影像分群

3.1 演算法介紹

生物智能演算法主要是模擬生物行為模式所發展出來的演算法，常見的有，螞蟻最佳化演算法(Ant Colony Optimization) [18]、粒子群最佳化演算法(Particle Swarm Optimization) [19]-[22]、人工蜜蜂演算法(Artificial Bee Colony) [23]-[28]，和基因演算法(Genetic Algorithm) [3]。

螞蟻最佳化演算法主要利用每隻螞蟻走過路徑，留下費洛蒙的濃度之比例，轉換成機率去選擇要走的方向，每隻螞蟻走過一條路徑都會讓費洛蒙濃度增加，為了避免陷入區域最佳解，每疊代完一次會讓所有費洛蒙降低，並把最好的解做費洛蒙權重提升。

人工蜜蜂演算法透過蜜蜂找尋食物的概念去尋求最佳解，從所有蜜蜂的解當中，選出較好的一半數量，分別在半徑內再做一次搜尋，並淘汰掉較差的一半，重新加入新蜜蜂，不斷疊代到收斂或條件符合為止。

基因演算法是以達爾文的進化論理念發展而來，在解問題中常以二位元編碼，透過不斷交配(Crossover)，由優秀的母代交換位元資訊來找出更好的解，另外加入了突變(Mutation)機制，將部份的基因做改變，以隨機選到的位元做反向，0 改成 1 或 1 改成 0，防止陷入局部最佳解，還可以強化搜尋全域最佳解的能力。

這些仿生物演算法都有類似的基本的架構，大致分成 5 個步驟：

(1) 初始化生物形態數目，如蜜蜂、螞蟻、粒子的數量。

(2) 定義可以解決問題的方法，並以亂數的方式產生一組解。

(3) 初始化/更新 他們的搜尋範圍、移動方向。

(4) 透過每一隻生物形態去蒐尋問題解的資料，並比較適應值(Fitness Value)的好壞，把較好的解記住，較差的解捨去。

(5) 判斷是否收斂，是則結束；若否，回到步驟(3) 。

目前很多問題都無法在有限的時間內解決，若運用了這些生物智能演算法去做最佳化的處理，可以在接受的時間內找出全域最佳解或是近似全域最佳解。

3.1.1 蜜蜂群之行為模式

蜜蜂是一種群體居住、共同合作的昆蟲，像是以母性為主的王國，由女王蜂、雄蜂、工蜂所組成；女王蜂負責產卵，不需要尋找食物；雄蜂數量較少，也不須要做其他工作，主要與女王蜂進行交配，完成傳宗接代任務，也是唯一可以隨意進出其他蜂巢，而不會遭受到其他蜜蜂的攻擊；工蜂性別同女王蜂都是雌性，在數量及要做的工作上是涵蓋最廣的，工作性質可分成內勤與外勤。

內勤的工蜂必須整理蜂室、擔任保家衛國的守衛，外勤工蜂主要負責修築蜂巢與採集花蜜的工作，從採集花蜜的工蜂又可分為以下三類，第一種稱作引領蜂(Leader)，在偵測到花粉來源後，會飛回蜂巢，以奇特的跳舞姿勢展現給跟隨蜂(Follower)看，表達出該食物地點及其方向，此外舞蹈的劇烈程度與食物源的價值成正比。跟隨蜂會學著舞蹈一起跳舞，看完數遍舞蹈後，會飛往該食物目標地去採蜜，若其他引領蜂跳舞表達出找到的食物源效益比較低，就會放棄當前的食物源，轉為偵查蜂(Scouter)繼續尋找新的食物目標。從引領蜂跳舞的方式傳遞訊息告訴其他工蜂去找尋食物方向，是一種很重要的訊息交

換，同時也會比較食物源的收益程度進行取捨，因此蜜蜂的採蜜方式有互助合作、尋找最大效益的食物目標等優點。

3.1.2 人工蜂群演算法

人工蜂群 (Artificial Bee Colony) 演算法，以模仿蜂群採集花蜜行為模式提出的優化方法，是一種群體智能演算法。在解題目前要先了解問題的複雜度，如果問題比較大、比較複雜，那我們初始化的蜜蜂個數就要增加，尋求一般問題的解答，數量 20 隻的蜜蜂已經很足夠。初始化蜜蜂的數量與搜尋半徑，接著我們便可以隨機把蜜蜂灑在問題之中，讓它去搜尋並算出適應值，等到所有蜜蜂都做完，將資訊帶回來分析，並從中找出蜜蜂數量之一半較好的解，去做局部搜尋，在這些蜜蜂範圍內加入新蜜蜂，重新尋找是否有更好的解。不斷的淘汰掉較差的解，保留較佳的蜜蜂進行區域搜尋，再以亂數產生新的蜜蜂放入問題解中，如此不斷疊代，從較好的解持續延伸去找更好的解，以亂數方式取代被淘汰的蜜蜂，便有機會獲得更好資訊，防止陷入局部最佳解，圖 3.1 為蜜蜂演算法流程圖。

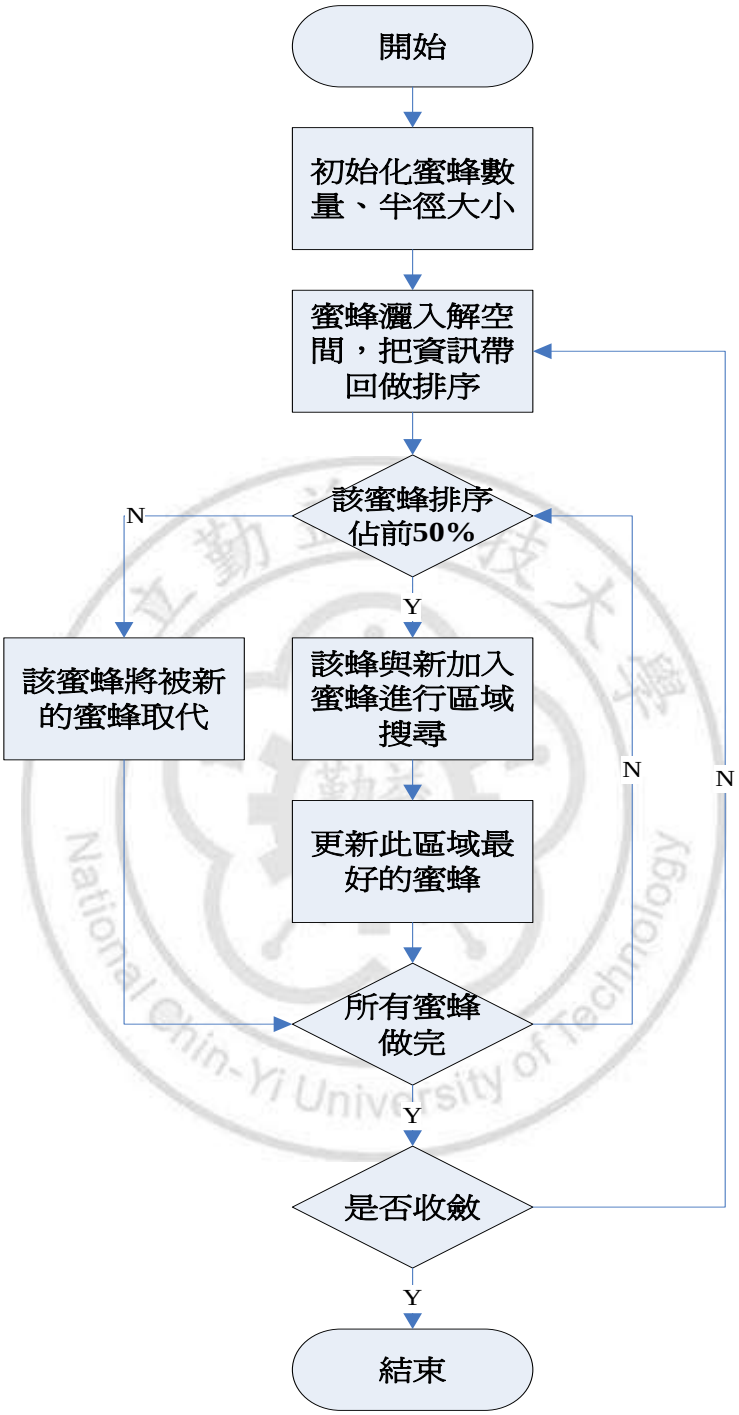

圖 3.1 蜜蜂演算法流程圖

從實際的範例做測試，以人工蜂群演算法來解決問題，用 Matlab 程式語言撰寫繪出 2 元 3 次方程式 $y = x - \cos(x^3) - \sin(2 \times x^2)$，其 x 範圍介於-2.5 到 2.5，每隔 0.001 間距繪出一個點，如圖 3.2 所示，曲線由 5001 個點所組成。此題目要找出曲線上的最大峰值位置，定義的目標函數(Objective function)為代入方程式 $y = x - \cos(x^3) - \sin(2 \times x^2)$，計算出變數 y 之最大值。

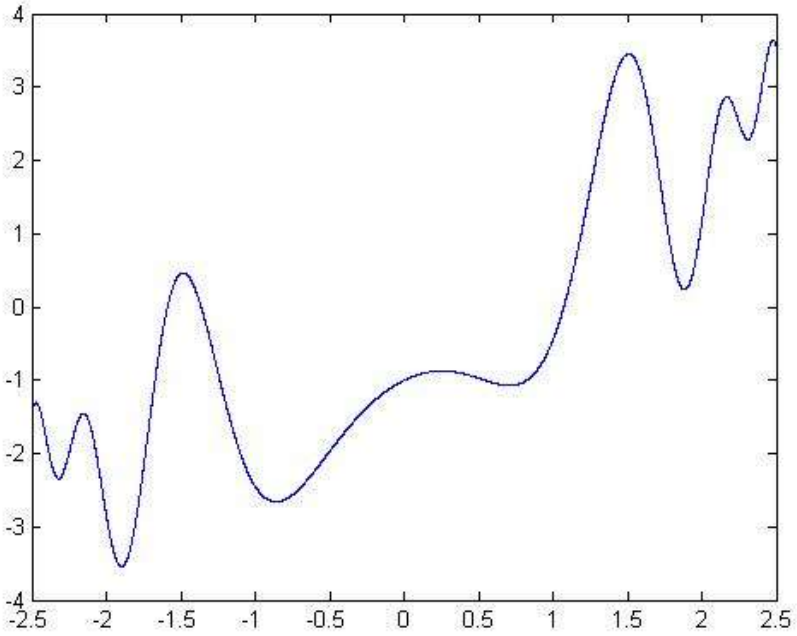

圖 3.2 曲線 $y = x - \cos(x^3) - \sin(2 \times x^2)$

先初始化問題解所需之蜜蜂數量，在本範例中設定 10 隻蜜蜂，如圖 3.3 所示，位置以亂數方式產生座標灑在曲線上。接著計算這些蜜蜂的適應值，從中淘汰掉適應值較差的蜜蜂，數量為總數的一半，另外在剩下的優秀蜜蜂中進行區域搜尋，希望可以找出更好的解，因此在當前最優秀及第二優秀的蜜蜂之半徑內隨機加產生 2 隻新蜜蜂(黑色點)，剩餘 3 隻在半徑內隨機產生 1 隻新蜜蜂(綠色點)，如圖 3.4 所示。在同個半徑內的蜜蜂，取出最優秀的一隻出來，其結果如圖 3.5 所示。之後再亂數增加 5 新隻蜜蜂(紅色)，補齊蜜蜂總數量，並持續選出較優秀的蜜蜂進行區域搜尋，如圖 3.6 所示。最後直到收斂條件完成，持續搜尋結果都沒有任何變化，較佳蜜蜂的位置沒有改變，就可以得出最後的結果，如圖 3.7 所示。最後從這些蜜蜂中找出最大 y 值，即可求出此問題之答案。

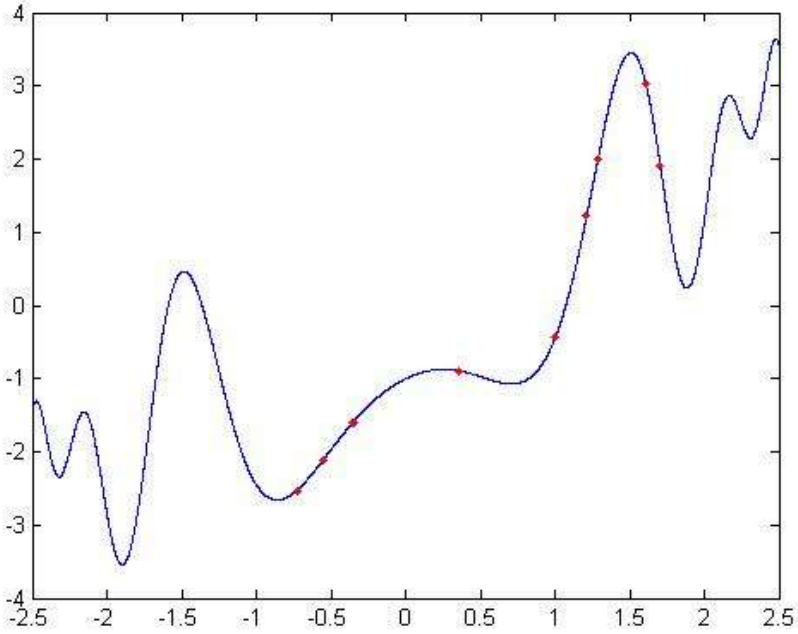

圖 3.3 初始化蜜蜂座標

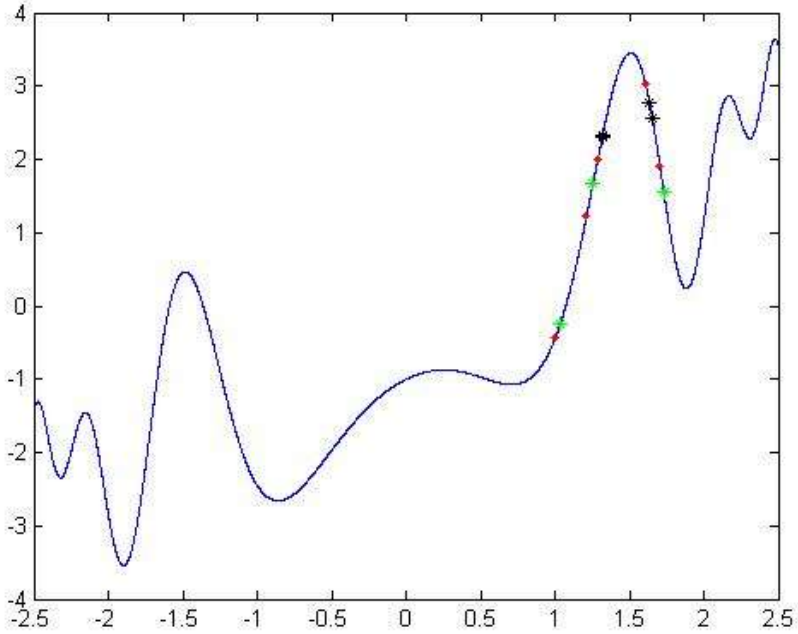

圖 3.4 優秀的蜜蜂進行區域搜尋

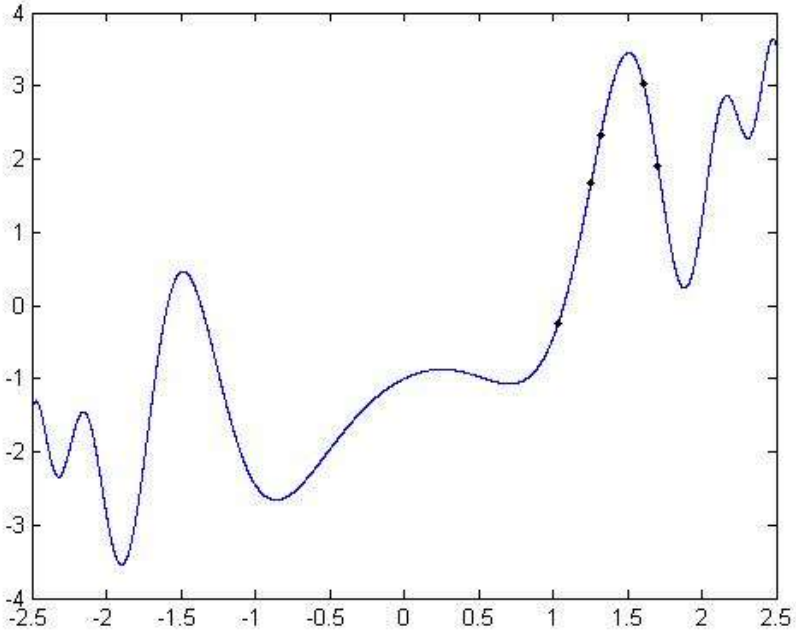

圖 3.5 區域搜尋完留下優秀的蜜蜂

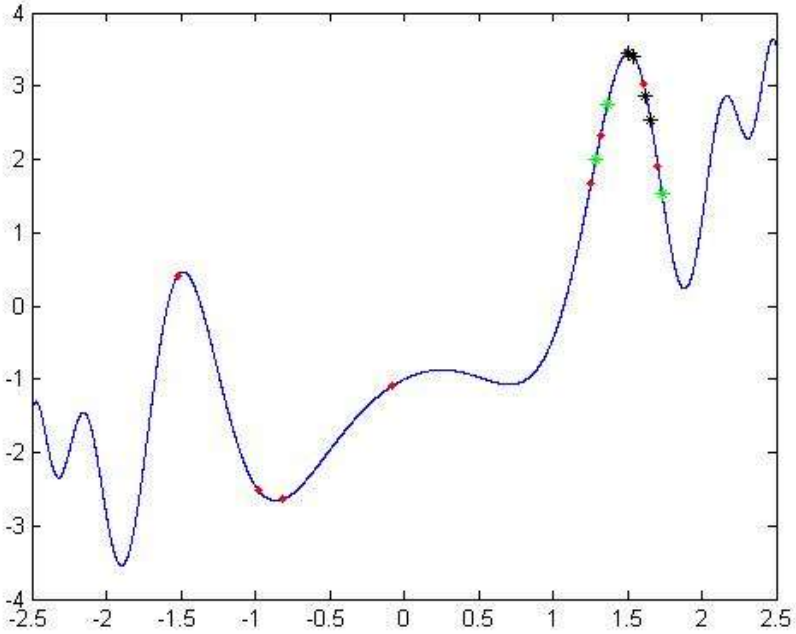

圖 3.6 加入新蜜蜂與區域搜尋

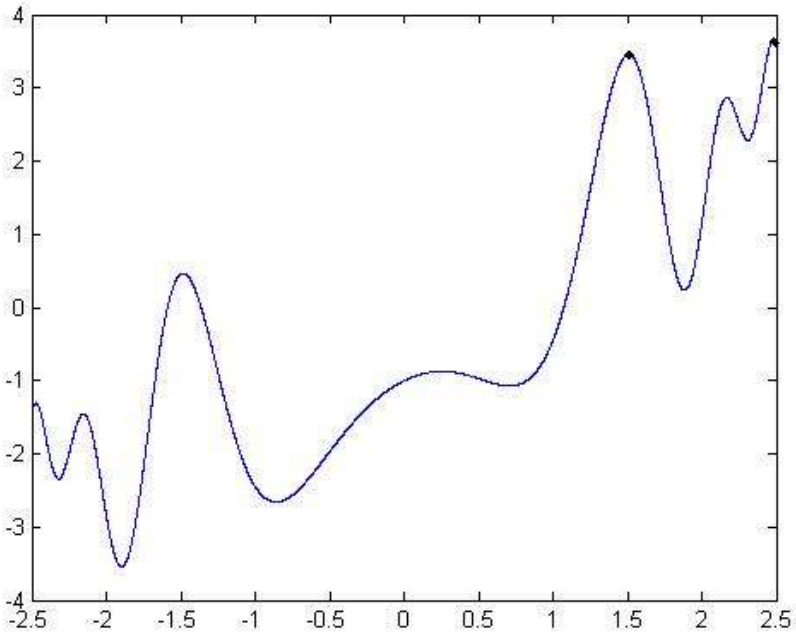

圖 3.7 收斂結束後，較佳蜜蜂的位置

3.1.3 粒子群最佳化

PSO 在 1995 年由 Kennedy and Eberhart 所提出，從觀察鳥類飛行與魚兒游水的族群特性發展出來，有群體行為的理論，概念來自於鳥類或是魚類在移動時，能透過個體間互相傳遞訊息，使團體朝向同一目標或是避開危險。因此每個粒子在問題解空間中都屬於候選解，各自擁有其速度，並且根據自我過去最好的經驗，與當前群體之最佳值進行移動搜尋，經過不斷修正，粒子群會漸漸接近最佳解。

由於相當多學者均投入於粒子群最佳化的研究中，因此版本種類很多，以最基本PSO為架構，在每一次疊代中，粒子 X_i 會去參考以前移動過程來找到最好的解位置，以及粒子群移動當中最好的一個解位置，來計算粒子的位移方向，其速度和位置更新如公式(3-1)和(3-2)所示。

$$v_{ij}(t+1) = v_{ij}(t) \times w + c_1 r_1 [P_{best_{ij}}(t) - X_{ij}(t)] + c_2 r_2 [G_{best}(t) - X_{ij}(t)] \quad (3\text{-}1)$$

$$X_{ij}(t+1) = X_{ij}(t) + v_{ij}(t+1) \quad (3\text{-}2)$$

v_{ij} 代表在d維的第j個解空間內，粒子群中第i個的粒子之速度或偏移量；$P_{best_{ij}}$ 代表在d維解空間中，記錄第i個粒子從過去到目前最佳的解位置；G_{best} 是從所有粒子群中，找出一個目前最佳解的粒子；r_1, r_2 為介於0 ~ 1的亂數值；c_1, c_2 則是一個常數值；公式(3-3)中 w 是慣性權重，其值會隨著疊代次數變化而慢慢變小，即一開始粒子是偏向做全域搜尋，再慢慢轉向區域搜尋。$w_{\max}, w_{\min}$ 是設定慣性權重的最大邊界值、最小邊界值；t 是目前的疊代次數；$iter_{\max}$ 是最大疊代次數。另外，為了避免移動距離太大而導致過快收斂，也必須設定 $v_{\max}, v_{\min}$ ，其值分別為0.9與0.4。

$$w = w_{\max} - t * \frac{w_{\max} - w_{\min}}{iter_{\max}} \tag{3-3}$$

圖 3.8 所示，我們以實際範例來說明 P_{best} 和 G_{best} 的更新，X 之位置是我們要搜尋的食物，初始化 A、B、C、D 之 4 個粒子之位置，並設為 $P_{best_{A1}}$ 、$P_{best_{B1}}$ 、$P_{best_{C1}}$ 、$P_{best_{D1}}$ ，與目標點 X 最近距離為 B1，因此 G_{best} 為當前 B1 位置，以 $G_{best_{B1}}$ 表示。

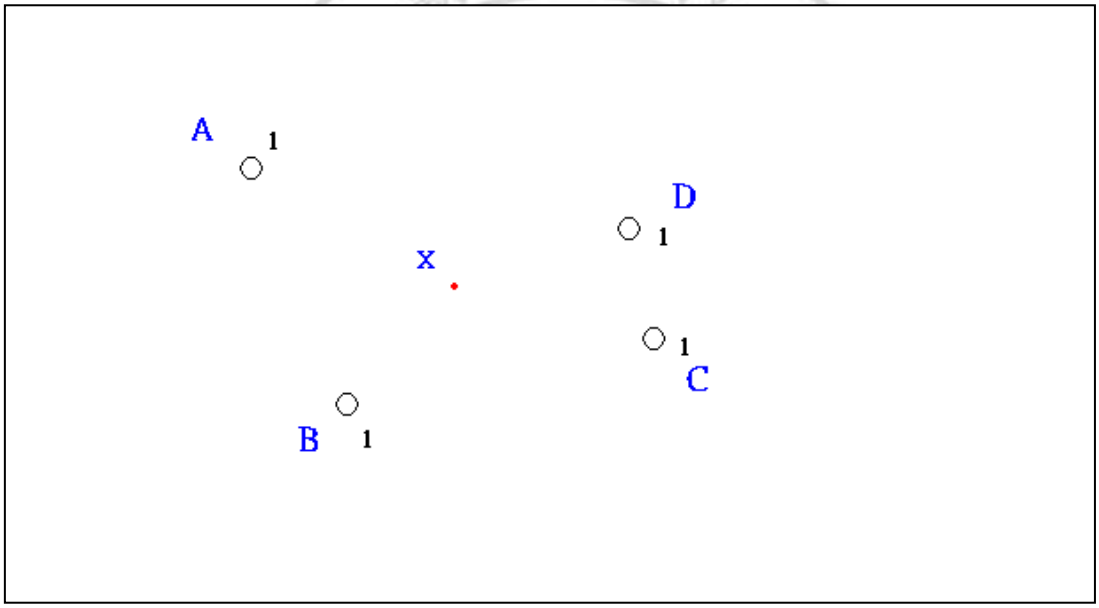

圖 3.8 初始化粒子位置

進行第一次疊代，以公式(3-1)、(3-2)和(3-3)更新粒子移動和位置，可以看到 A、B、C、D 粒子往不同的方向搜尋，A1 的位置更新到 A2，與目標 X 距離更近，因此更新 A 粒子的 P_{best} ，從 $P_{best_{A1}}$ 改為 $P_{best_{A2}}$ ，

而 B、C、D 的新位置也比之前的好，也做更新 P_{best} 動作，改為 $P_{best_{B2}}$ 、$P_{best_{C2}}$ 、$P_{best_{D2}}$ ，這些 P_{best} 與之前 $G_{best_{B1}}$ 比較，選擇離目標 X 最近之距離，更新為 $G_{best_{B2}}$ ，如圖 3.9 所示。

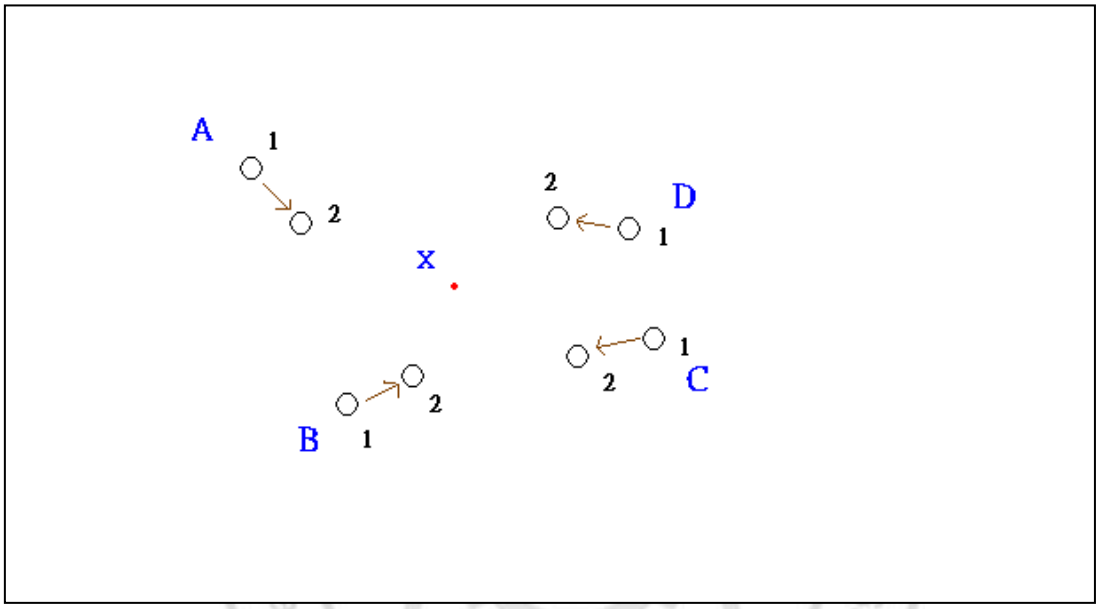

圖 3.9 第一次疊代，更新粒子移動

進行第二次疊代，產生新的位置 A3、B3、C3、D3 粒子， 每一粒子與自己過往的經驗去比較，選出經驗最好的 P_{best} 與目標 X 距離最近，為 $P_{best_{A3}}$ 、$P_{best_{B3}}$ 、$P_{best_{C2}}$ 、$P_{best_{D3}}$ ，再與 $G_{best_{B2}}$ 做比較，發現 B3 與 D3 的位置比 $G_{best_{B2}}$ 好，但 D3 與目標 X 距離最近，因此更新為 $G_{best_{D3}}$ ，如圖 3.10 所示。

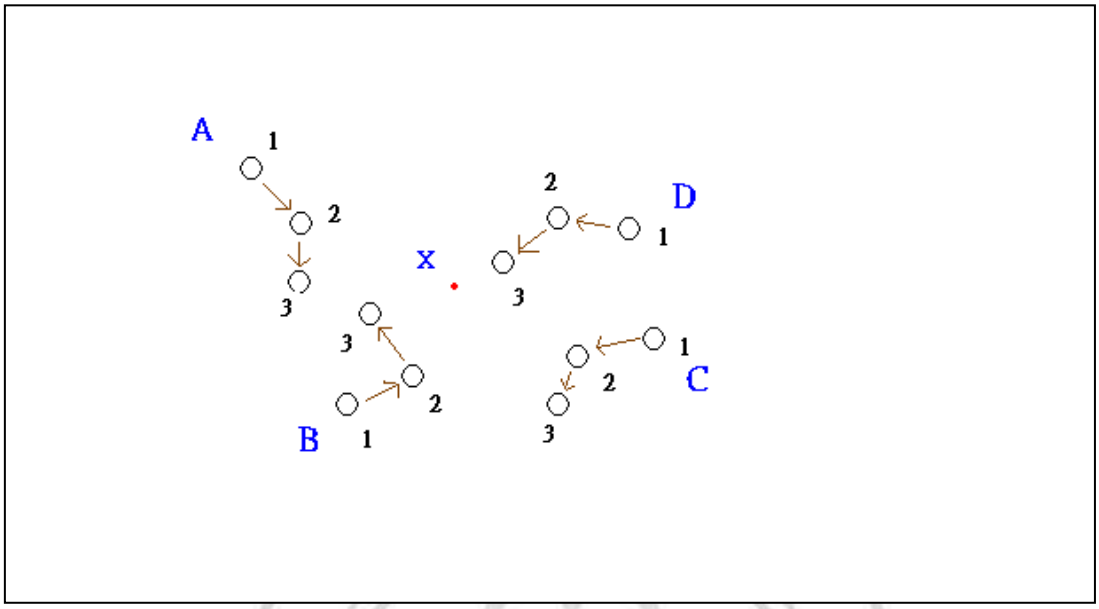

圖 3.10 第二次疊代，更新粒子移動

要解一般問題的架構流程，必先初始化粒子數目 M ，並隨機初始化每個粒子 i $(0 < i <= M)$ 的速度及位置，將 M 個粒子的位置代入fitness function求解，記錄當作初始 P_{best_i} ，並從 M 個粒子當中找出最佳fitness解，當作 G_{best} 。透過公式(3-1) (3-2) (3-3)更新粒子速度及位置，把更新後的粒子位置各別代入fitness function求解，判斷第i個粒子的適應解，是否有比過去自己經驗最好的 P_{best_i} 還要好，若有，則把這次解的位置及適應值取代 P_{best_i} ，並繼續比較 G_{best} 的適應值，如果比較好，則將第 i 粒子的位置取代 G_{best} ，如果沒有，則判斷下一粒子，直到一次疊代完成為止，一直到總疊代次數做完，或是收斂條件符合，即結束。

3.2 分群概念

分群演算法(Clustering Algorithm)主要是將所收集到的資料，進行有效的分類，並可以針對使用者的需求，調整細分的程度，應用的領域非常廣泛。在資料分群中，找出資料內數量較多或是較重要的幾個中心點，取代與中心點相似的數據，如同資料壓縮、降低計算量；分析顧客的購買行為與習慣，針對不同的消費族群，推出適當的產品。在影像的分群中，可以幫助我們把重要的圖形或是特徵分離出來，進行追蹤或辨識，或是透過分群系統處理核磁共振影像，協助醫生做快速檢視病變的地方。

在傳統影像分類方法中，可分為二種：監督式(supervised)與非監督式(unsupervised)，監督式分類必須決定分組數目及名稱，並找出各具代表性的區域後，再做分類，此方法比較耗時，容易有偏差產生；而非監督式分類是指人們事先對分類過程不加以經驗認知，透過不斷疊代來修正群集中心或門檻值，達到收斂條件以完成分類。

3.2.1 分群技術

影像分群最著重於如何分割出正確的特徵輪廓，以及在速度上效率越快越好，常見的分類方法有 Hard C-Mean (HCM)、Fuzzy C-Mean (FCM) 與門檻值分割法。

HCM 先以亂數方式決定群集中心，透過歐式距離運算，個體與群集中心之距離，選出與中心距離最近的群集，個體就被歸屬為該群集，再更新群集中心，重複先前運算，直到符合疊代條件才結束。此方法雖快，卻容易因為初始位置不佳，而陷入局部最佳解。

HCM 演算法敘述如下：

(1) 初始化分群數目為 a 群，並以亂數產生 a 個群集中心值，以 C_i 表示，$0<i\leq a$。

(2) 讀取一張影像(長寬為 M、N)，其影像的像素值以 X_j 表示，$0<j\leq M*N$，歸屬權重為 W_{ji}。

(3) 把該點像素值與群集中心比較距離，找出數值最小的，其歸屬權重設為 1，否則為 0，如公式(3-4)到公式(3-7)。

$$value[i] = \left\| X_j - C_i \right\| \tag{3-4}$$

$$if\left(value[i] == \min\left(value\right)\right), \left(W_{ji} = 1\right), else\left(W_{ji} = 0\right) \tag{3-5}$$

且須滿足 $$\sum_{i=1}^{a} W_{ji} = 1 \tag{3-6}$$

與

$$\sum_{i=1}^{a}\sum_{j=1}^{M*N} W_{ji} = M * N \tag{3-7}$$

(4) 計算如公式(3-8)的目標函數 J，若此次 J 值與上一次運算的值相同，代表收斂，即可結束，否則繼續步驟 5。

$$J = \sum_{i=1}^{a} J_i = \sum_{i=1}^{a}\sum_{j=1}^{M*N} W_{ji} \left\| X_j - C_i \right\| \tag{3-8}$$

(5) 更新所有群集中心，如公式(3-9)，回到步驟 3。

$$C_i = \frac{\sum_{j=1}^{M*N} W_{ji} * X_j}{\sum_{j=1}^{M*N} W_{ji}} \tag{3-9}$$

Bezdek [6]首先提出 FCM 演算法，改良了 HCM 的權重歸屬方式，加入了模糊概念，讓每個個體不再僅歸屬於某一特定群集，以其歸屬程度來表現與各群集中心之間的影響比例。

FCM 演算法步驟：

(1) 讀取一張影像(長寬為 M、N)，其影像的像素值以 X_j 表示，$0 < j \le M * N$ 。

(2) 初始化分群數目為 a 群，初始權重矩陣 $W_{current}$，其亂數產生介於 0~1 之間的值，但需滿足該像素值對應到其他群集中心之比例總合為 1，如公式(3-10) 。

$$\sum_{i=1}^{a} W_{ji} = 1, \forall j = 1,2,....., M * N \qquad (3\text{-}10)$$

(3) 計算群集中心，如公式(3-11)，m 代表權重指數。

$$C_i = \frac{\sum_{j=1}^{M*N} W_{ji}^{m} * X_j}{\sum_{j=1}^{M*N} W_{ji}^{m}} \qquad (3\text{-}11)$$

(4) 計算如公式(3-12)之目標函數 J，若與上次的目標函數值差異甚小則當作收斂完成；另外亦可將此次的權重矩陣 $W_{current}$ 與上次的權重矩陣 W_{old} 相減，得到的新矩陣內 W_{new}，若此矩陣內的最大值小於一個非常小的數，代表權重矩陣已收斂完成，如公式(3-13)。只要有一個條件符合，及代表收斂結束，否則繼續步驟 5。

$$J = \sum_{i=1}^{a} J_i = \sum_{i=1}^{a} \left(\sum_{j=1}^{M*N} W_{ji}^{m} \left\| X_j - C_i \right\|^2 \right) \tag{3-12}$$

$$W_{new} = W_{current} - W_{current} \quad , \quad Max(W_{new}) < 0.0001 \tag{3-13}$$

(5) 記錄當前權重矩陣，並更新計算權重矩陣，如公式(3-14)與(3-15)，並回到步驟 3。

$$W_{old} = W_{current} \tag{3-14}$$

$$W_{current_{ji}} = \frac{1}{\sum_{t=1}^{a} \left(\frac{\left\| X_j - C_i \right\|}{\left\| X_j - C_t \right\|} \right)^{\frac{2}{m-1}}} \tag{3-15}$$

門檻值分割法，則透過直方圖統計分析，利用影像中每一個像素灰階值，出現次數所統計出來的一個分佈圖，搭配演算法找出最佳門檻值，並以此門檻值來當作分群條件。

Kapur 提出最大熵值門檻法，運用了 Shannon 熵的概念進行影像分割，找出一個適當門檻灰階值能夠劃分出背景(background)與物件(Object)，並且讓這 2 個區域內擁有最大變化量。L 代表此灰階影像的最大範圍，t 代表在解空間中的任一灰階值，計算方法如公式(3-16)與公式(3-17)所示，$H(t)$代表影像中 entropy 的值，假設在一維度空間，$h(i)$ 代表第 i 點灰階值的出現在影像中的總數；N 代表所有影像中的像素的個數，如公式(3-18)所示，試圖找出最佳的門檻值 t，能讓$H(t)$計算出來的值最大。

$$H(t) = H_{object}(t) + H_{background}(t)$$
$$= -\sum_{i=0}^{t} \frac{p_i}{p_t} \ln \frac{p_i}{p_t} - \sum_{i=t+1}^{L-1} \frac{p_i}{1-p_t} \ln \frac{p_i}{1-p_t} \quad (3\text{-}16)$$

$$P_t = \sum_{i=0}^{t} P_i \ , \ P_i = h(i)/N \ . \quad (3\text{-}17)$$

$$\phi = Arg\max_{0<t<L-1} H(t) \tag{3-18}$$

將多個門檻值情況下，去運算每一個灰階值 i，如公式(3-19)與(3-20)所示，讓門檻值範圍內出現在整體的機率。

$$\begin{aligned} &H(t_1, t_2, \cdots, t_n) = H(t_1) + H(t_2) + \cdots + H(t_n) \\ &= -\sum_{i=0}^{t_1-1} \frac{P_i}{P_{t_1}} \ln \frac{p_i}{P_{t_1}} - \sum_{i=t_1}^{t_2-1} \frac{P_i}{P_{t_2}} \ln \frac{p_i}{P_{t_2}} - \cdots - \sum_{i=n}^{L-1} \frac{P_i}{P_{L-1}} \ln \frac{p_i}{P_{L-1}} \end{aligned} \tag{3-19}$$

$$\begin{aligned} p_{t_1} &= \left(\sum_{j=0}^{t_1-1} P_j \right), p_j = h(j)/N, \\ P_{t_2} &= \left(\sum_{j=t_1}^{t_2-1} p_j \right), p_j = h(j)/N, \cdots, \\ p_{t_n} &= \left(\sum_{j=n}^{L-1} p_j \right), p_j = h(j)/N \end{aligned} \tag{3-20}$$

將不同的門檻值，代入 entropy 計算公式去運算，不斷搜尋找出最大的解，最後以門檻值內的成員視為同一群，即完成門檻值分割法。

3.3 影像切割

本節之目的在於以生物智能概念搭配各種分群演算法，進行影像

分割。

3.3.1 退火排程法之人工蜂群模糊系統

在本論文中，我們提出了退火排程法之模糊人工蜂群系統，系統中把每隻蜜蜂以亂數方式灑在影像上，進行空間域上的資料探查，資料取樣以蜜蜂半徑內的所有像素灰階值，進行 FCM 的分群統計，透過全部蜜蜂取得的食物，以排序擇優的方法選擇，並把食物源較豐富的地帶，以更多的蜜蜂進行區域搜尋。

其演算法步驟如下：

(1) 初始化蜜蜂數量 n、分群數目為 c、總疊代次數 t 和蜜蜂的搜尋半徑 r。

(2) 以亂數方式產生座標，決定 n 蜜蜂的位置，灑在影像空間上。

(3) 把每隻蜜蜂半徑內的像素值，代入 FCM 進行分類，並以分群完結果，運算該群佔半徑內的權重比例。

(4) 選出權重比例比較好的蜜蜂，數量為總蜜蜂數之一半，以該蜜

蜂的半徑內，加入 2 隻新蜜蜂做區域搜尋，並把區域內較好的蜜蜂進行保留動作，其他捨去。

(5) 組合權重比例高的群聚當成主要群集中心，判斷疊代是否完成，完成則以群集中心進行分類；若疊代沒完成，則進入步驟 6。

(6) 以亂數方式產生總數量之一半蜜蜂座標，取代之前被淘汰掉的，如公式(3-21)，以退火排程法更新蜜蜂的搜尋半徑，並回到步驟 3 繼續運行。

$$r(t) = \frac{1}{\varepsilon}\left[\varepsilon + \tanh(w)^t\right] \times r(t-1) \tag{3-21}$$

r 代表蜜蜂的搜尋半徑，w 的範圍在 0 < w < 1，是一個很小的常數，t 是疊代次數。使用退火排程目的，在於隨著疊代次數漸漸縮減半徑的範圍，可以更精準且更有效率的尋找每塊區域上的局部最佳解。

傳統上的分類方法，較少利用空間上的訊息，此演算法以蜜蜂的全

面性搜尋，搭配FCM歸類後取得的空間上資訊，以權重最好的部分，做為整體的群集中心，此演算法簡稱FABCS(Fuzzy Artificial Bee Colony System with Cooling Schedule for the Image Segmentation)，其演算法流程圖，如圖3.11所示。

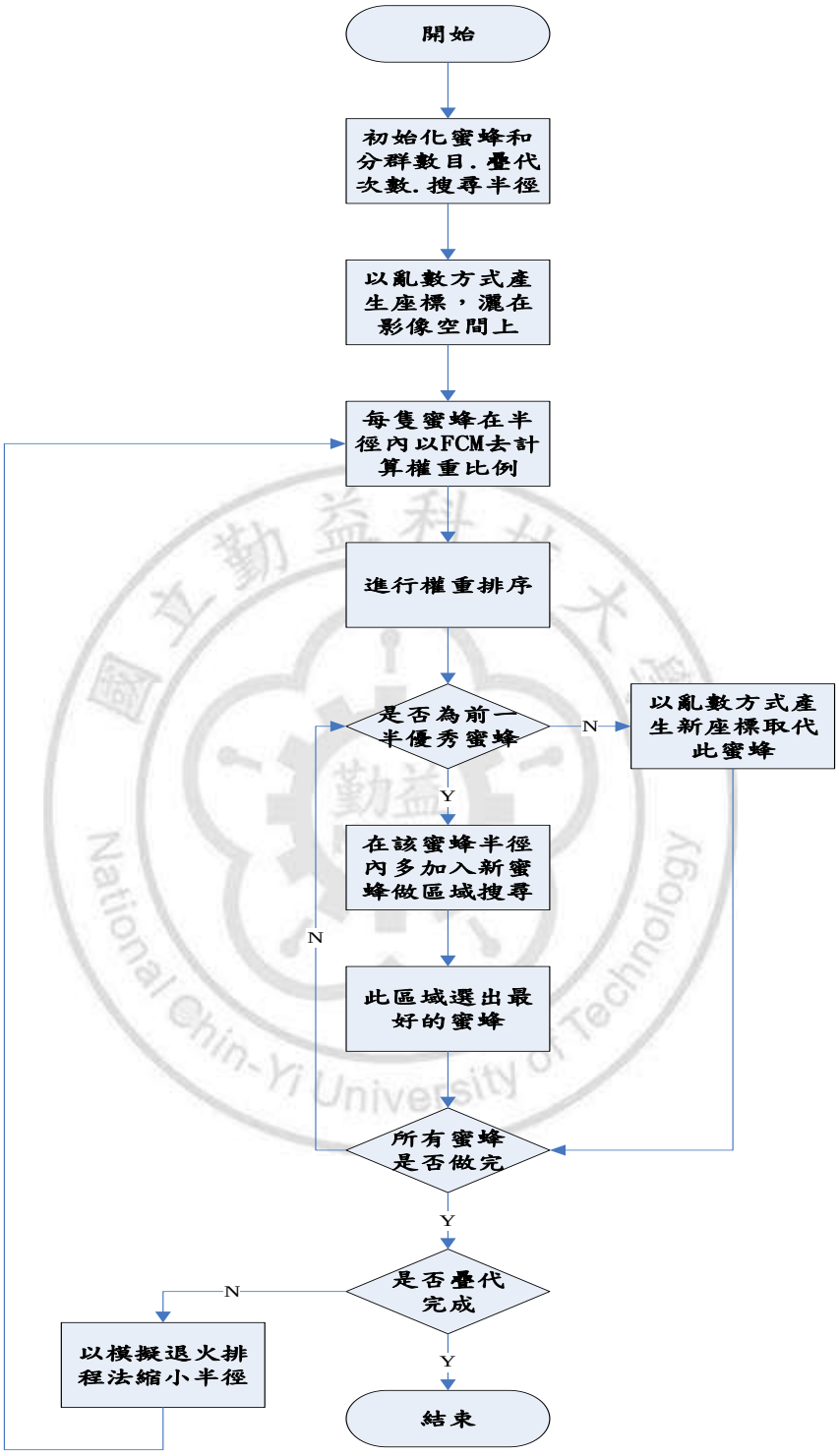

圖 3.11　FABCS 流程圖

3.3.2 建構 entropy 於粒子群最佳化演算法之門檻值演算法

把門檻值與群集中心的演算法最搭配，藉由最大熵值門檻法和均勻度方法以架構的粒子群最佳化，找出最佳門檻值，透過各門檻值範圍內的像素灰階值，算出全部像素出現在影像中出現機率，搭配範圍內像素值的平均計算，也就是以群集中心的密度當做評估，由粒子不斷的疊代計算最佳門檻值。

均勻度是對門檻值的效能評估，其概念在於使用每個區域內的值，跟該範圍內的平均值相減後再加總，如公式(3-22)所示，所以門檻取的越好，其均勻度就越大：

$$u = 1 - 2 * \frac{\sum_{j=0}^{k} \sum_{i \in R_j} \left(f_i - m_j \right)^2}{N * \left(f_{\max} - f_{\min} \right)^2} \tag{3-22}$$

均勻度的值介於 0 到 1 之間，其值越大越好，其中 k 代表門檻值數目；i 代表門檻值內的像素；f_i 代表該點像素灰階值；m_j 代表該區域的平均值；N 為整張影像的像素大小；$f_{\max}, f_{\min}$ 代表整張影像的最大灰階值及最小灰階值。

其演算法步驟如下:

<1> 讀取一張影像，由使用者決定分群數目 N，門檻值個數為 $(N-1)$ 個，以 K 表示。

<2> 初始化粒子數目 M；隨機亂數設定每個粒子 i $(0<i<=M)$ 的速度及位置；若為8bits影像之灰階值0~255範圍，隨機挑選設定 K 個門檻值，並計算均勻度公式；K 個門檻值設定有 K 個子集空間。

<3> 將 M 個粒子的位置分別取代第 j 個子集空間 $(0<j<=K)$ 的門檻值，去運算entropy，即公式(3-19)、(3-20)。

<4> 計算出來每個粒子的解，並與自身 p_{best} 的適應值比較，若較佳，即把當前粒子的位置跟適應值取代自己的 p_{best}。M 個粒子做完，找出最優秀之第 i 個粒子，當作 $p_{subswarm\_best_{ij}}$，重複步驟<3>，直到 $j=K$，進入步驟5。

<5> 把 K 個 $p_{subswarm\_best}$ 排列，取出最好的 $p_{subswarm\_best_{ij}}$ 並比較 G_{best} 的適應值，若較好，則把位置及適應值取代 G_{best}。

<6> 把 M 個粒子，代入速度及位置更新，如公式(3-1)、(3-2)和(3-3)。

<7> 把 K 個門檻值與 $p_{subswarm\_best}$ 做統計學的排列組合，代入均勻度公式，取出最大的一組，與 K 個門檻值去比較均勻度值，如公式(3-22)，若有比較好，則取代當前門檻值，並把 K 個 $p_{subswarm\_best}$ 和 P_{best} 及 G_{best} 適應值清空，避免陷入區域最佳值。

<8> 重複第<3>步驟到第<7>步驟，直到疊代次數做完，或粒子位置不再變化、門檻值也沒再變動等收斂條件符合，即結束。

<9> 以結果得到的最佳門檻值，做分類切割影像。

其演算法架構流程圖，如圖3.12所示。

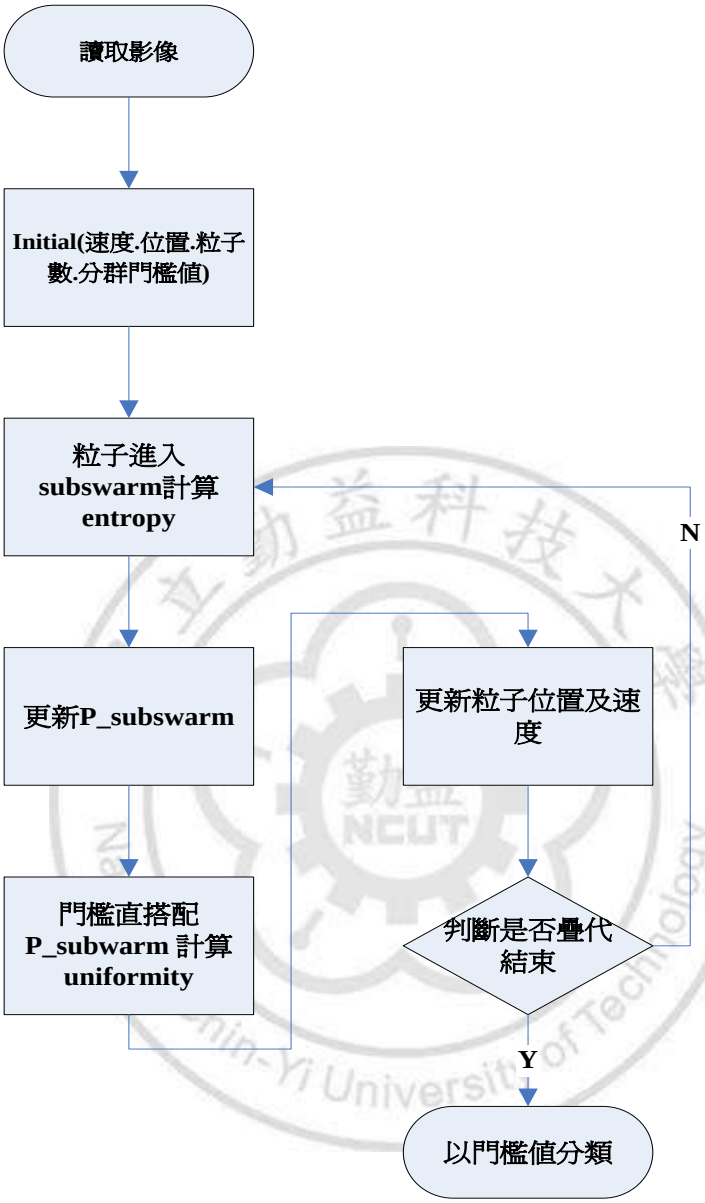
讀取影像
Initial(速度.位置.粒子數.分群門檻值)
粒子進入subswarm計算entropy
更新P_subswarm
門檻直搭配P_subwarm 計算uniformity
更新粒子位置及速度
判斷是否疊代結束
N
Y
以門檻值分類

圖3.12　演算法流程圖

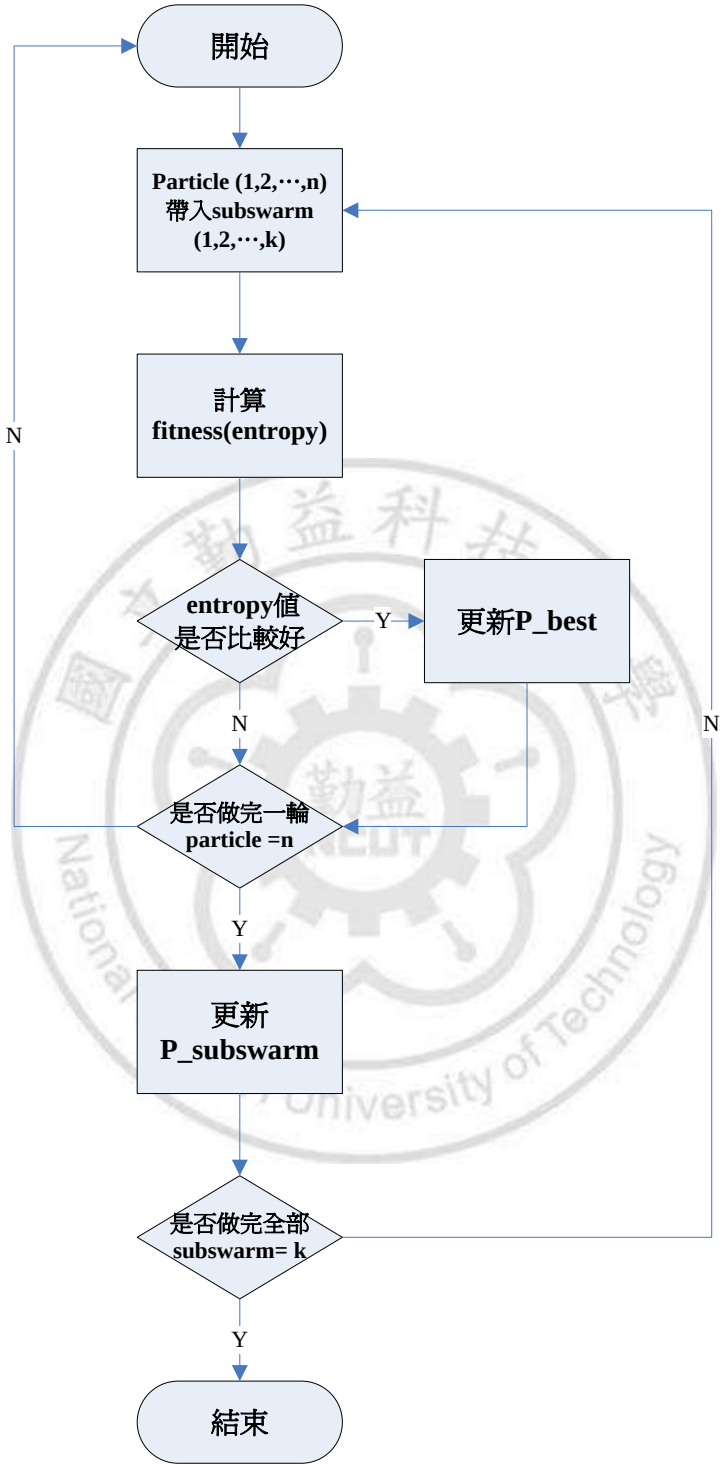

圖3.13　粒子進入subswarm計算entropy

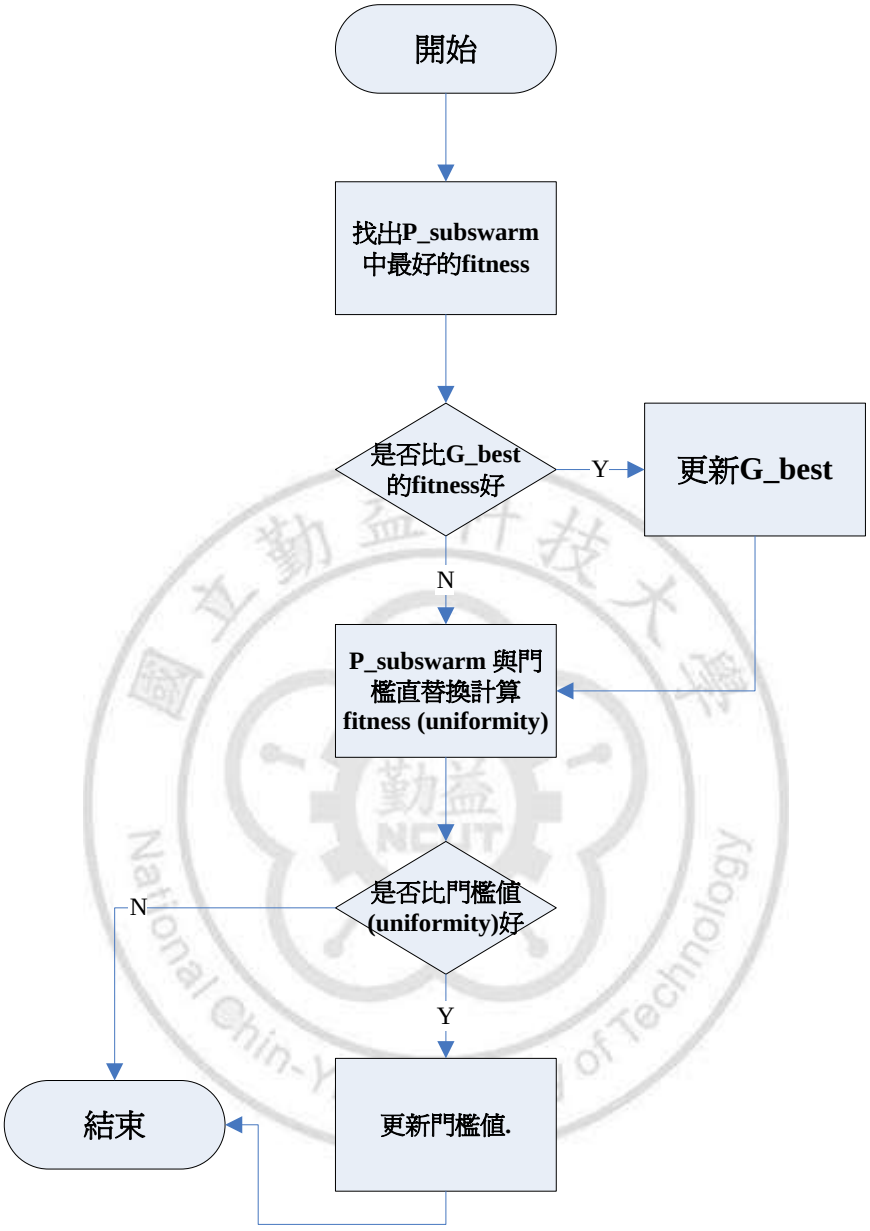

圖3.14　門檻直搭配P_subswarm 計算 uniformity

第四章 實驗結果

4.1 實驗結果

本論文之實驗環境， 均在 Pentium 雙核心個人電腦上運算， 並以 Matlab 為程式實作工具來完成實驗。演算法中利用生物智能演算法進行影像分割處理，以人工蜂群法搭配 FCM 和 HCM，作人腦病變核磁共振影像，再與原始分群法 HCM 和 FCM 比較其效能；另外在人眼睛的分割部份，先以影像前處理進行解決色彩偏差，再以粒子群演算法搭配最大熵值門檻法，確切的切割出瞳孔。

4.2 蜂群演算法分類結果

如圖 4.1 所示，首先我們先完成人腦切片測試樣本的圖形，透過已知的數據做效能上的檢測。先建立一個大小 256*256 的一個矩陣，其內部灰階值設成 0，再利用橢圓方程式 $\frac{x^2}{a^2}+\frac{y^2}{b^2}=1$ 劃出 7 個圖形，如公式(4.1)到公式(4.7)，其內部以不同灰階值表示。

$$y = 115 \times \sqrt{1 - \frac{(x-128)^2}{80^2}} + 128$$, x 的範圍由 48 到 208,間隔為 0.1 (4.1)

$$y = 105 \times \sqrt{1 - \frac{(x-128)^2}{70^2}} + 128$$, x 的範圍由 58 到 198,間隔為 0.1 (4.2)

$$y = 20 \times \sqrt{1 - \frac{(x-168)^2}{50^2}} + 168$$, x 的範圍由 78 到 178,間隔為 0.1 (4.3)

$$y = 20 \times \sqrt{1 - \frac{(x-88)^2}{50^2}} + 88$$, x 的範圍由 78 到 178,間隔為 0.1 (4.4)

$$y = 90 \times \sqrt{1 - \frac{(x-128)^2}{40^2}} + 128$$, x 的範圍由 88 到 168,間隔為 0.1 (4.5)

$$y = 50 \times \sqrt{1 - \frac{(x-143)^2}{10^2}} + 143$$, x 的範圍由 118 到 138,間隔為 0.1 (4.6)

$$y = 50 \times \sqrt{1 - \frac{(x-113)^2}{10^2}} + 113$$, x 的範圍由 118 到 138,間隔為 0.1 (4.7)

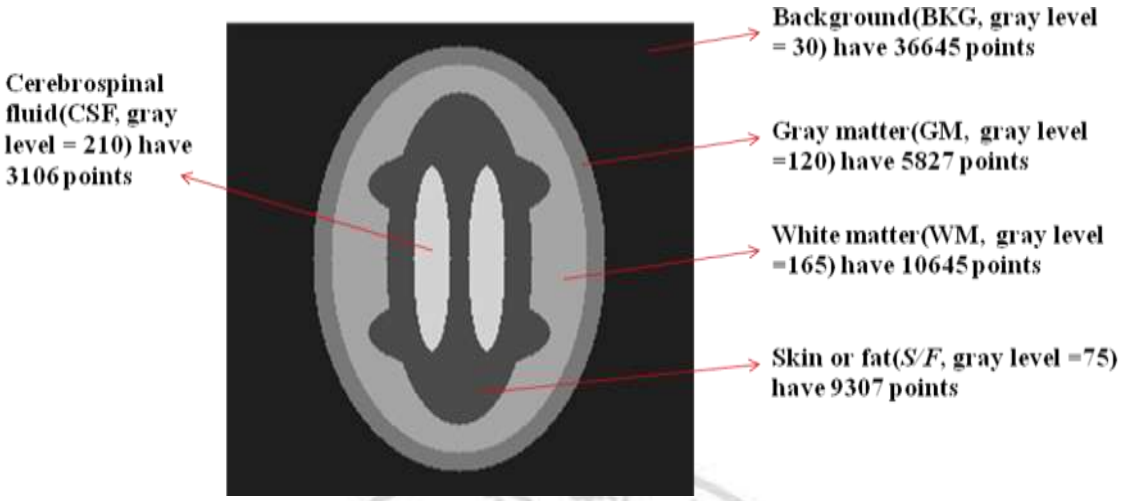

圖 4.1　測試樣本圖

把測試樣本圖加入均勻分布的雜訊 n，分別為 15、20、25、30，雜訊 n 代表整張影像的每一點像素值，以亂數之正負 n 範圍取代原來像素值。舉例來說，n 為 15，影像上某一點的像素值為 100，其加入雜訊後，該點像素值介於$100-15 \le pixel \le 100+15$，以亂數方式產生。圖 4.2 為 256*256 的原始圖，圖 4.3 為雜訊度 15，圖 4.4 為雜訊度 20，圖 4.5 為雜訊度 25，圖 4.6 為雜訊度 30。以各種演算法 HCM、FCM、蜂群加上 HCM、蜂群加上 FCM 做比較，分類結果如圖 4.7 到圖 4.14。

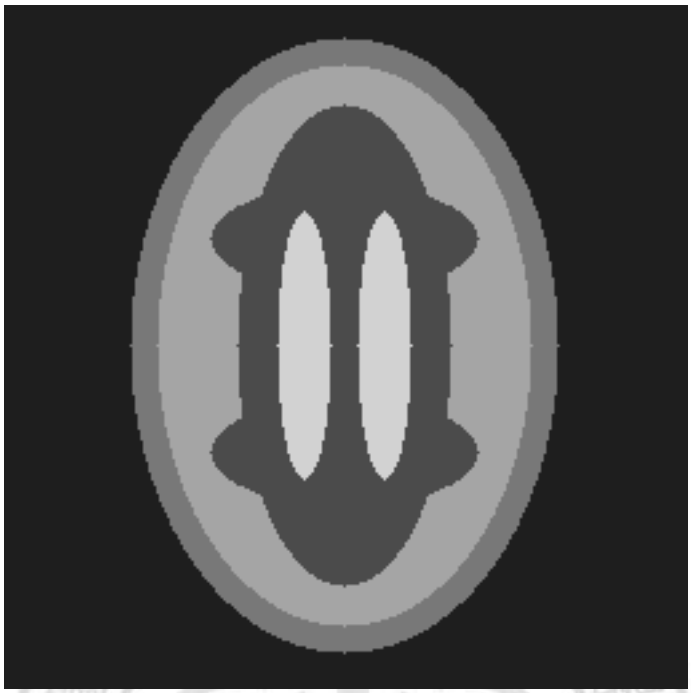

圖 4.2 測試樣本之原始圖

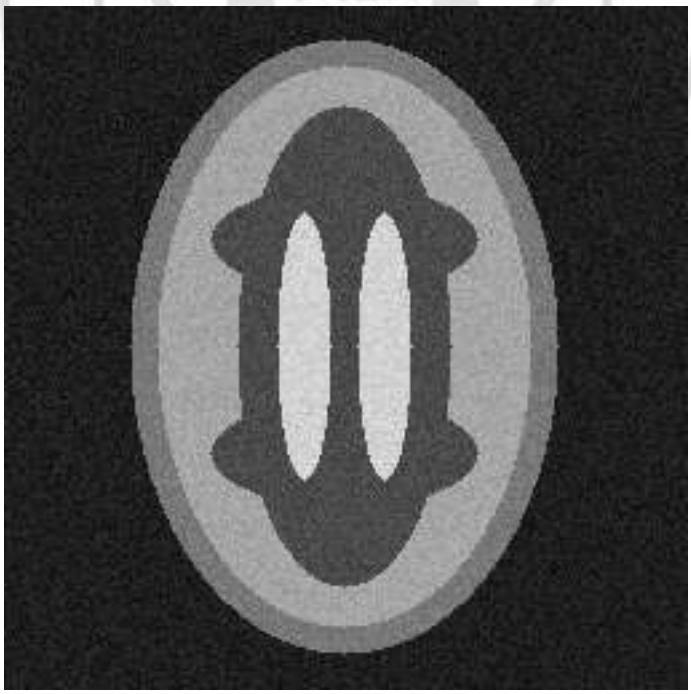

圖 4.3 加入雜訊度 15

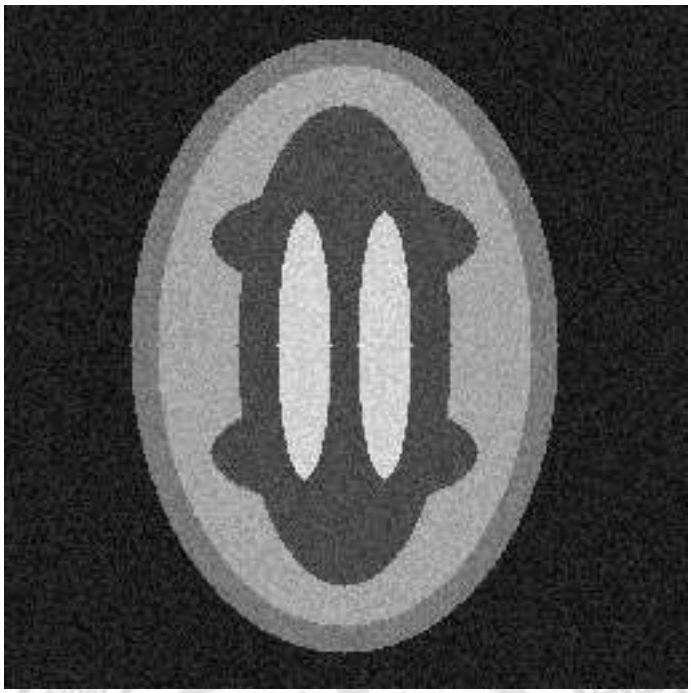

圖 4.4 加入雜訊度 20

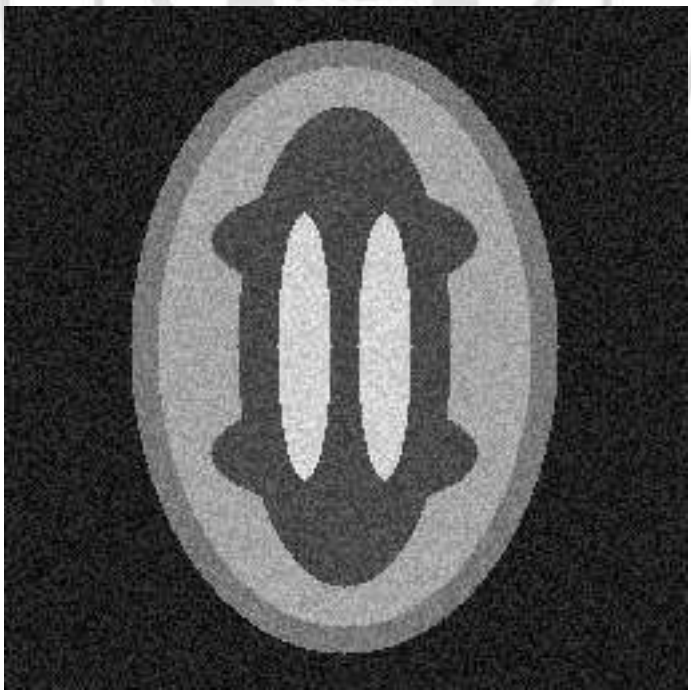

圖 4.5 加入雜訊度 25

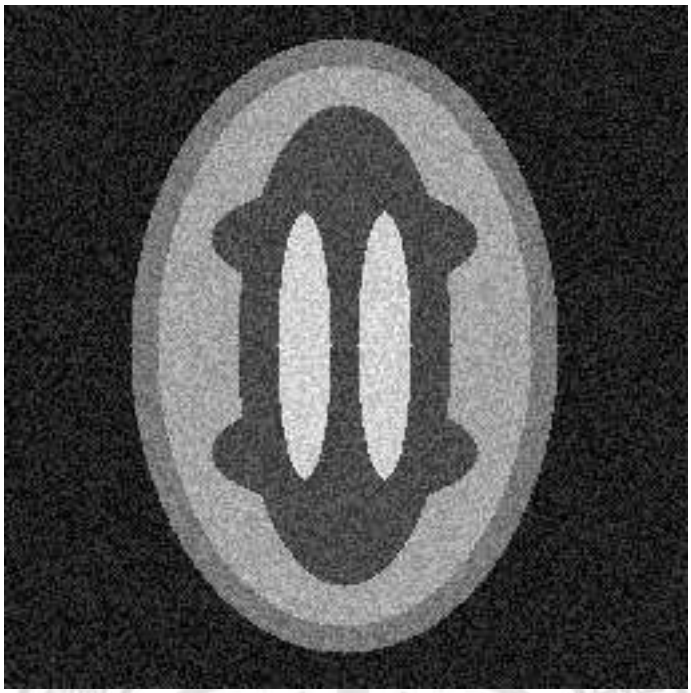

圖 4.6 加入雜訊度 30

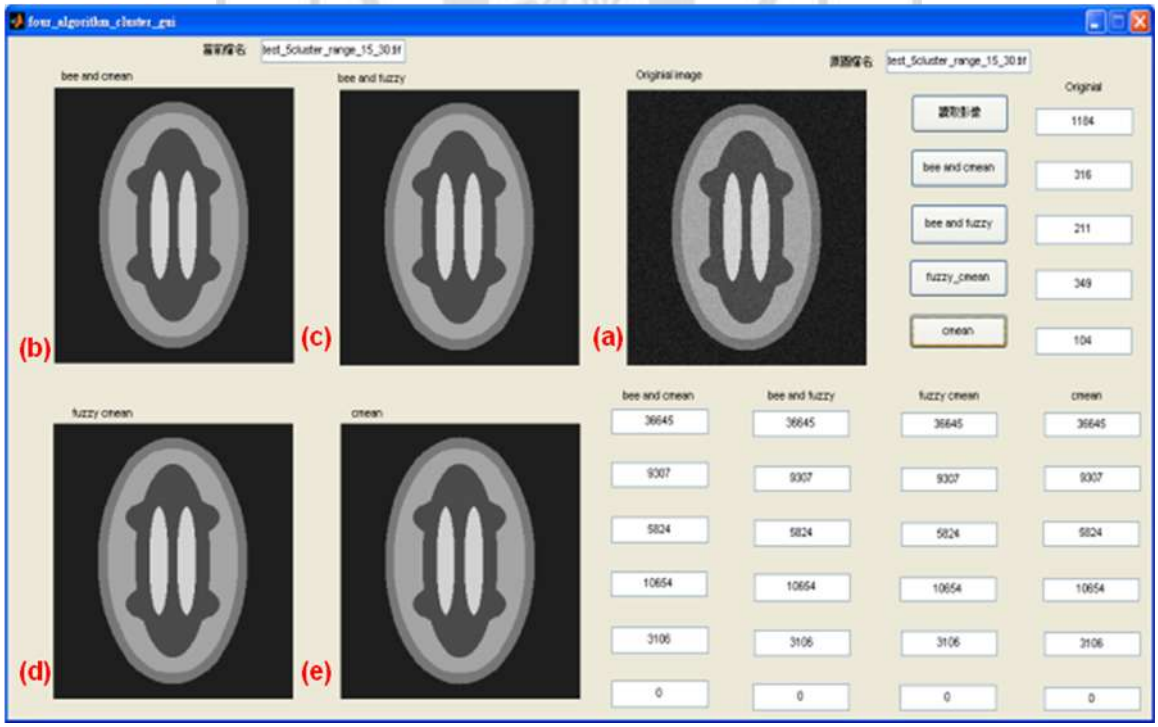

圖 4.7 雜訊度 15 的方法比較；(a)為原始圖 (b)為 Bee+HCM (c)為 Bee+FCM (d)為 FCM (e)為 HCM

TABLE I
THE SEGMENTATION PERFORMANCE FOR HCM, FCM, BEE + HCM, AND THE PROPOSED FABCS ALGORITHM USING THE TEST PHANTOM WITH $k <= 15$.

Simulate	Actual pixels	HCM	FCM	Bee + HCM	FABCS
Background	36645	36645	36645	36645	36645
S/F	9307	9307	9307	9307	9307
GM	5824	5824	5824	5824	5824
WM	10654	10654	10654	10654	10654
CSF	3106	3106	3106	3106	3106
Average error		0%	0%	0%	0%

圖 4.8 雜訊度 15 的平均錯誤率

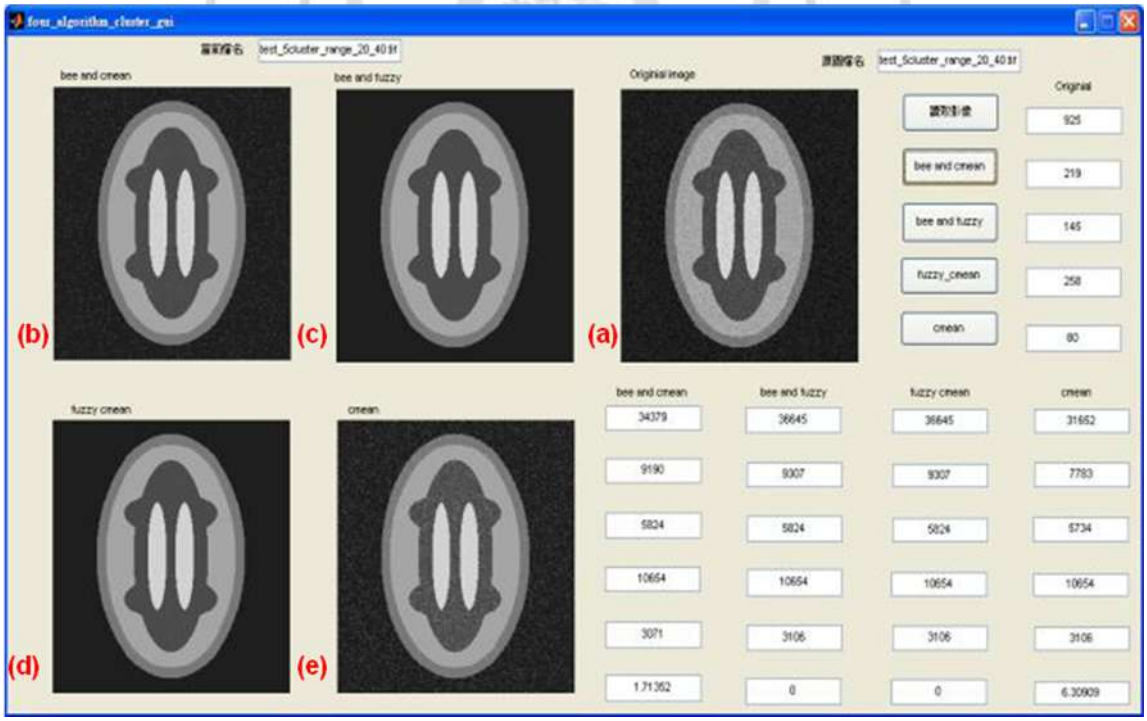

圖 4.9 雜訊度 20 的方法比較；(a)為原始圖 (b)為 Bee+HCM (c)為 Bee+FCM (d)為 FCM (e)為 HCM

TABLE II
THE SEGMENTATION PERFORMANCE FOR HCM, FCM, BEE + HCM, AND THE PROPOSED FABCS ALGORITHM USING THE TEST PHANTOM WITH $k <= 20$.

Simulate	Actual pixels	HCM	FCM	Bee + HCM	FABCS
Background	36645	31652	36645	34379	36645
S/F	9307	7783	9307	9190	9307
GM	5824	5734	5824	5824	5824
WM	10654	10654	10654	10654	10654
CSF	3106	3106	3106	3071	3106
Average error		6.31%	0%	1.71%	0%

圖 4.10 雜訊度 20 的平均錯誤率

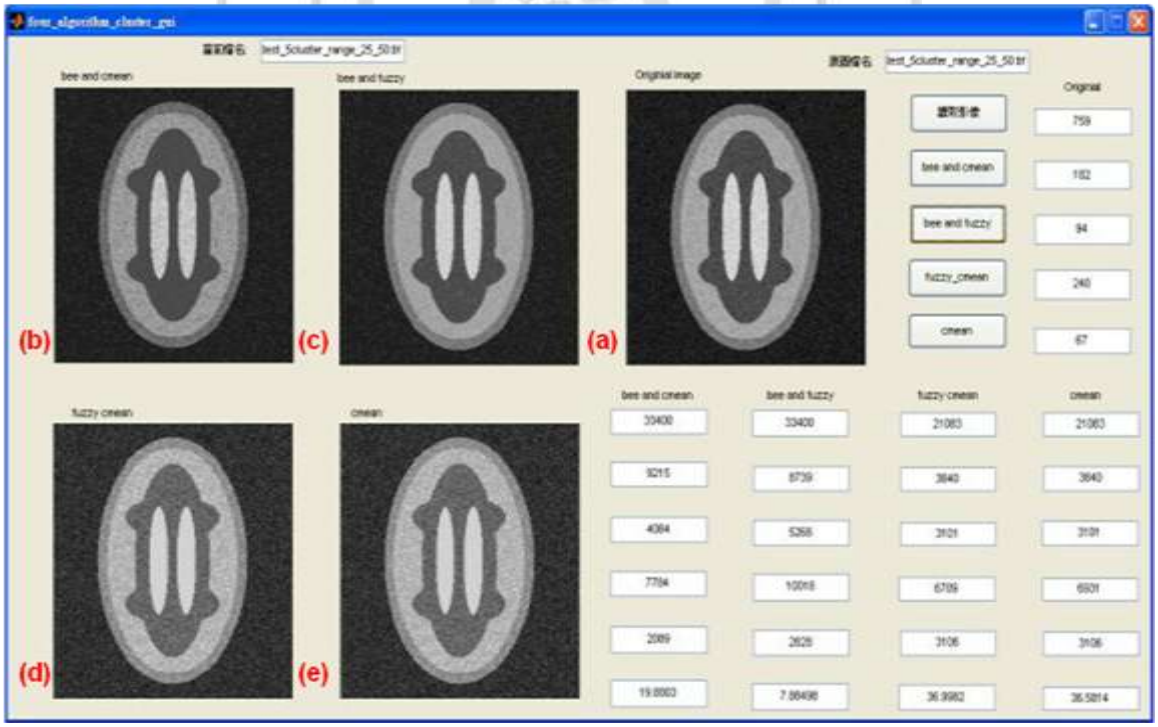

圖 4.11 雜訊度 25 的方法比較；(a)為原始圖 (b)為 Bee+HCM (c)為 Bee+FCM (d)為 FCM (e)為 HCM

TABLE III
THE SEGMENTATION PERFORMANCE FOR HCM, FCM, BEE + HCM, AND THE PROPOSED FABCS ALGORITHM USING THE TEST PHANTOM WITH $K <= 25$.

Simulate	Actual pixels	HCM	FCM	Bee+HCM	FABCS
Background	36645	21083	21083	33400	33400
S/F	9307	3840	3840	9215	8739
GM	5824	3101	3101	4084	5268
WM	10654	6931	6709	7784	10018
CSF	3106	3106	3106	2089	2828
Average error		36.58%	37.0%	19.88%	7.88%

圖 4.12 雜訊度 25 的平均錯誤率

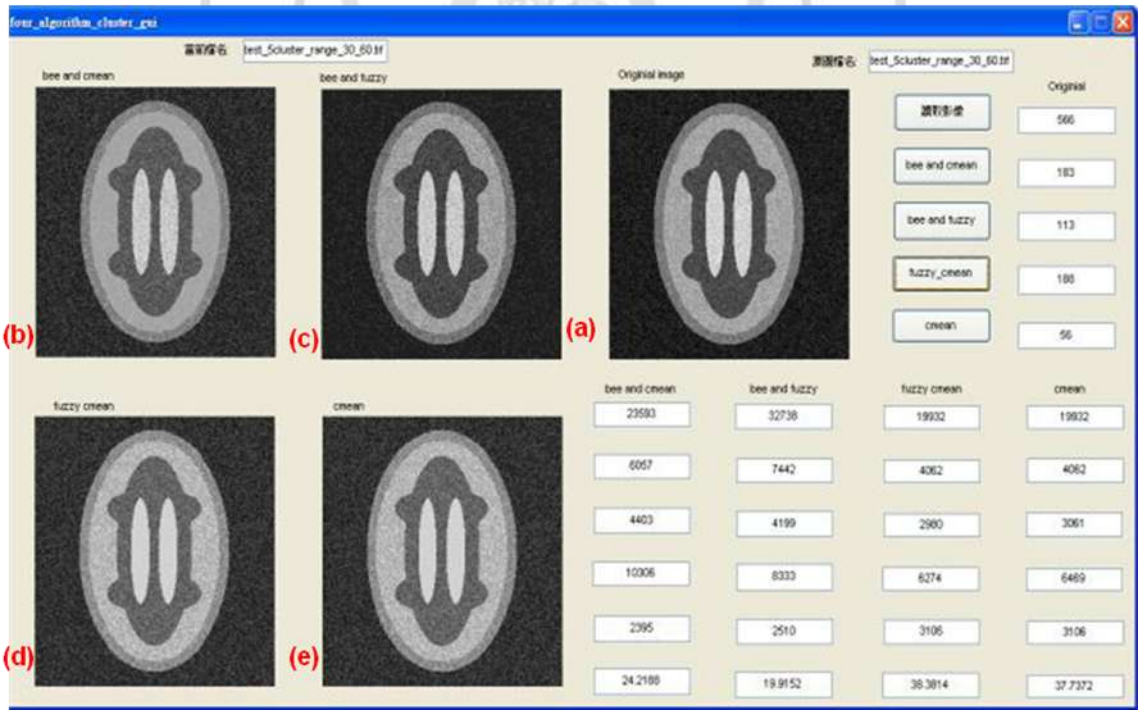

圖 4.13 雜訊度 30 的方法比較；(a)為原始圖 (b)為 Bee+HCM (c)為 Bee+FCM (d)為 FCM (e)為 HCM

TABLE IV
THE SEGMENTATION PERFORMANCE FOR HCM, FCM, BEE + HCM, AND THE PROPOSED FABCS ALGORITHM USING THE TEST PHANTOM WITH $k <= 30$.

Simulate	Actual pixels	HCM	FCM	Bee+HCM	FABCS
Background	36645	19932	19932	23593	32738
S/F	9307	4062	4062	6057	7442
GM	5824	3061	2980	4403	4199
WM	10654	6469	6274	10306	8333
CSF	3106	3106	3106	2395	2510
Average error		37.74%	38.38%	24.22%	19.92%

圖 4.14 雜訊度 30 的平均錯誤率

從圖 4.7 到圖 4.14 可以明顯看出 Bee + FCM 在不同的雜訊度條件下，均有較低的平均錯誤率，因此透過測試樣本圖片，可以知道 FABCS 在這 4 種方法裡面是最好的。如圖 4.15 和圖 4.16 所示，利用各種方法對核磁共振影像做分群。

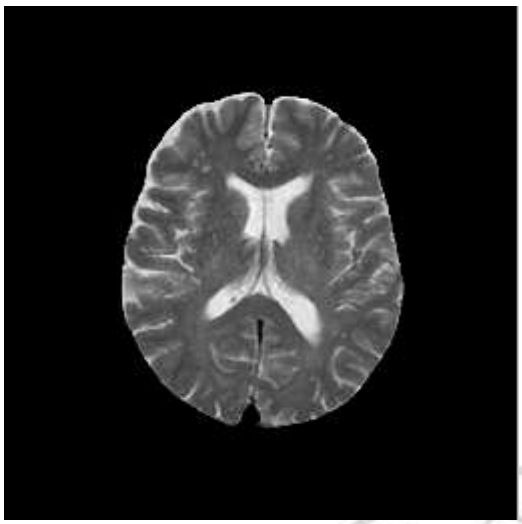

原始 MRI

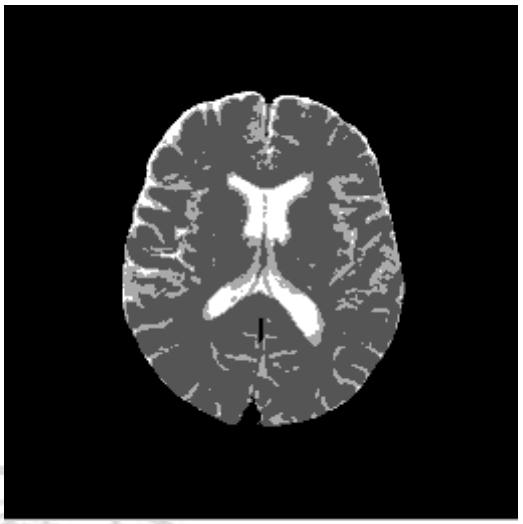

分 4 群 Bee + HCM

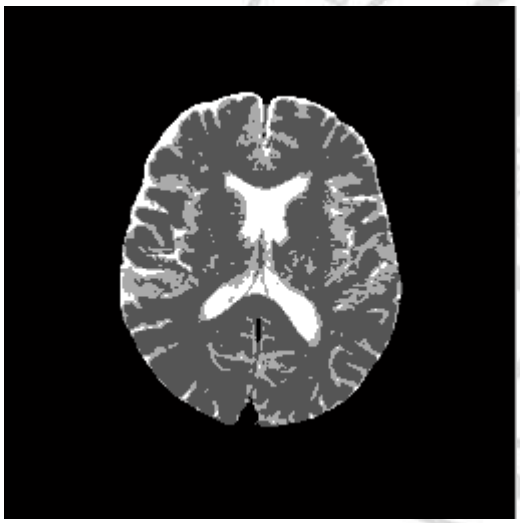

分 4 群 FCM

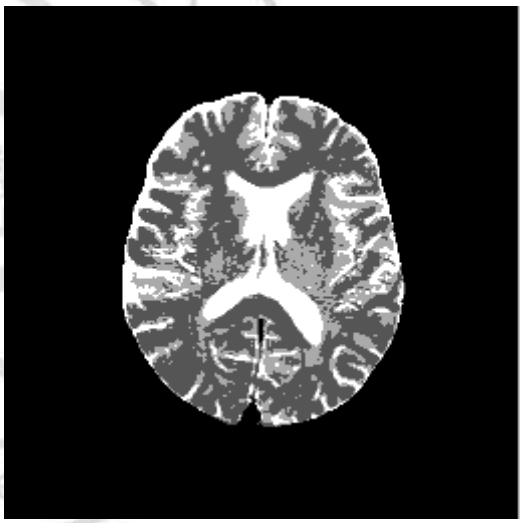

分 4 群 Bee + FCM

圖 4.15 實際測試 MRI 影像

原始 MRI

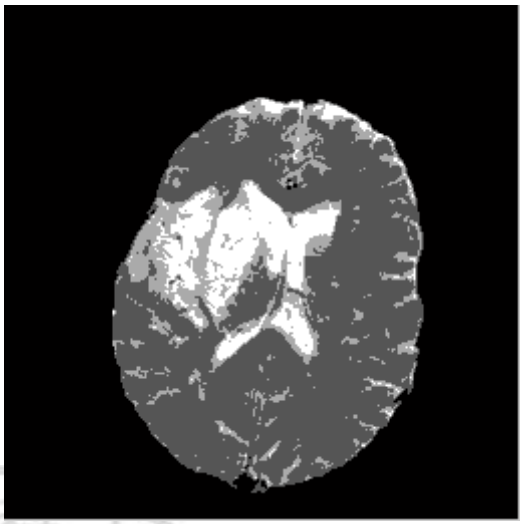

分 4 群 Bee + HCM

分 4 群 FCM

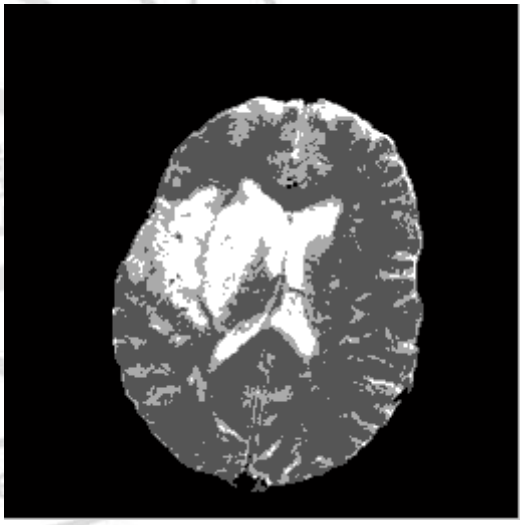

分 4 群 Bee + FCM

圖 4.16 實際測試 MRI 影像

4.3 粒子群演算法切割結果

本論文方法與 COCLPSO [21]進行比較，效能評量方面採用熵值與均勻度來當作依據，其結果如表 4.1 與表 4.2。

Image	k	Proposed PSO		HCOCLPSO [21]	
		Optimal thresholds	Entropy	Optimal thresholds	Entropy
Lena	2	88, 165	17.76	97, 164	17.8130
	3	72, 125, 179	22.0278	82, 126, 175	22.0993
	4	70, 117, 163, 197	25.8766	64, 97, 138, 179	25.9864
	5	53, 86, 123, 160, 207	29.1873	63, 94, 128, 163, 194	29.7348
Pepper	2	70, 146	18.0233	72, 144	18.0280
	3	56, 109, 164	22.4350	53, 102, 155	22.4694
	4	50, 98, 146, 196	26.3321	53, 98, 143, 191	26.5234
	5	35, 71, 106, 141, 191	30.3217	42, 74, 109, 149, 191	30.3483
barbara	2	90, 169	18.2646	98, 163	1832765
	3	72, 135, 187	22.6534	76, 127, 178	22.7182
	4	60, 111, 168, 208	26.6182	61, 100, 143, 187	26.7712
	5	66, 99, 135, 170, 208	30.5861	57, 92, 129, 166,199	30.6238

表 4.1 進行 entropy 效能比較

Image	k	Uniformity	
		Proposed PSO	HCOCLPSO[21]
Lena	2	0.9889	0.9883
	3	0.9899	0.9886
	4	0.9904	0.9893
	5	0.9920	0.9903
Pepper	2	0.9878	0.9876
	3	0.9890	0.9875
	4	0.9918	0.9914
	5	0.9916	0.9914
barbara	2	0.9898	0.9893
	3	0.9911	0.9901
	4	0.9925	0.9911
	5	0.9921	0.9919

表 4.2 進行 uniformity 效能比較

分群數目	粒子數目：20	記憶體空間			
		Proposed PSO		HCOCLPSO[21]	
5	P_best (記錄最佳位置、fitness)	20*2	總共需要 92	20*2*5	總共需要 410
	G_best	2		2*5	
	粒子速度	20		20*5	
	粒子位置	20		20*5	
	Sub_swarm	4*5		0	
n	P_best (記錄最佳位置.fitness)	20*2	總共需要 82+4*n	20*2*n	總共需要 82*n
	G_best	2		2*n	
	粒子速度	20		20*n	
	粒子位置	20		20*n	
	Sub_swarm	4*n		0	

表 4.3 進行記憶體使用量比較

以 PSO 演算法搭配 entropy 和 uniformity 進行影像進行分群，其切割成果如圖 4.17 到圖 4.22。

圖 4.17 Lena 原始圖

圖 4.18 Lena 分 6 群

圖 4.19 Pepper 原始圖

圖 4.20 Pepper 分 6 群

圖 4.21 barbara 原始圖

圖 4.22 barbara 分 6 群

4.4 演算法加入霍式轉換進行眼睛瞳孔分割

霍式轉換(Hough Transform)在 1962 年由 P. Hough 提出[29]，在 1972 年發表，初期只能用於直線的偵測，後來由 Duda 和 Hart 使用到圓形的偵測[30]，將影像中的每一點轉換到參數平面上做分析，再累計轉換後的參數值，以最大的累計參數值求得圓心。它的優點在於即使初始的資訊不完整，還是可以經由映射到新的平面上找出區域內累計器中最高的部份，去搜尋出可能的候選解。

首先從影像邊界的位置，去運算這些邊緣的梯度向量，利用 Sobel 的垂直、水平遮罩可以求 G_x 與 G_y，如公式(4-8)與公式(4-9)所示，並計算其梯度向量的角度，如公式(4-10)所示。把邊界上的每一點，移動圓之半徑長度，若為圓形形狀，轉換出來的參數平面上，會有較密集的區域，便可以找出圓心。

$$G_X = \begin{bmatrix} -1 & -2 & -1 \\ 0 & 0 & 0 \\ 1 & 2 & 1 \end{bmatrix} \times \begin{bmatrix} Matrix_{i-1,j-1} & Matrix_{i-1,j} & Matrix_{i-1,j+1} \\ Matrix_{i,j-1} & Matrix_{i,j} & Matrix_{i,j+1} \\ Matrix_{i+1,j-1} & Matrix_{i+1,j} & Matrix_{i+1,j+1} \end{bmatrix} \tag{4-8}$$

$$G_y = \begin{bmatrix} -1 & 0 & 1 \\ -2 & 0 & 2 \\ -1 & 0 & 1 \end{bmatrix} \times \begin{bmatrix} Matrix_{i-1,j-1} & Matrix_{i-1,j} & Matrix_{i-1,j+1} \\ Matrix_{i,j-1} & Matrix_{i,j} & Matrix_{i,j+1} \\ Matrix_{i+1,j-1} & Matrix_{i+1,j} & Matrix_{i+1,j+1} \end{bmatrix} \quad (4\text{-}9)$$

$$\theta = \arctan\left(\frac{Gy}{Gx}\right) \quad (4\text{-}10)$$

如圖 4.23 所示，欲求圓心 O 之座標，先運算 P 點的梯度向量角度 θ_1，代入公式(4-8)到公式(4-10)，若 G_y 是負值則把 $\theta_1 + 180^\circ$，同時透過三角形定理得知 $\theta_1 = \theta_2$，即可推算圓心夾角為 $\frac{\pi}{2} - \theta_2$，再利用極座標求取圓心 $X_c = x + r \times \cos\left(\frac{\pi}{2} - \theta_2\right), Y_c = y + r \times \sin\left(\frac{\pi}{2} - \theta_2\right)$；其中 r 值是未知的，必須給定一個範圍，透過疊代計算找出密度最高的部份。

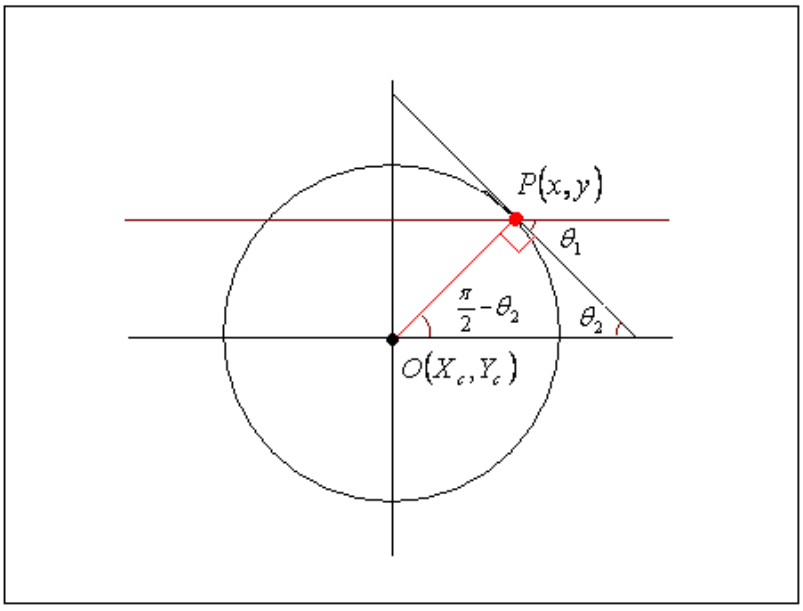

圖 4.23 展示圖

如圖 4.24 所示，在瞳孔分割部份，以粒子群最佳化演算法完成分群；如圖 4.25 所示，以相似度計算像素值黑色部份的合併；以 Sobel 的3×3水平及垂直遮罩，完成邊緣檢測，如圖 4.26 所示；再代入霍式轉換來做圓形偵測，如圖 4.27 所示；偵測出眼睛瞳孔的位置，如圖 4.28 所示；最後進行瞳孔的切割，如圖 4.29。

圖 4.24 眼睛原始圖

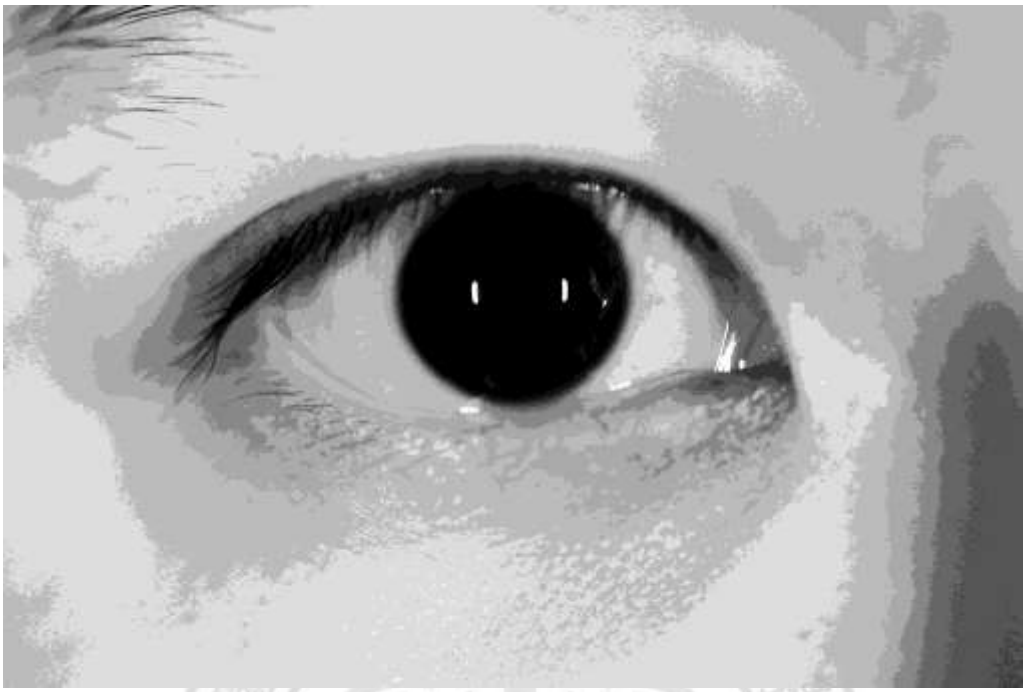

圖 4.25 粒子群最佳化演算法分群

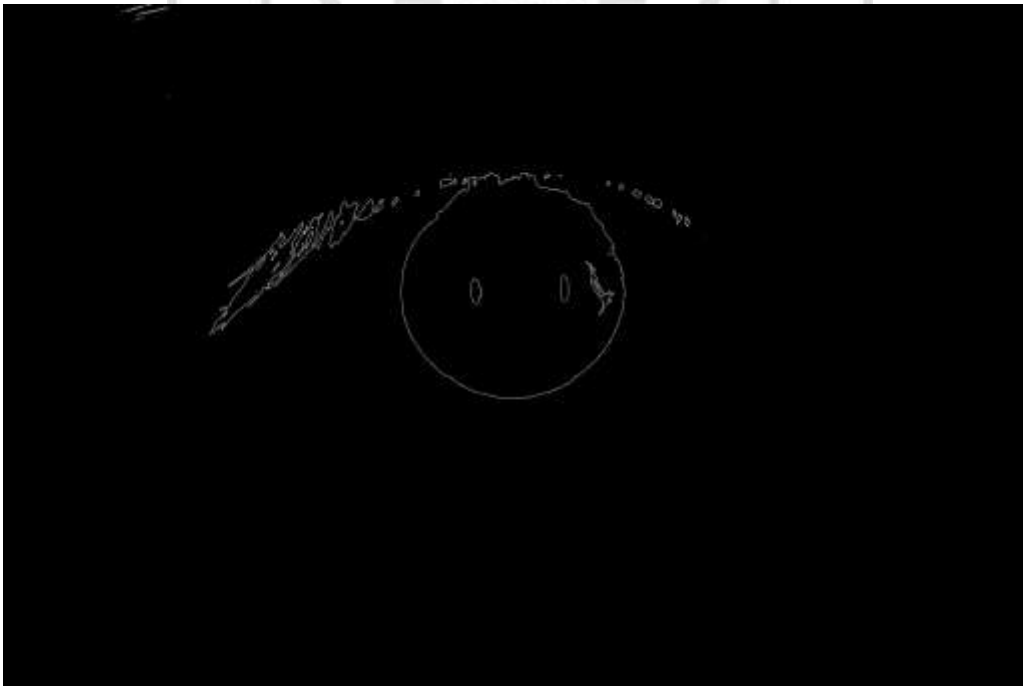

圖 4.26 Sobel 邊緣檢測

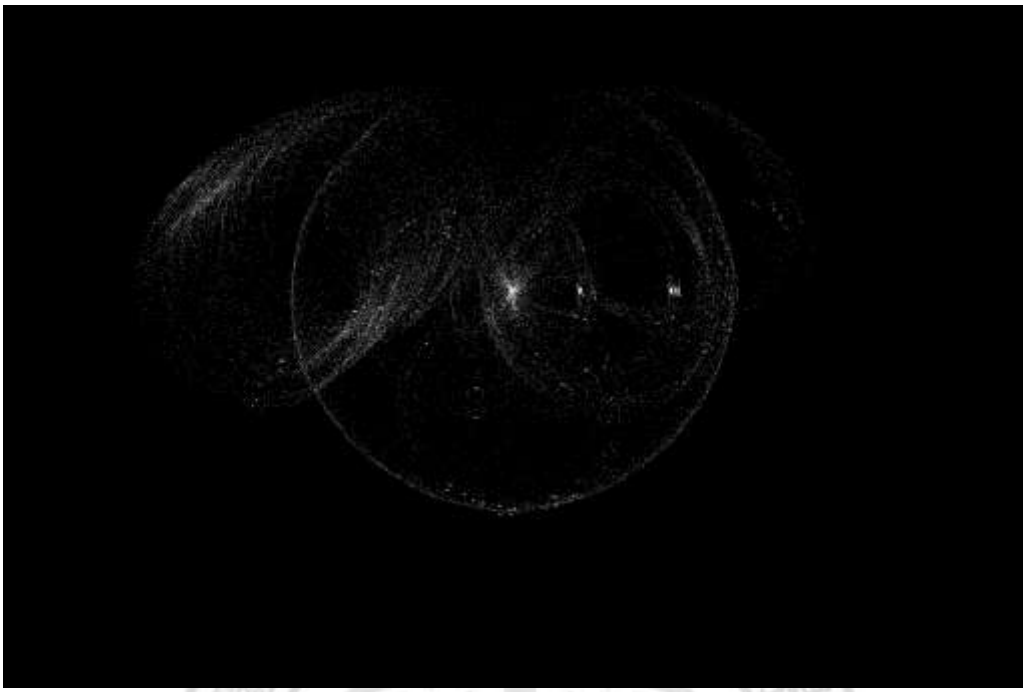

圖 4.27 霍式轉換

圖 4.28 瞳孔偵測圖

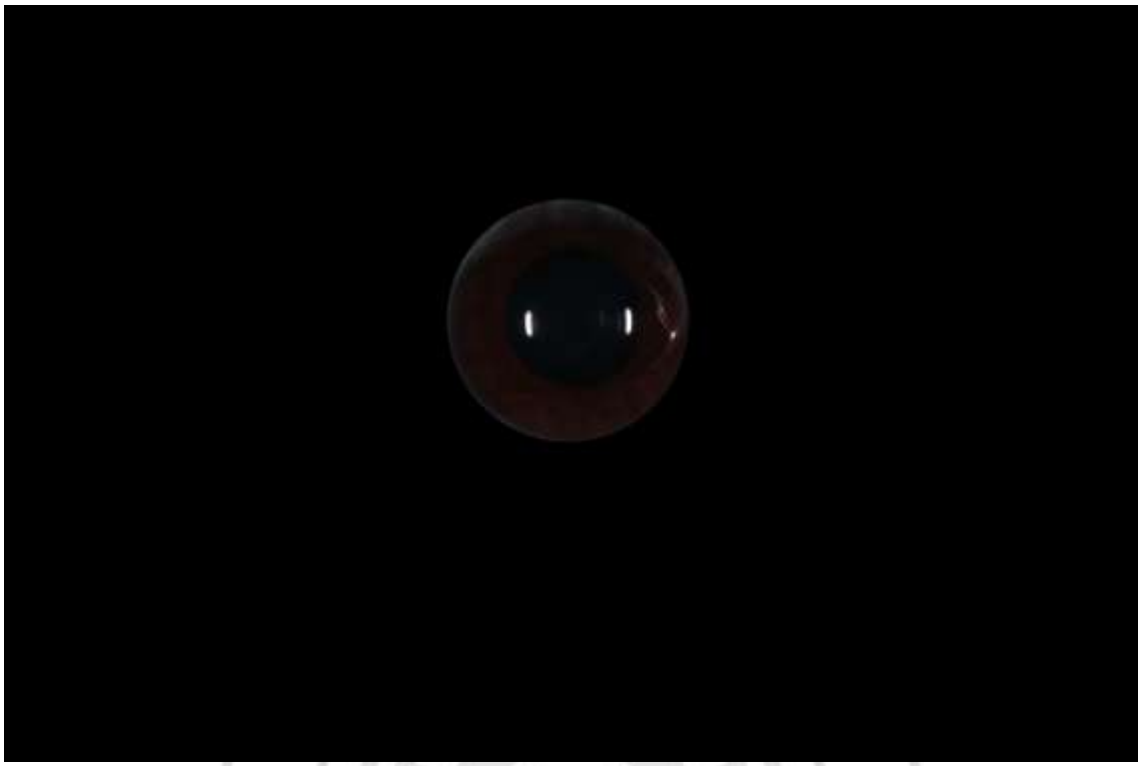

圖 4.29 瞳孔切割圖

第五章 結論與未來展望

5.1 結論

利用簡單的統計出色偏後，透過影像前處理之白平衡，搭配攝影技巧的觀念，把分區曝光系統代入到白平衡演算法祛除色偏，以減少之後要進行影像分類的誤差，而這一個步驟也可以讓許多攝影玩家，能夠在拍攝後進行影像的後處理。在影像分割部份，利用生物智能演算法的優點，以人工蜂群處理空間上資訊搜尋，結合 FCM 的分類權重，並以模擬退火排程做蜜蜂搜尋半徑的縮減，進行 MRI 的分類。在這部份，處理的速度比 FCM 快上許多，分類效果也較佳，因為 FCM 每疊代一次要計算全部歸屬程度的部分，是相當耗時，而蜜蜂只需搜尋範圍內的資料。此外在空間上有雜訊的部份，會被其他蜜蜂找到更好食物源而淘汰，比較不會直接影響到整張影像的權重。

以眼睛分割部份，建構 entropy 於粒子群最佳化演算法找出門檻值，並加入均勻度做群集中心與其區域內成員之計算，以取得更好的門檻值。在記憶體空間使用量，只需用一組粒子群陣列，傳統上每一

維度空間，需使用一組粒子群，因此當分群數目越多，所使用的陣列空間就越大。透過霍式轉換參數空間，以疊代方式去尋找出最佳的圓形之半徑，而求解出圓心，最後完成瞳孔分割。演算法開發是一個重要步驟，可以幫助解決許多問題或是加強效能，在記憶體使用量減少、速度上有突破性的提升。

5.2 未來展望

本論文之研究主要將其成果應用於實務上之醫學影像方面及照相機功能的精進，在這科技發達的時代，晶片設計、嵌入式系統的發展非常快速，讓使用者越來越便利，若能夠把白平衡處理方法，加入在拍攝之後的自動偵測，也就是拍攝到的畫面偵測到色偏，會立即詢問使用者是否做校調來還原正常色彩，可以增加許多便利性，省去很多的後製的處理。

在醫學影像方面，把分割出的眼睛影像，由醫生做出專業的判斷病變部份的位置與程度，進行資料庫統計與訓練，完成專家系統，之後便可以協助醫生，做迅速的初步診斷。

參考文獻

[1] Dongju Liu, Jian Yu, “Otsu method and K-means,” Hybrid Intelligent System, vol. 1, pp. 344-349, 2009.

[2] Huiyu Zhou, Gerald Schaefer “Anisotropic mean shift based fuzzy c-mean segmentation of dermoscopy images,” IEEE JOURNAL OF SELECTED TOPICS IN SIGNAL PROCESSING, vol. 3, no. 1, pp. 26 - 34, 2009.

[3] M. Awad, K.Chehdi, A. Nasri, “Multi-component image segmentation using a hybrid dynamic genetic algorithm and fuzzy C-means,” Image Processing, IET, vol. 3, pp. 52-62, 2009.

[4] M. S. Yang, Y. J. Hu, K. C. R. Lin, and C. C. L. Lin, “Segmentation techniques for tissue differentiation in MRI of ophthalmology using fuzzy clustering algorithms,” Magn. Reson. Imaging, vol. 20, pp. 173-179, 2002.

[5] M. N. Ahmed, S. M. Yamany, N. Mohamed, A. A. Farag, T. Moriarty, “A modified fuzzy c-means algorithm for bias field estimation and segmentation of MRI data,” IEEE Trans Med Imaging, vol. 21, pp. 193-199, 2002.

[6] Nikhil R. Pal and James C. Bezdek “On Cluster Validity for the Fuzzy c-Means Model”, IEEE Transactions Fuzzy System, vol.3, pp. 370-379, 1995.

[7] X. Wang, Y. Wang, L. Wang, “Improving fuzzy c-means clustering based on feature-weight learning,” Pattern Recognit Lett, vol. 25, pp. 1123-1132, 2004.

[8] J. Kittler, J. Illingworth, “Minimum error threshold,” Pattern Recognition, vol. 19, lssue 1,pp. 41-47,1986.

[9] Madhubanti Mairta, Amitava Chatterjee “A hybrid cooperative-comprehensive learning based PSO algorithm for image segment using multilevel threshilding,” Expert System with Applications, vol. 34, pp. 1341-1350, 2008.

[10] Cheng-Lun Chen; Shao-Hua Lin; , "Automatic white balance based on estimation of light source using fuzzy neural network," IEEE Conference on Industrial Electronics and Applications, pp.1905-1910,May 2009.

[11] Lam, E.Y.; , "Combining gray world and retinex theory for automatic white

balance in digital photography", Proceedings of the Ninth International Symposium on Consumer Electronics, pp. 134- 139, June 2005

[12] Hong-Kwai Lam; Au, O.S.; Chi-Wah Wong; , "Automatic white balancing using standard deviation of RGB components", Proceedings of the International Symposium on Circuits and Systems, vol.3, pp. 921-924, May 2004

[13] Jun-yan Huo; Yi-lin Chang; Jing Wang; Xiao-xia Wei; , "Robust automatic white balance algorithm using gray color points in images", IEEE Transactions on Consumer Electronics, vol.52, no.2, pp. 541- 546, May 2006

[14] Ansel Adams, "The Negative", Ansel Adams Photography, Book 2, Little Brown and Company; Bulfinch.

[15] Joseph Chiang, "Gray World Assumption", PSYCH221/EE362 curse project, Department of Psychology, Stanford University, U.S.A. 1999.

[16] Daniel J. Jobson, Zia-ur Rahman, Glenn A. Woodell, "A Multiscale Retinex for Bridging the Gap Between Color Images and the Human Observation of Scenes", IEEE Transactions on Image Processing, Vol. 6, No. 7, pp. 965-976, July. 1997

[17] EH Land, JJ McCANN "Lightness and retinex theory", Journal of the Optical society of America, Vol. 61, No. 1, pp.1-11 1971.

[18] Bo Zhao, Zhongxiang Zhu, Enrong Mao, Zhenghe Song, "Image Segmentation Based on Ant Colony Optimization and K-Means Clustering", Automation and Logistics, 2007 IEEE International Conference on, pp. 18-21 Aug. 2007.

[19] James Kennedy, Russell Eberhart, "Particle Swarm Optimuzation", IEEE International Conference on Neural Networks, pp. 1942 - 1948 Dec.1995

[20] Russell C. Eberhart, Yuhui Shi, "Particle Swarm Optimization: Developments, Applications and Resources", Evolutionary Computation, Vol. 1, pp.81-86, 2001

[21] Madhubanti Mairta, Amitava Chatterjee "A hybrid cooperative-comprehensive learning based PSO algorithm for image segment using multilevel threshilding," Expert System with Applications, vol. 34, pp. 1341-1350, 2008.

[22] Tang Hongmei, Wu Cuixia, Han Liying, Wang Xia, "Image segment based on Improved PSO" Computer and Communication Technologies in Agriculture Engineering, pp. 191-194, 2010.

[23] Chengbo Yu, Jin Zhang , Yimeng Zhang, "Maximum entropy image segmentationis based on improved QPSO algorithm", Electronic and Mechanical

Engineering and Information Technology (EMEIT), pp. 12-14 Aug. 2011.

[24] B. Basturk, D. Karaboga, “An artificial bee colony (ABC) algorithm for numeric function optimization,” IEEE Swarm Intelligence Symposium, Indiana, USA, 2006.

[25] D. Karaboga, B. Basturk, “Artificial bee colony (abc) optimization algorithm for solving constrained optimization problems,” LNCS: Advances in Soft Computing: Foundations of Fuzzy Logic and Soft Computing, vol. 4529, pp. 789-798, Springer-Verlag, 2007.

[26] D. Karaboga, B. Basturk, “A powerful and efficient algorithm for numerical function optimization: artificial bee colony (ABC) algorithm,” Journal of Global Optimization, vol. 39, pp. 459-171, 2007.

[27] D. Karaboga, “An idea based on honey bee swarm for numerical optimization,” Technical Report-TR06, Erciyes University, Engineering Faculty, Computer Engineering Department, 2005.

[28] B. Basturk, D. Karaboga, “An artificial bee colony (ABC) algorithm for numeric function optimization,” IEEE Swarm Intelligence Symposium, Indiana, USA, 2006.

[29] Hough, P. V. C., “Method and means for recognizing complex patterns,” US Patent 3069654, December 1962.

[30] Duda, R. O., and Hart, P. E., “Use of the Hough transformation to detect lines and curves in pictures,” Communications of the ACM, vol. 15, pp.11-15, Jan.1972

附錄

發表論文:

國際期刊：

[1] Jzau-Sheng Lin, **Shou-Hung Wu**, "Fuzzy Artificial Bee Colony System with Cooling Schedule for the Segmentation of Medical Images by Using of Spatial Informatio," International Journal of World Academy of Science Engineering and Technology (ISSN 2010-376X) (EI) (已被接受)

會議：

[1] Yu-Yi Liao, Jzau-Sheng Lin, **Shou-Hung Wu** and Shen-Chuan Tai, "Automatic white balance using simple statistics with zone system", The 18thNational Conference on Fuzzy Theory and Its Applications (中華民國第十八屆模糊理論及其應用研討會), pp. 470-475, Dec 2010.

[2] Jzau-Sheng Lin, **Shou-Hung Wu**, "A PSO-based Algorithm with Subswarm Using Entropy and Uniformity for Image Segmentation," International Congerence on Genetic and Evolutionary Computing(已被接受)

2012 The Fifth International Conference on Intelligent Computation Technology and Automation

(ICICTA 2012)

Dear Author,

Congratulations! Your paper has been accepted by the International Conference on the Fifth International Conference on Intelligent Computation Technology and Automation (ICICTA 2012), and it will be published by the international journal World Academy of Science, Engineering and Technology (ISSN 2010-376X，EI 检索 JA 型）. Please verify the following items to ensure their accuracies:

(1) Please confirm the following:

Paper ID: 888

Title: Fuzzy Artificial Bee Colony System with Cooling Schedule for the Segmentation of Medical Images by Using of Spatial Information

Contact Authors: Jzau-Sheng Lin, Shou-Hung Wu

E-mail: jslin@ncut.edu.tw

(2) Your paper will NOT be published unless your registration be completed during scheduled date.

Thank you again for your contribution to the ICICTA2012, and we look forward to seeing you in Zhangjiajie.

Best regards,
ICICTA 2012

ICICTA2012 会务组

Fuzzy Artificial Bee Colony System with Cooling Schedule for the Segmentation of Medical Images by Using of Spatial Information

Jzau-Sheng Lin and Shou-Hung Wu

Abstract**—**In this paper, segmentation of medical images using a fuzzy artificial bee colony algorithm with a cooling schedule is created. In this paper, we embed fuzzy inference strategy into the artificial bee colony system to construct a segmentation system named Fuzzy Artificial Bee Colony System (FABCS). A conventional FCM algorithm did not utilize the spatial information in the image. We set a local circular area with a variable radius by using a cooling schedule for each bee to search suitable cluster centers with the FCM algorithm in an image. The cluster centers can be calculated by each bee with the membership states in the FABCS and then updated iteratively for all bees in order to find near-global solution in MR image segmentation. The proposed FABCS found the cluster centers with local spatial information in stead of global pixels' intensities. In the simulation and real medical-image segmentation results, the proposed FABCS network can reserve the segmentation performance.

Keywords**—**FCM, Medical Image segmentation, Artificial bee colony system.

I. Introduction

MAGNETIC resonance imaging (MRI) is the preferred imaging modality for examining many neurological conditions which alter the shape, volume, and distribution of brain tissue. Reliable measurement can be performed by using image segmentation for these alterations. Several approaches [1-5] have been developed to automate such measurements by segmentation. However, some of these methods do not take advantage of the MRI images. The analysis of such medical images can be accomplished by using supervised or unsupervised classification methods. In supervised classification strategies, the region of interest (ROI) is defined by the associated human interaction and the approach trains on the ROI and flags each pixel in the scenes associated with a given signature. However, a supervised approach is very time-consuming for large volumes and heavy biases may be introduced by an unskilled technician. The unsupervised classification methods classify the target data sets without the aid of training sets, but a post-processing step is required to correct misclassified pixels.

The fuzzy clusters are generated by dividing the training samples in accordance with the membership function. The fuzzy c-means (FCM) [3-5] algorithm used the memberships of a training sample across clusters that sum up to 1, which means the different grades of a training sample are shared by distinct clusters. Membership state is important for the correct feature of data substructure in clustering problem. If a training sample has been classified to a suitable cluster, then membership is a better constraint for which the training sample is closest to this cluster. In this paper, we embedded the FCM strategy into an artificial bee colony to construct the FABCS and used to the application of Medical MRI images segmentation.

Swarm intelligence is an interesting research field that models the population of interacting agents or swarms that can be able to organize by themselves. Swarm intelligence systems are popular in the natural world such as immune system, ant colony, a flock of birds or bacterial foraging. Artificial bee colony algorithm, an optimization strategy based on the intelligent behavior of honey bee swarm, is one of the swarm intelligence systems.

Artificial Bee Colony (ABC) algorithm was proposed by Karaboga [6-9] for optimizing numerical problems. The algorithm simulates the intelligent foraging behavior of honey bee swarms. It is a robust stochastic optimization algorithm. Several well-known heuristic strategies such as Genetic Algorithm (GA) [10], Differential Evolution (DE) [11], Particle Swarm Optimization (PSO) [12-13] on constrained and unconstrained problems were proposed to compare the performance with the ABC algorithm.

On an image, the pixels are highly correlated one another. That is the pixels in the neighborhood own nearly the same feature data. Therefore, the spatial relationship of neighboring pixels is an important characteristic that can be of great aid in imaging segmentation. In this paper, we randomly put several bees into an image to find cluster centers on a local circular area with a fixed radius by using of FCM algorithm with a cooling schedule to decrease the searching radius iteratively. Then we select the suitable cluster centers iteratively with the bees' searching strategy till the terminal condition is met. The purpose of selecting local area is to reserve the local feature data to segment an image effectively.

Jzau-Sheng Lin, is with the National Chin-Yi University of Technology, Taichung, Taiwan, R. O. C. (phone: 886-4-23924505; fax: 886-4-23917426; e-mail: jslin@nuct.edu.tw).

Shou-Hung Wu, is is with the National Chin-Yi University of Technology, Taichung, Taiwan, R. O. C. (phone: 886-4-23924505; fax: 886-4-23917426; e-mail: jslin@nuct.edu.tw).

II. Clustering Techniques

Clustering techniques are the process of recognizing clusters in testing samples based on some similarity measures. Distance measurement is generally used for evaluating similarities between training data. Hard c-means (HCM) is the simplest and most commonly used clustering method. It represents each cluster by the mean value of the data points within the cluster. In a target space, given *n* objects, the HCM allocate each object to one of *C* clusters and minimize the sum of squared Euclidean distances between each object and the center of the cluster belonging to every such allocated object. The object function of HCM is defined as Eq. (1)

$$J_{HCM} = \frac{1}{2}\sum_{x=1}^{n}\sum_{i=1}^{c}\left\| z_x^i - \varpi_i \right\|^2 \quad (1)$$

where z_x^i is the *x*th data point belonging to the *i*th cluster, ϖ_i is the cluster center of the *i*th cluster, *c* is the number of clusters and *n* is the number of data points in cluster *i*.

First, the HCM takes *c* randomly selected pixels and makes them the initial centers of the *c* clusters being formed. And, this algorithm assigns each pixel to the cluster with *c*entre closest to it. Then, the centers of the *c* clusters are recalculated, and the pixels are redistributed. This step is repeated for a specified number of iterations or until there is no change to the membership of the clusters over two successive iterations. It is known that the HCM algorithm maybe trap at local optimal solutions, depending on the choice of the initial cluster centers.

The theory of fuzzy logic provides a mathematical environment to capture the uncertainties as the same human cognition processes. The fuzzy clusters are generated by dividing the training samples in accordance with the membership functions. A component in the membership matrix denotes the grade of membership that a training sample belongs to a cluster. Real data unavoidably involves some noises, either from interface due to noise sources which exist in the natural environment or from the equipment itself. Therefore, the drawback of FCM will be significant while processing improper data. The purpose of the FCM approaches, like the conventional clustering techniques, is to group data into clusters or similar items by minimizing a least-squared error measure. The FCM algorithms used the probabilistic constraint to enable the memberships of a training sample across clusters to sum up to 1, which means the different grades of a training sample are shared by distinct clusters but not as degrees of typicality. In contrast, each component generated by the FCM corresponds to a dense region in the data set. Each cluster is independent of the other clusters in the FCM strategy. The objective function of the FCM can be formulated as

$$J_{FCM} = \frac{1}{2}\sum_{x=1}^{n}\sum_{i=1}^{c}\mu_{x,i}^{m}\left\| z_x - \varpi_i \right\|^2 \quad (2)$$

where Memberships and centroids are defined as

$$\mu_{x,i} = \left(\sum_{\ell=1}^{c} \frac{(\left\| z_x - \varpi_i \right\|^2)^{1/(m-1)}}{(\left\| z_x - \varpi_\ell \right\|^2)^{1/(m-1)}} \right)^{-1}, \; x = 1, 2, \ldots, n, \; i = 1, 2, \ldots, c, \quad (3)$$

and

$$\varpi_i = \frac{1}{\sum_{y=1}^{n}(\mu_{y,i}^{m})}\sum_{x=1}^{n}(\mu_{x,i}^{m})z_x \quad (4)$$

The value *m*, so-called fuzzification parameter, would alleviate the noise effect when the centroids are computed. The larger the value of *m*, the greater will be the sensitivity to noise.

III. Artificial Bee Colony (ABC) algorithm

A colony of honey bees can extend itself over long distances in order to search food sources. The foraging process is begun in a colony by scout bees to search for plentiful flower patches. More bees visit flower patches with large amounts of pollen or nectar that can be collected with less effort, whereas patches with less pollen or nectar attract fewer bees. During the warm season, a colony continues its foraging process, keeping a percentage rate of the population as scout bees. When scout bees return to the hive, they found a patch rated above a certain quantity threshold deposit their nectar or pollen and go to the "dance floor" to perform a "waggle dance" dance. This special dance is essential for bees' communication in a colony, and includes three kind of information regarded a flower patch: its distance from the hive, the direction in which it will be found, and its quantity rating. These information help the colony to assign its bees to flower patches accurately, without any guide or map. This dance enables the colony to calculate the relative value of different patches according to both the quantity of the food they supply and the amount of energy needed to collect it. After waggle dancing on the dance floor, the scout bees go back to the flower patches with follower bees that were waiting inside the hive. More follower bees are assigned to more hopeful patches. This process allows the colony to collect food efficiently and quickly. While harvesting from a patch, the bees monitor their food level. When bees return to the hive, it is necessary to decide the next waggle dance. If the patch is always good enough as a food source, it will be noticed waggle dance and more bees will be recruited to that source. The conventional ABC algorithm is described as

1. Load the training patterns.
2. Initialize the bees' population.
2. calculate the fitness of the population.
3. While (stopping condition is not met)
//Forming new population.
4. Select sites for neighborhood search.
5. Recruit bees for selected sites (more bees for the best *e* sites) and evaluate fitness.
6. Select the fittest bee from each site.

7. Assign remaining bees to search randomly and evaluate their fitnesses.
8. End While.

IV. The Proposed Fuzzy Artificial Bee Colony System

In an image, one of the important characteristics is that neighboring pixels are greatly correlated. In other words, similar feature values are possessed by these neighboring pixels. The spatial information is important in clustering problem, but it is not considered in a standard FCM algorithm.

In the proposed FABCS, the clustering is a two-pass process each iteration. In the first pass, the scout bees were randomly put in the space domain of a target image. And the spatial information are searched by using of the function of ABC. The second pass is the same as that in standard FCM to calculate the membership function in the spatial domain for each scout bee. Then, the local cluster process is stopped when the maximum difference between two cluster centers at two successive processes is less than a threshold. In order to find near-optimal solution efficiently, we embedded a cooling schedule to narrow the area iteratively for the candidate bees to recruit bees for the best sites and poor sites randomly. In this paper, the decrement function shown as in Eq. 5 [14] is used as cooling schedule.

$$r(t) = \frac{1}{\varepsilon + 1}\left[\varepsilon + \tanh(w)^t\right] r(t-1) \tag{5}$$

where r is the radius of the searching circle for a candidate bee and w a small constant which closes to unit as well as ε is also a constant. Additionally, t is the iterations. Lin [14] showed that Eq. (5) can result in a faster decrement speed than that resulted from the conventional decrement functions. In Eq. (5), a suitable value of w can be set as $0.0 < w < 1.0$. A smaller value of w was selected; the convergent time can speed up but fall in a local minimum easily. The flowchart of the proposed FABCS algorithm is shown as in Fig. 1. After the convergence, defuzzification is applied to assign each pixel to a specific cluster for which the membership is maximal.

V. Experimental Results

In order to show the performance, all simulations are executed with the interpreter language of MATLAB in a personal computer. The performances for two frequently-used methods i.e., the HCM and FCM, and the proposed FABCS algorithm were first compared in the simulation study. And, the real medical images were segmented by the proposed FABCS algorithm.

A. Computer simulations

The computer generated image was made up of seven overlapping ellipses. Each ellipse represents one structural area of tissue. From the periphery to the center, they were the background (BKG, gray level = 30), skin or fat *(S/F,* gray level = 75), gray matter (GM, gray level = 120), white matter (WM, gray level = 165), and cerebrospinal fluid (CSF, gray level = 210), respectively. The gray levels for each region were set to a constant value. In addition, the noise of uniform distribution with the gray levels ranging from -*K* to *K* was then added to the simulated phantoms. The noise level *K* for different cases was set to be 15, 20, 25, and 30, respectively.

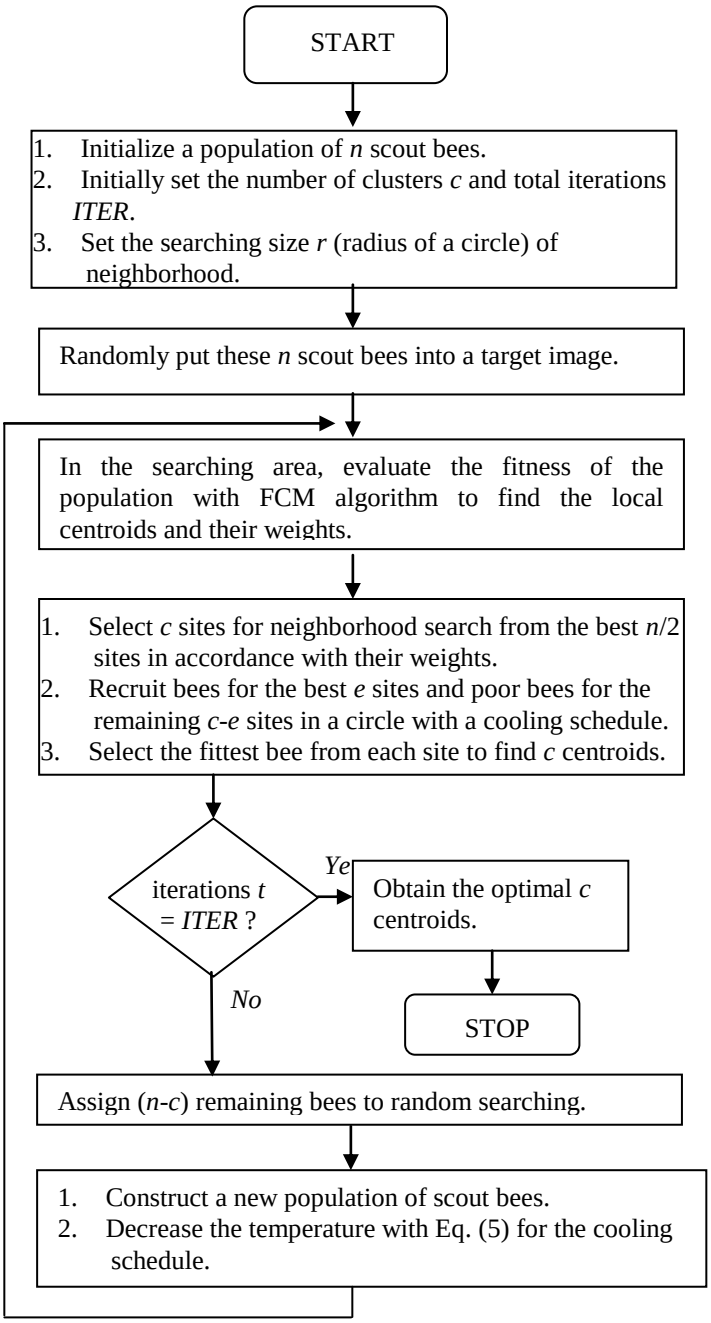

Fig. 1 The flowchart of the proposed FABCS algorithm.

The segmented images for the test phantom are shown in Figs. 3 - 5. The accuracy for the four image segmentation methods described above are listed in TABLEs I-IV. From these tables, they can easily be seen that all the methods would extract the objects very accurately for the noise levels K = 15 and 20, respectively. For larger noise levels of K = 25 and 30, the proposed FABCS algorithm would be more accurate in image segmentation than the other three methods. An average accuracy is 92.12 % for K = 25, and 80.08% for K = 30 may be achieved

using the FABCS approach.

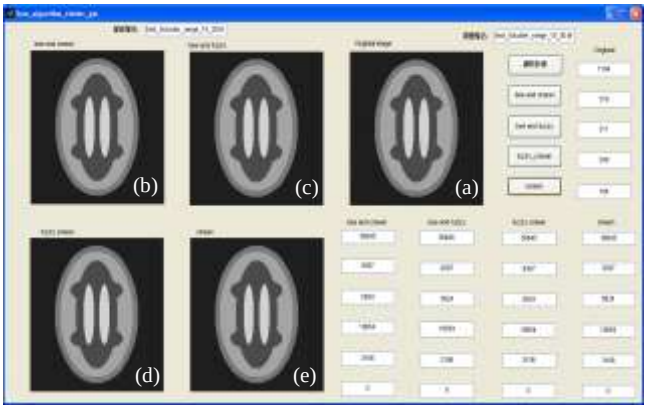

Fig. 2 The test phantom of four objects with added noise *(k*< = 15*)* in (a) and the result images shown in (b), (c), (d) and (e) using the ABC+HCM, FABCS, FCM, and HCM methods, respectively.

TABLE I
THE SEGMENTATION PERFORMANCE FOR HCM, FCM, BEE + HCM, AND THE PROPOSED FABCS ALGORITHM USING THE TEST PHANTOM WITH *k* <= 15.

Simulate	Actual pixels	HCM	FCM	Bee + HCM	FABCS
Background	36645	36645	36645	36645	36645
S/F	9307	9307	9307	9307	9307
GM	5824	5824	5824	5824	5824
WM	10654	10654	10654	10654	10654
CSF	3106	3106	3106	3106	3106
Average error		0%	0%	0%	0%

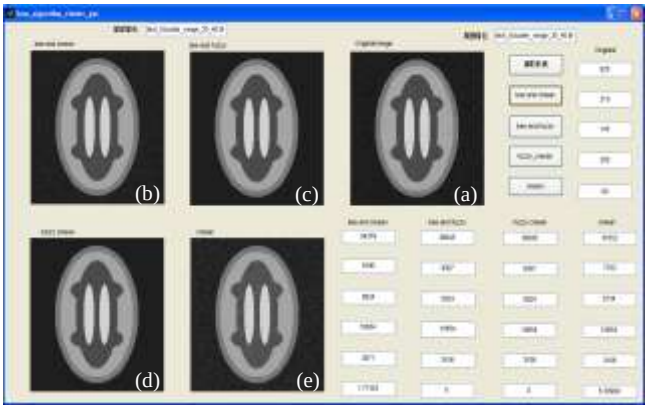

Fig. 3 The test phantom of four objects with added noise *(k*< = 20*)* in (a) and the result images shown in (b), (c), (d) and (e) using the ABC+HCM, FABCS, FCM, and HCM methods, respectively.

B. Real MRI image segmentation

The second experiment showed the segmentation performance with medical images. These real medical images in Figs. 6 and 7 are acquired with T_2-weighted sequences. The acquisition parameters with different repetition time (*TR*) and echo time (*TE*) are *TR*/*TE* = 2500ms/75ms for Figs. 6(a) and 6(b).

In Fig. 7(a), different regions were classified by the FABCS from Fig. 1 such as background (BKG), gray matter (GM), white matter (WM), and cerebral spinal fluid (CSF), respectively.

The next example is a medical image classification in head MR image of a patient diagnosed with cerebral infarction. Fig. 7(b) shows 5 regions BKG, GM, WM, CSF, and cerebral infarction (CI) classified by the proposed FABCS respectively. The abnormal region with CI classified by the FABCS can be clearly classified in Fig. 7(b).

TABLE II
THE SEGMENTATION PERFORMANCE FOR HCM, FCM, BEE + HCM, AND THE PROPOSED FABCS ALGORITHM USING THE TEST PHANTOM WITH *k* <= 20.

Simulate	Actual pixels	HCM	FCM	Bee + HCM	FABCS
Background	36645	31652	36645	34379	36645
S/F	9307	7783	9307	9190	9307
GM	5824	5734	5824	5824	5824
WM	10654	10654	10654	10654	10654
CSF	3106	3106	3106	3071	3106
Average error		6.31%	0%	1.71%	0%

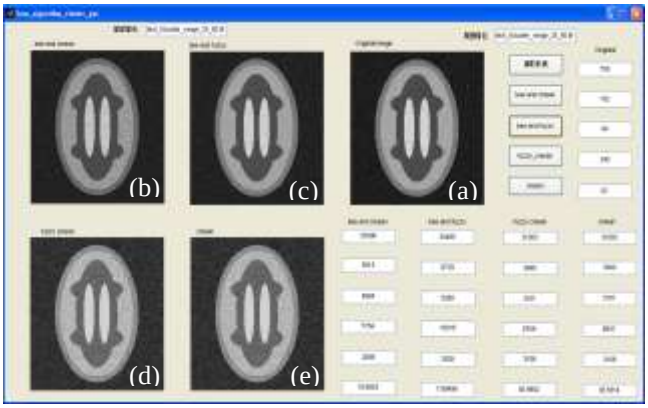

Fig. 4 The test phantom of four objects with added noise *(k*< = 25*)* in (a) and the result images shown in (b), (c), (d) and (e) using the ABC+HCM, FABCS, FCM, and HCM methods, respectively.

TABLE III
THE SEGMENTATION PERFORMANCE FOR HCM, FCM, BEE + HCM, AND THE PROPOSED FABCS ALGORITHM USING THE TEST PHANTOM WITH K <= 25.

Simulate	Actual pixels	HCM	FCM	Bee+HCM	FABCS
Background	36645	21083	21083	33400	33400
S/F	9307	3840	3840	9215	8739
GM	5824	3101	3101	4084	5268
WM	10654	6931	6709	7784	10018
CSF	3106	3106	3106	2089	2828
Average error		36.58%	37.0%	19.88%	7.88%

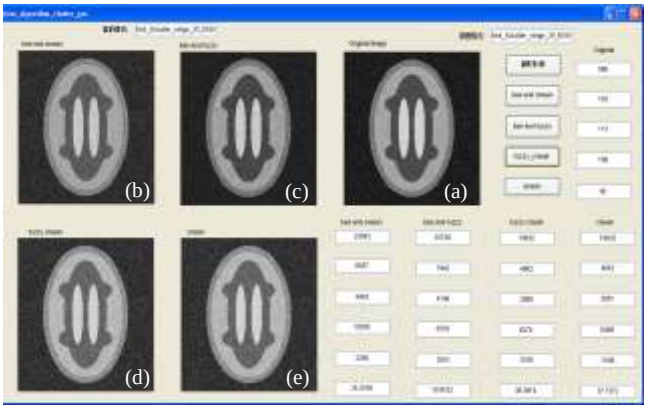

Fig. 5 The test phantom of four objects with added noise *(k*< = 30*)* in (a) and the result images shown in (b), (c), (d) and (e) using the ABC+HCM, FABCS, FCM, and HCM methods, respectively.

TABLE IV
THE SEGMENTATION PERFORMANCE FOR HCM, FCM, BEE + HCM, AND THE PROPOSED FABCS ALGORITHM USING THE TEST PHANTOM WITH k <= 30.

Simulate	Actual pixels	HCM	FCM	Bee+HCM	FABCS
Background	36645	19932	19932	23593	32738
S/F	9307	4062	4062	6057	7442
GM	5824	3061	2980	4403	4199
WM	10654	6469	6274	10306	8333
CSF	3106	3106	3106	2395	2510
Average error		37.74%	38.38%	24.22%	19.92%

VI. CONCLUSIONS

An artificial bee colony system by means of fuzzy c-means with cooling schedule called Fuzzy Artificial Bee Colony System (FABCS) is proposed to medical image segmentation in this paper. Every bee in the proposed FABCS owns a searching circular area with a variable radius decreased by a cooling schedule iteratively. In the searching area, the pixels classified several clusters by means of the FCM strategy to find the best local cluster centroids. Finally, the clusters' cnetroids for each bee are integrated to merge near-global centroids when the iterations were terminated. In order to show the classification performance, the test phantom images can be classified into more suitable clusters by the proposed FABCS than the other strategies. In the application of MRI medical image classification, The promising results can be obtained by using of the proposed FABCS.

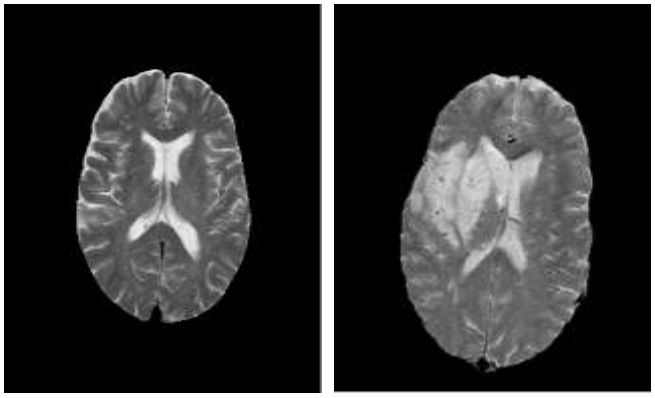

(a) normal with *TR*/*TE* = 2500ms/75ms (b) cerebral-infarction with *TR*/*TE* = 2500ms/75ms

Fig. 6 T_2-weighted brain Images

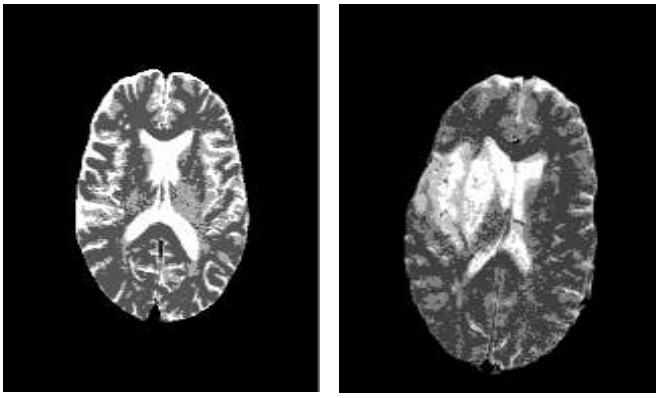

(a) (b)

Fig. 7 classified results of Figs. 1 and 2 by means of the proposed FABCS; (a) 4 regions with background (BKG), gray matter (GM), white matter (WM), and cerebral spinal fluid (CSF), respectively; (b) 5 regions with BKG, GM, WM, CSF, and cerebral infarction (CI), respectively.

ACKNOWLEDGMENT

This work was supported by the National Science Council, TAIWAN, under the Grants NSC99-2221-E-167-010 -.

REFERENCES

[1] J. –S. Lin "Annealed chaotic neural network with nonlinear self-feedback and its application to clustering problem," *Pattern Recognition*, vol. 34, no. 5, pp. 1093-1104, 2001.

[2] M. S. Yang, Y. J. Hu, K. C. R. Lin, and C. C. L. Lin, "Segmentation techniques for tissue differentiation in MRI of ophthalmology using fuzzy clustering algorithms," *Magn. Reson. Imaging*, vol. 20, pp. 173-179, 2002.

[3] X. Wang, Y. Wang, L. Wang, "Improving fuzzy c-means clustering based on feature-weight learning," *Pattern Recognit Lett*, vol. 25, pp. 1123-1132, 2004.

[4] M. N. Ahmed, S. M. Yamany, N. Mohamed, A. A. Farag, T. Moriarty, "A modified fuzzy c-means algorithm for bias field estimation and segmentation of MRI data," *IEEE Trans Med Imaging*, vol. 21, pp. 193-199, 2002.

[5] N. S. Lyer, A. Kandel, M. Schneider, "Feature-based fuzzy classification for interpretation of mammograms," *Fuzzy Sets Syst*, vol.114, pp. 271-280, 2002.

[6] D. Karaboga, "An idea based on honey bee swarm for numerical optimization," Technical Report-TR06, Erciyes University, Engineering Faculty, Computer Engineering Department, 2005.

[7] B. Basturk, D. Karaboga, "An artificial bee colony (ABC) algorithm for numeric function optimization," *IEEE Swarm Intelligence Symposium*, Indiana, USA, 2006.

[8] D. Karaboga, B. Basturk, "Artificial bee colony (abc) optimization algorithm for solving constrained optimization problems," LNCS: Advances in Soft Computing: Foundations of Fuzzy Logic and Soft Computing, vol. 4529, pp. 789-798, Springer-Verlag, 2007.

[9] D. Karaboga, B. Basturk, "A powerful and efficient algorithm for numerical function optimization: artificial bee colony (ABC) algorithm," *Journal of Global Optimization*, vol. 39, pp. 459-171, 2007.

[10] A.Kumar Dey, S. Saha, A. Saha, and S. Ghosh, "A Method of Genetic Algorithm (GA) for FIR Filter Construction: Design and Development with Newer Approaches in Neural Network Platform," *Int. J. of Advanced Computer Science and Applications*, vol. 1, no. 6, p.87-90, 2010.

[11] S. Paterlini, T. Krink, "Differential evolution and particle swarm optimization in partitional clustering," *Comput. Stat. Data Anal.* vol. 50, pp.1220-1247, 2006.

[12] M. Omran, A. Engelbrecht, A. Salman, "Particle swarm optimization method for image clustering," *Int. J. Pattern Recognit. Artif. Intell.*, vol. 19, no. 3, pp. 297-322, 2005.

[13] J. -S. Lin, Y.-Y. Chang and S. –Y. Huang, "2-D filters designed by using singular-value decomposition based on an annealed particle swarm optimization," *J. of Technology*, vol. 24, no.1, pp.69-75, 2009.

[14] J.-S. Lin, "Image vector quantization using an annealed Hopfield neural network," *Opt. Eng.*, vol. 38, pp. 599-604, 1999.

Jzau-Sheng Lin was born at Taichung, Taiwan, R.O.C. in 1956. He is a Professor of the Department of Computer Science and Information Engineering at National Chin-Yi University of Technology, Taichung, Taiwan, R. O. C. He received the B.S. degree in electronic engineering from Taiwan University of Science and Technology in 1980, the M.S. and Ph.D degrees in electrical engineering from National Cheng Kung University in 1989 and 1996 respectively. And he is a Director of TFSA now.

Professor Lin was a member of the SPIE. His research interests involve BCI, neural network, image processing, pattern recognition, and medical image analysis

Shou-Hung Wu, is a graduate student. His research interests involve neural network and image processing.

Automatic white balance using simple statistics with zone system

Yu-Yi Liao[1] Jzau-Sheng Lin[2] Shou-Hung Wu[3] Shen-Chuan Tai[4]

[1, 4] Institute Computer and Communication Engineering

National Cheng Kung University

E-mail:liao.yuyi@gmail.com, sctai@mail.ncku.edu.tw

[2, 3] Department of Computer Science and Information Engineering

National Chin-Yi University of Technology

E-mail:jslin@ncut.edu.tw, happy_like92@yahoo.com.tw

摘要

當處理彩色影像時因為不同光源之色溫導致影像產生色偏時，白平衡即是改善這問題很重要的步驟。分區曝光系統將影像所能表現的所有色階分為11區，從第一區0的全黑到最後一區 X 的全白，而中間區 V 是反射率為18%的中灰色影調。在這篇文章中，我們提出利用簡單的影像統計方法和分區曝光系統的概念經由 YCbCr 色彩空間的色階分佈圖以達成自動白平衡的功能。經實驗證實此方法可以有效率的改善影像色偏的問題。

關鍵詞：自動白平衡，分區曝光系統。

Abstract

White balancing is an important step to correct the color value of pixels under varied color temperature of illuminations for color image processing. The Zone system divides the full tonal capabilities of the display medium into eleven zones ranging from zone 0 (pure black) to zone X (pure white), with zone V representing subjective middle gray which corresponding to 18% reflectance. In this paper, we utilize simple image statistic and the concept of the zone system through the histogram of YCbCr color space to solve the color cast problem. Experimental results exhibit that the proposed method gets the fine image.

Keywords：automatic white balance, zone system.

1. Introduction

Light is one of important factor to affect the quality of color images. Color temperature gives a way to represent the spectrum of colors in light and is recorded on the pixels of image thought the camera sensor. A white object will appear nature white as daylight, but it will appear reddish color or bluish color under low color temperature or high color temperature. The human eyes have a marvelous ability to adjust different light conditions due to the "color constancy" of the vision perception. The digital camera sensor or photo image processing utilizes the white balance algorithm to remove the impractical color casts, so that objects which appear white in human eyes are rendered similar white in color image. Therefore, several methods have been proposed in the literatures for automatic white balance in the past years [3-10, 13-15].

Gray world assumption is one of the commonly known white balance methods [7]. It exhibits that an image can be found the average value of the primary color components (RGB) and then uses the average to determine an overall gray value. Nevertheless, it will lose the completeness of color when the certain color dominates. The Retinex theory is base on the visual color constancy and to remove the unfavorable illumination effects from a given image [5]. It computes independently the mean value of primary color of relative reflectance through the randomness and number of paths. It has some shortcomings such as hallows and iterative solution. Multi-Scale Retinex (MSR) balances dynamic range compression, color consistency and color rendition [4]. MSR causes the color deviation while RGB proportion is out of balance. The color temperature is not crisp but fuzzy. Therefore, the white balance method with the fuzzy logic rules is proposed [14]. It minimizes the color temperature difference of various light sources and then to determinate the color parameters for digital camera. The automatic white balance with fuzzy neural network is also proposed [3]. The training phase of the fuzzy neural network predicts pixel-level color temperatures, and then the testing phase estimates the color temperature value from the image pixels to achieve the white balance.

The Zone system, formulated by Ansel Adams [1], is a photographic technique for providing photographers with a systematic method to determine optimal film exposure and development. In this paper, a new simple and efficient method is proposed, which used the concept of Zone system to define the unrealistic color casts and then the simple statistic to

regulate the RGB gains by the adjusted pixels.

The rest of the paper is organized as follows. Section 2 describes the Zone system and histogram of YCbCr color space. Following section exhibits the proposed methods. Section 4 presents the experimental results. Finally, section 5 gives the conclusion.

2. The zone system and histogram of YCbCr color space

The quality of color image is depending on correct light source and the exposure. Ansel Adams, who is a famous photographer and environmentalist, develops the Zone system to determine the correspondence between portion of the scene and tones in the print [1]. The Zone system has been applied the display medium to describe images with the full tonal capabilities although it originated with black and white sheet film. The Zone system is divided the tonal gradation into eleven discrete zones, shown in Table 1, numbered 0 through X from dark to light. Each zone represents a doubling or halving of the luminance in the field of scene. Zone 0 is pure black, zone X is pure white, and Zone V is subjective middle gray, corresponding to reflectance of about 18%. Three zones are especially important: the zone III used to measure for the shadows for film, the zone V used for 18% middle gray exposure, and the zone VII used to measure the highlights for digital. Hence, the exposure of subject with a zone V, dark area within zone III and bright area within zone VII will be resulted in a mid-tone rendering in the final image.

A histogram is a graphical representation of the tonal distribution in an image. Each pixel in an image has a color which has been produced by some combination of the primary colors (RGB). The horizontal axis represents the brightness value ranging from 0 to 255 for digital color image with a bit depth of 8 bits and the vertical axis counts how many pixel are at each levels. In the proposed method, the histogram was divided equally 11 areas to represent the Zone system, illustrated in Figure 1.

The YCbCr color space is widely used in video compression standards (e.g. MPEG and JPEG) and digital photography systems since it is perceptually uniform [2]. Y is the luminance or brightness component, Cb and Cr is the blue-difference and red-difference chrominance components respectively. The following basic equations convert between RGB color space and YCbCr color space.

$$\begin{aligned} Y &= 0.299\,R + 0.587\,G + 0.114\,B \\ Cb &= -0.1687\,R - 0.3313\,G + 0.5B + 128 \\ Cr &= 0.5R - 0.4187\,G - 0.0813\,B + 128 \end{aligned} \quad (1)$$

$$\begin{aligned} R &= Y + 1.402(Cr - 128) \\ G &= Y - 0.34414(Cb - 128) - 0.71414(Cr - 128) \\ B &= Y + 1.772(Cb - 128) \end{aligned} \quad (2)$$

The equation (2) indicates that the gray pixel under the standard light source, its color value between the RGB and YCbCr color space have the following relation:

$$Y=R=G=B,\ Cb=Cr=128 \quad (3)$$

The values of Cb and Cr fall into the zone V and the color value of RGB and Y change correspondingly. Figure 2 shows the histogram of YCbCr under different color temperature. In each figure, M represents the mean which describes the central tendency of values of YCbCr. Figure 2 (a) shows that an image will appear reddish color under the tungsten light that is rich in reds and poor in blues, that is, the mean of Cr lies in brighter area (zone VII) and the mean of Cb lies in darker area (zone IV). On the other hand, Figure 2 (b) demonstrates the bluish image, downloaded from [11], which the mean of Cb and almost the Cb components locate in brighter area (zone VI) and the mean of Cr locates at darker area (zone V). Finally, figure 2 (c) presents the averages of all YCbCr components locate in zone V to result the fine image downloaded form [12].

3. The proposed method

Generally, an automatic color balancing method is achieved by two steps such as illuminant estimation and actual adjusting. The proposed method also includes two steps. The first step is to determine the color temperature and adjusted pixels by estimating blue-difference and red-difference of all pixels in YCbCr color space. The second step is luminance and automatic color balance adjustment which can be accomplished through adjusted pixels as reference to calculate the RGB channel grains.

3.1. Color temperature and adjusted pixels estimation

First, an image is converted to YCbCr color space from RGB color space by equation (1). The Cb and Cr are examined to check the unrealistic color cast. Let an image $I(x,y)$ has size $M*N$, where x and y denote the indices of the pixel position. $I_y(x,y)$, $I_{Cb}(x,y)$ and $I_{Cr}(x,y)$ denote the luma component Y and two chroma components of Cb and Cr. We computed the average of three components as following equations

$$Y_{avg} = \frac{1}{MN}\sum_{x=1}^{M}\sum_{y=1}^{N} I_y(x,y)$$
$$Cb_{avg} = \frac{1}{MN}\sum_{x=1}^{M}\sum_{y=1}^{N} I_{Cb}(x,y) \quad (4)$$
$$Cr_{avg} = \frac{1}{MN}\sum_{x=1}^{M}\sum_{y=1}^{N} I_{Cr}(x,y)$$

In probability theory, Chebyshev's inequality guarantees that in any data sample differ from its mean by more then k standard deviations is less then or equal to K^{-2}. Therefore, we use the following equation to get the candidate of adjusted pixels.

$$I_{adjusted}(x,y) = Cb_{adjusted}(x,y) \wedge Cr_{adjusted}(x,y) \quad (5)$$

and

$$Cb_{adjusted}(x,y) = (I_{Cb}(x,y) - (Cb_{avg} + Cb_{ad})) < (\theta \times Cb_{ad})$$
$$Cr_{adjusted}(x,y) = (I_{Cr}(x,y) - (Cr_{avg} + Cr_{ad})) < (\theta \times Cr_{ad}) \quad (6)$$

where Cb_{ad} , Cr_{ad} and θ are the average deviation of Cb, the average deviation Cr and multiples respectively. θ gives the number of the candidate of adjusted pixels will be kept. It is set double or half of standard deviation of Cb and Cr because each zone represents a doubling or halving of the luminance in the field of scene.

3.2. Luminance and color balancing adjustment

According to equation (2), the luminance component (Y) affects all of three primary colors. Strictly speaking, the color cast is improved since the bright or middle areas are adjusted. Therefore, the equation (7) exhibits the top of 80% pixels will be kept after the arranging of candidate of adjusted pixels from high to low sequence.

$$I_{gain}(x,y) = I_y(I_{adjusted}(x,y)) \geq num \times 20\% \quad (7)$$

where num presents the number of the candidate of adjusted pixels.

The new gains of the R,G, and B channel are then adjusted by equation (8)

$$R_{new} = R_{old} * \frac{\min(Y)}{(mean(R(I_{gain}(x,y))) + \min(R(I_{gain}(x,y))))/2}$$
$$G_{new} = G_{old} * \frac{\min(Y)}{(mean(G(I_{gain}(x,y))) + \min(G(I_{gain}(x,y))))/2} \quad (8)$$
$$B_{new} = B_{old} * \frac{\min(Y)}{(mean(B(I_{gain}(x,y))) + \min(B(I_{gain}(x,y))))/2}$$

4. Experimental Results

This section we present the experiments were simulated in a Pentium-IV personal computer by using of the language Matlab and then compare the result with the Gray world and Retinex algorithms.

Figure 3 shows the mean of Cb and Cr lay in the same zone V after the reddish image was adjusted by the proposed method with the different θ . Figure 4 shows the mean of Cb and Cr also located in the same zone V after the bluish image was adjusted by the proposed method with the different θ . All of results exhibit that the luminance component Y will be changed when chrominance components Cb and Cr are adjusted. Finally, we compare the experimental results with other methods in Figures 5-6.

5. Conclusion

In this paper, we describe an automatic white balance method which is base on the principle of the Zone system and the simple image statistic for digital color image. The Zone system classifies the full tonal range in scenes and prints into eleven discrete zones and zone V is subjective middle gray corresponding to a reflectance of about 18%. The histogram show how the tones in the image maps onto the zone scale. Therefore, we apply the zone V in the histogram of YCbCr color space as the reference range to analyze and calculate the gain of RGB channels by simple statistic. Finally, we also get the fine outcome when comparing the adjusted results of the propose method with other automatic white balance methods.

Reference

[1] Ansel Adams, "The Negative", Ansel Adams Photography, Book 2, Little Brown and Company; Bulfinch.

[2] C.A. Poynton, A Technical Introduction to Digital video. John Wiley & Sons, 1996.

[3] Cheng-Lun Chen; Shao-Hua Lin; , "Automatic white balance based on estimation of light source using fuzzy neural network," IEEE Conference on Industrial Electronics and Applications, pp.1905-1910,May 2009.

[4] Daniel J. Jobson, Zia-ur Rahman, Glenn A. Woodell, "A Multiscale Retinex for Bridging the Gap Between Color Images and the Human Observation of Scenes", IEEE Transactions on Image Processing, Vol. 6, No. 7, pp. 965-976, July. 1997

[5] EH Land, JJ McCANN "Lightness and retinex theory", Journal of the Optical society of America, Vol. 61, No. 1, pp.1-11 1971

[6] Hong-Kwai Lam; Au, O.S.; Chi-Wah Wong; , "Automatic white balancing using standard deviation of RGB components", Proceedings of the International Symposium on Circuits and Systems, vol.3, pp. 921-924, May 2004

[7] Joseph Chiang, "Gray World Assumption", PSYCH221/EE362 curse project, Department of Psychology, Stanford University, U.S.A. 1999

[8] Jun-yan Huo; Yi-lin Chang; Jing Wang; Xiao-xia Wei; , "Robust automatic white balance algorithm

using gray color points in images", IEEE Transactions on Consumer Electronics, vol.52, no.2, pp. 541- 546, May 2006
[9] Lam, E.Y.; , "Combining gray world and retinex theory for automatic white balance in digital photography", Proceedings of the Ninth International Symposium on Consumer Electronics, pp. 134- 139, June 2005
[10] Po-Min Wang; Chiou-Shann Fuh; , "Automatic White Balance with Color Temperature Estimation", International Conference on Consumer Electronics, pp.1-2, Jan. 2007
[11] Test image: http://www.cs.sfu.ca/~colour/publications/IST-2000/index.html
[12] Test image: http://www.mathworks.co.uk/matlabcentral/fileexchange/23772
[13] Varsha Chikane and Chiou-Shann Fuh, “Automatic White Balance for Digital Still Cameras”, Journal of Information Science and Engineering, Vol.22, pp. 497-509, 2006
[14] Yung-Cheng Liu, Wen-Hsin Chan and Ye-Quang Chen, “Automatic White Balance for Digital Still Camera”, IEEE Transactions on Consumer Electronics, Vol. 41, No.3, p.p.460-466, Aug. 1995
[15] Zhong Jian; Yao Suying; Xu Jiangtao; , "Development and Implementation of Automatic White Balance Based on Luminance Compensation,", Second International Symposium on Intelligent Information Technology Application, vol.2, pp.206-210, Dec. 2008

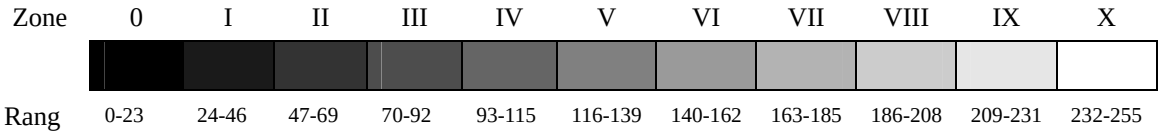

Fig. 1 Histogram versus Zone system

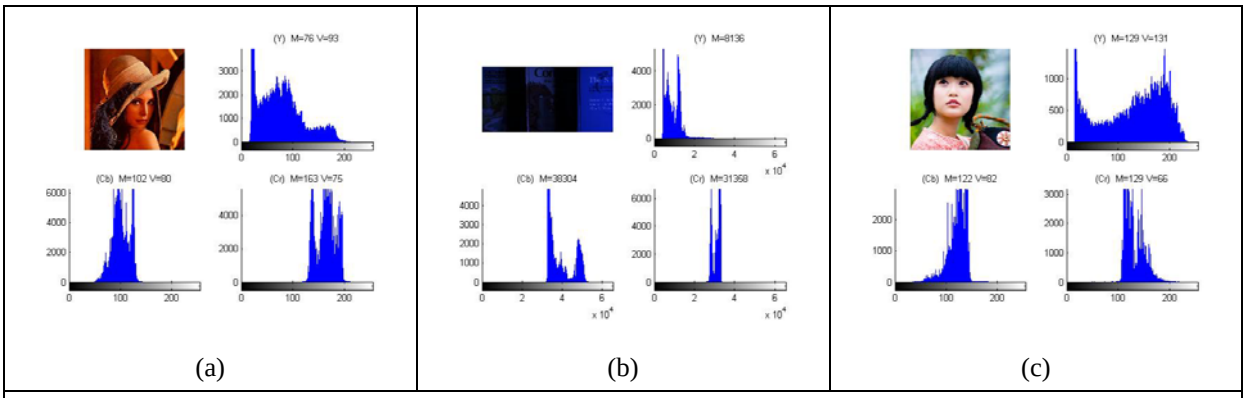

(a) (b) (c)

Figure 2 (a) The image will appear reddish when the mean of Cr lies in brighter area (zone VII) and the mean of Cb lies in darker area (zone IV). (b) The image will appear bluish when the mean of Cb and almost the Cb components locate at brighter area (zone VI) and the mean of Cr locates at darker area (zone V).(c) The mean of YCbCr components of the fine image located in zone V.

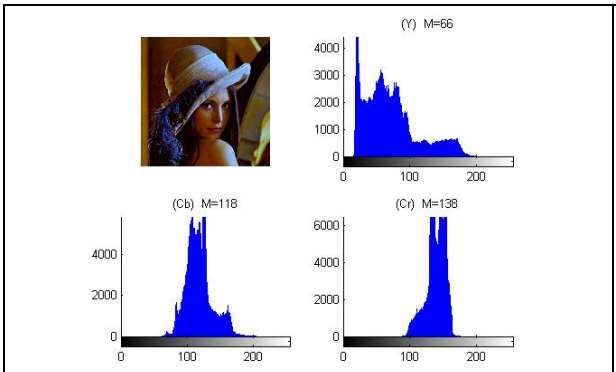

(a) θ=1.5

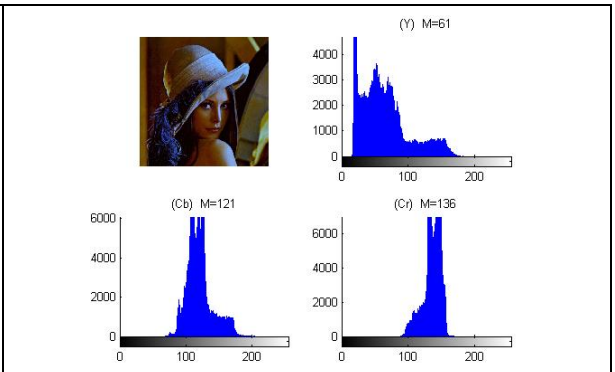

(b) θ=2

Figure 3 the mean of Cb and Cr components of the reddish image are adjusted into zone V by the proposed method with different value of θ

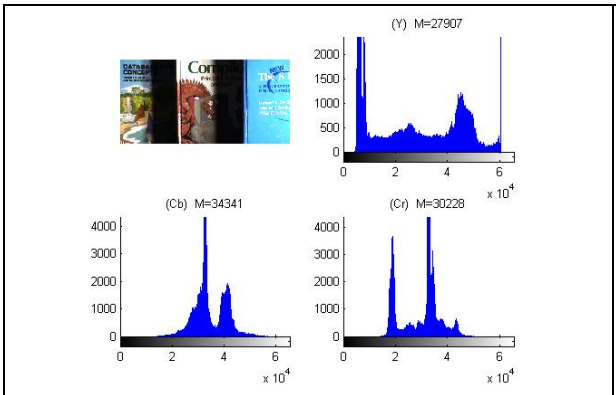

(a) θ=1.5

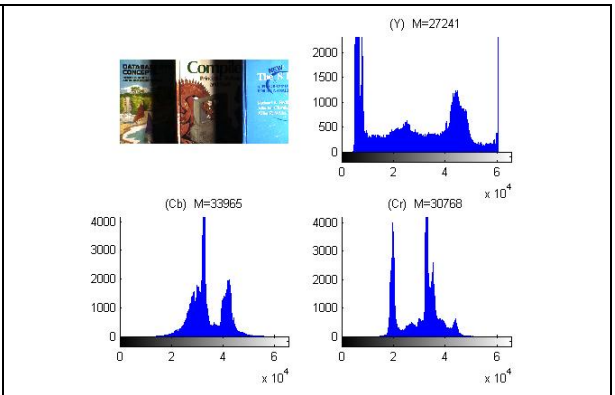

(b) θ=2

Figure 4 the mean of Cb and Cr components of the bluish image are adjusted into zone V by the proposed method with different value of θ

(a) (b) (c) (d)

Figure 5 Adjusted results of an reddish image use the different automatic white balance methods: (a) original image (b) gray world assumption method (c) multi-scale retinex theory method (d) the proposed method

(a) (b) (c) (d)

Figure 6 Adjusted results of an bluish image use the different automatic white balance methods: (a) original image (b) gray world assumption method (c) multi-scale retinex theory method (d) the proposed method

Table 1 is described the zone scale and its relationship to typical scene elements [1].

Zone	Description
0	Total black
I	Near black, with slight tonality but no texture
II	Dark gray-lack. textured black; the darkest part of the image in which slight detail is recorded
III	Very dark gray, average dark materials and low values showing adequate texture. This is where you will want to place shadow details.
IV	Medium-dark gray, average dark foliage, dark stone, or landscape shadows
V	Middle gray; Standard Kodak 18% gray reflectance card, clear north sky; dark skin, average weathered wood
VI	Rich mid-tone gray, average Caucasian skin; light stone; shadows on snow in sunlit landscapes
VII	Off white or bright light gray, very light skin; shadows in snow with acute side lighting, highest zone that will still hold good details.
VIII	Lightest tone with texture; textured snow
IX	Slight tone without texture; glaring snow
X	Pure white; light sources and specular reflections

The Sixth International Conference on Genetic and Evolutionary Computing

August 25-28, 2012, Kitakyushu, Japan
http://bit.kuas.edu.tw/~icgec12

Dear Prof. Jzau-Sheng Lin,

Thank you for your submission to the Sixth International Conference on Genetic and Evolutionary Computing (ICGEC-2012), to be held on August 25-28, 2012, in Kitakyushu, Japan. We are pleased to inform you that your paper

Paper No.: ICGEC-2012-259
Paper Title: A PSO-based Algorithm with Subswarm Using Entropy and Uniformity for Image Segmentation
Author(s): Jzau-Sheng Lin, Shou-Hung Wu

has been accepted for presentation in ICGEC-2012. Your paper will be published in the conference proceeding with the Conference Publishing Services of the IEEE Computer Society. Please do take the comments and suggestions of the reviewers into account in the revision to further improve the quality of your paper. Please refer to http://bit.kuas.edu.tw/~icgec12 for further information regarding the conference registration and to the online Author Guide at http://bit.kuas.edu.tw/~icgec12 for detailed procedures in the preparation of your camera-ready copy and copyright release form. Both deadlines are July 7, 2012.

We are looking forward to meeting you in Kitakyushu. Further information on ICGEC-2012 can be obtained from the conference web sites: http://bit.kuas.edu.tw/~icgec12

Sincerely Yours,

Chin-Shiuh Shieh, Program Committee Chair
National Kaohsiung University of Applied Sciences, Taiwan

Junzo Watada, Conference Chair
Waseda University, Japan

A PSO-based Algorithm with Subswarm Using Entropy and Uniformity for Image Segmentation

Jzau-Sheng Lin
Dept. of Computer Science and Information Engineering
Nat'l Chin-Yi University of Technology
Taichung City, TAIWAN
jslin@ncut.edu.tw

Shou-Hung Wu
Dept. of Computer Science and Information Engineering
Nat'l Chin-Yi University of Technology
Taichung City, TAIWAN
happy_like92@yahoo.com.tw

***Abstract*—In the image segmentation field, it needs several iterations to find optimization thresholds or cluster center to segment images. In this paper, we embedded a scheme based on maximum entropy and uniformity into the particle swarm optimization with subswarm structure named MEUPSOS to find the optimization threshold values iteratively. Instead of using the conventional PSO, swarm was divided into several subswarms for the purpose of getting local optimal solutions with a fitness function based on maximal entropy and uniformity. Additionally, just one-swarm particles were used to replace *k*-swarm (*k* is the number of threshold values) particles in order to upgrade the computation performance. Then, the local optimal solutions ware used to update global parameter in the global swarm. Through iterations updating the velocities and locations of particles, we can calculate the near optimal threshold values on an image based on the fitness functions of maximum entropy and uniformity. Finally, we can find that the proposed method can get more promising results than the other method.**

Keywords- PSO; image segmentation; entropy; uniformity

I. INTRODUCTION

Segmentation in an image is a very important step for the image processing. Great deals of literatures, based on region growing [1], edge detection [2], pixel classification [3-4], and histogram threshold [5], have been proposed in the research field of image segmentation. Region growing strategies start at known pixels and append all neighbors which are similar in gray level, color, texture, or other properties, to the known pixels in order to form a region. The local discontinuities are detect first and then connected to form complete boundaries in edge detection approaches. A pixel classification approach is one that classifies pixels based on global of local information such as their gray levels or colors in an image. In the traditional pixel classification approaches, they can be divided into two schemes such as supervised and unsupervised classification approaches. The supervised strategy classifies pixels into representative regions with known properties like number of regions or cluster centroids. Then these regions are merged into suitable clusters. The supervised method is so troublesome that it is time consuming. The unsupervised approach is a classification process that does not need to be experience cognitive. It just modifies cluster centers through several iterations to achieve the convergence condition in order to complete the classification.

Generally, a thresholding algorithm is one that determines optimal threshold values based on a certain criterion. A single threshold value is used for the whole image in a global thresholding method as well as several threshold values are used to segment a given image into subregions in a local thresholding. There are several optimal algorithms in thresholding segmentation have bee proposed such as maximum entropy threshold [6] and Minimum error threshold [7-8]. In order to find optimal threshold values and reduce the time consumption, biological intelligence algorithms, such as Artificial ant algorithm [9], Particle Swarm Optimization [10], Artificial Bee Colony [11-12] , Genetic Algorithm[13], and Bacterial Evolutionary[14], have been embedded into thresholding segmentation method to find global or near global optimal solution.

Artificial ant algorithm is used to choose a correct path for travelling in accordance with the pheromone. The quantity of pheromone on a path can be increased when ants go through the same path. In order not to fall into a local optimal solution, pheromones on all paths have to be reduced but the pheromone weight on the best path has to be increased in accordance with a fitness function.

Artificial Bee Colony (ABC) algorithm was proposed by Karaboga [11-12] for optimizing numerical problems. The algorithm simulates the intelligent foraging behavior of honey bee swarms. It is a near robust stochastic optimization algorithm.

Genetic algorithm is a heuristic algorithm commonly used binary encoding. It exchanges bits of information to find a better solution through iterative crossover step from their good parent generation. Additionally, the mutation mechanism also used to prevent trapped in local optimal solutions.

PSO method, belonging to the category of swarm optimization, is a population-based algorithm and first demonstrated as a stochastic optimization algorithm by Eberhart and Kennedy [15]. It is modeled to simulate the social behavior of bird flocks and follow similar steps as evolutionary algorithms finding near-optimal solutions. During the last two decades, PSO has been popularly applied to several optimization problems such as minimax problems [16], integer programming problems [17], global optimization problems [18], and other applications in engineering [19-20].

The convergence of traditional PSO algorithm is so fast that it easily falls into the local optimal solution. In order to resolve this problem, the main framework of this paper divides the solution space into *n* subspaces named subswarms in the PSO scheme. The optimal threshold value was obtained in accordance with the local maximum entropy for the best position ever attained by a proper particle and the global maximum uniformity indicated the best position ever encountered by all particles in the subswarms. The experimental results show that promising thresholds can be obtained by means of maximum entropy and global maximum uniformity which are embedded into fitness function of particles.

II. Relative Algorithms

A. Maximum-entropy Thresholding

A maximum entropy threshold method, proposed by Jaynes [21], used the concept of Shannon entropy to image segmentation. It finds an appropriate grayscale threshold value which can divide pixels into the background and objects. And, let variances of pixels within these two regions be the largest amount, *L* represent the maximum range of the grayscale images and *t* is any one of the gray level value in the solution space. *H*(*t*), represented the entropy value of an image, can be calculated as follows:

$$\begin{aligned} H(t) &= H_{object}(t) + H_{background}(t) \\ &= -\sum_{i=0}^{t} \frac{p_i}{p_t} \ln \frac{p_i}{p_t} - \sum_{j=t+1}^{L-1} \frac{p_j}{1-p_t} \ln \frac{p_j}{1-p_t} \end{aligned} \tag{1}$$

and

$$P_t = \sum_{i=0}^{t} P_i \text{ and } P_i = h(i)/N, \tag{2}$$

where $h(i)$ is the total pixels with the graylevel value i as well as N is the total number of pixels in an image. Therefore, we can find an optimal threshold t which deduces maximum entropy as follows:

$$\phi = \underset{0<t<L-1}{Arg\max} H(t) \tag{3}$$

To find the optimal multi-threshold values $t_1, t_2, \cdots, t_n$ in the multi-thresholding problem, Eq. (1) can be modified as

$$\begin{aligned} &H(t_1, t_2, \cdots, t_n) = H(t_1) + H(t_2) + \cdots + H(t_n) \\ &= -\sum_{i=0}^{t_1-1} \frac{P_i}{P_{t_1}} \ln \frac{P_i}{P_{t_1}} - \sum_{j=t_1}^{t_2-1} \frac{P_j}{P_{t_2}} \ln \frac{P_j}{P_{t_2}} - \cdots - \sum_{k=t_n}^{L-1} \frac{P_k}{P_L} \ln \frac{P_k}{P_L} \end{aligned} \tag{4}$$

where $P_{T_1} = \left(\sum_{i=0}^{t_1-1} P_i \right), P_i = h(i)/N, P_{T_2} = \left(\sum_{j=t_1}^{t_2-1} p_j \right), P_j = h(j)/N$, and $P_L = \left(\sum_{k=t_n}^{L-1} p_k \right), P_k = h(k)/N$. Therefore, the fitness function, shown as in Eq. (5), is also defined the maximum entropy such that

$$Fit = \underset{0<t<t_n}{Arg\max} H(t_1, t_2, \cdots, t_n). \tag{5}$$

B. Uniformity

The uniformity is to evaluate the performance estimation for an image through thresholding processing. The greater the threshold value, the better the uniformity. The uniformity is defined as follows:

$$u = 1 - 2 * \frac{\sum_{j=0}^{k} \sum_{i \in R_j} (f_i - m_j)^2}{N * (f_{\max} - f_{\min})^2} \tag{6}$$

Uniformity value is ranged between 0 to 1. Where k is the number of thresholding values. i, f_i and m_j are the number of pixels, graylevel of pixel i, and the average graylevel in a cluster, respectively. $f_{\max}$ and $f_{\min}$ are the maximum and minimum graylevel in the target image.

C. Particle Swarm Optimization

PSO, proposed by Kennedy and Eberhart [15], is a stochastic optimization algorithm that is also a population-based strategy to take advantage of a population (named *swarm*) of individuals (called *particles*) and search promising areas in the search space. Initially, PSO algorithm generates a group of particles, in which a particle is defined by a position and a velocity. Each particle moves with an adaptable velocity based on a fitness function within the search space, and retain the best position it ever visited in the past. The velocity decides the moving direction and distance for a particle. In PSO, two optimal constraint parameters *gbest* (global parameter indicated the best position ever encountered by all particles) and *pbest* (local parameter for the best position ever attained by a proper particle) are used to update the velocity for all particles. Finally, an approximating optimal solution can be obtained through previous actions iteratively.

Assume a search space with n dimension, $N \subset R^n$ is a swarm consisting of M particles. Then the position and velocity for the i-th particle on an n-dimension coordinate are defined

$$S_i = (x_{i1}, x_{i2}, ..., x_{in})^T \in N \tag{7}$$

and

$$V_i = (v_{i1}, v_{i2}, ..., v_{in})^T \in N. \tag{8}$$

The best previous position (*pbest*) encountered by the i-th particle in N is defined as

$$pbest_i = (p_{i1}, p_{i2}, ..., p_{in})^T \in N. \tag{9}$$

In the meantime, the best previous position (*pbest*) among all the individuals of the swarm can be obtained by

$$gbest = \max(pbest_1, pbest_2, ..., pbest_M). \tag{10}$$

Therefore, the velocity $V_i(k+1)$ and position $S_i(k+1)$ for the i-th particle in the swarm at iteration k+1 can be defined as following equations:

$$V_i(k+1) = wV_i(k) + c_1 \times rand_1(pbest_i(k) - S_i(k)) + c_2 \times rand_2(gbest(k) - S_i(k)) \quad (11)$$

$$S_i(k+1) = S_i(k) + V_i(k+1). \quad (12)$$

where $i = 1,2,...,M$ is the index of particles, c_1 and c_2 are cognitive and social parameters, $rand_1$ and $rand_2$ are random numbers uniformly distributed between 0 and 1, and *w*, the weighting function, is defined as

$$w = w_{\max} - \frac{w_{\max} - w_{\min}}{k_{\max}} \times k. \quad (13)$$

In Eq. (11), the cognitive component $pbest_i(k) - S_i(k)$ represents the particles own experience as to where the best position is while the social component $gbest(k) - S_i(k)$ stands for the belief of the entire swarm as to where the best solution is during iteration *k*. In Eq. (13), $w_{\max}$ is the initial weight as well as $w_{\min}$ and $k_{\max}$ are defined the weight and the number of the last iteration respectively. The higher the value of iteration, the smaller the weight *w* will be. In the proposed MEUPSOS, Eq (10) is modified as

$$subbest_k = \max(pbest_1, pbest_2, ..., pbest_i). \quad (14)$$

$$gbest = \max(subbest_1, subbest_2, ..., subbest_k). \quad (15)$$

III. The Proposed PSO Based on Maximum Entropy and Uniformity

In this paper the constraints with maximum entropy and uniformity were embedded into the PSO algorithm with subswarm structure (named MEUPSOS). Swarm in the MEUPSO was divided into several subwarms in order to find several local optimal solutions to speed up global or near global threshold values being obtained. In order to upgrade the computation performance, we just used only one-swarm particles for all subswarms instead of one-population particles for each swaem.

In the proposed MEUPSOS, we added local optimal value named *subbest* for each subswarm. First, we used the entropy-based fitness function to update the parameter *pbest*. Then parameters *pbest*s were used to update *subbest* in a subswarm. Finally, *gbest* was updated with *subbest*s in the global swarm. The detail flowchart of the proposed MEUPSOS is shown as in Figure 1. In Figure 1, the processing flow went through two sub flowcharts named (A) and (B) to calculate the entropies for updating *subbest*s and compute uniformity to adjust the global parameter *gbest*. These two sub flowcharts are shown as in Figure 2 and Figure 3.

The main purpose in Figure 2 is to calculate the entropy-based fitness function of particles in every subswarm and updating parameters *pbest* with maximum entropy. Then, *pbest*s were used to update *subbest* in a subswarm.

In Figure 3, parameter *gbest* was updated by using of the best *subbest* with uniformity-based fitness function in subswarms. Additionally, the threshold values were updated with the better uniformity.

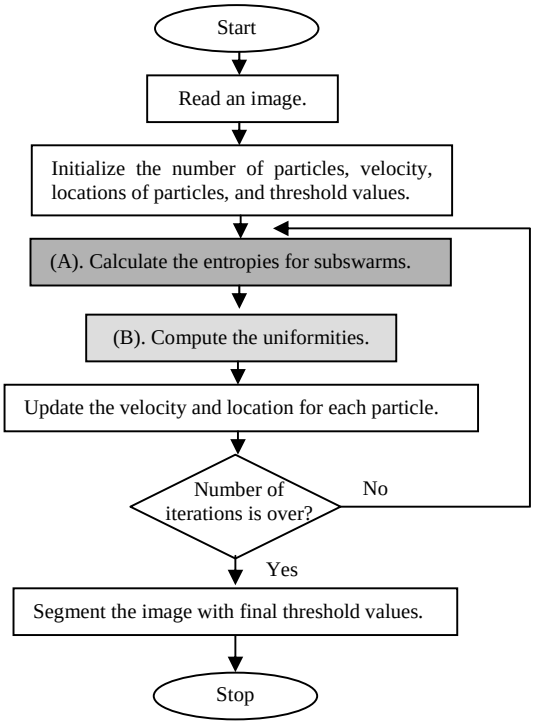

Figure 1. Flowchart of the proposed MEUPSO.

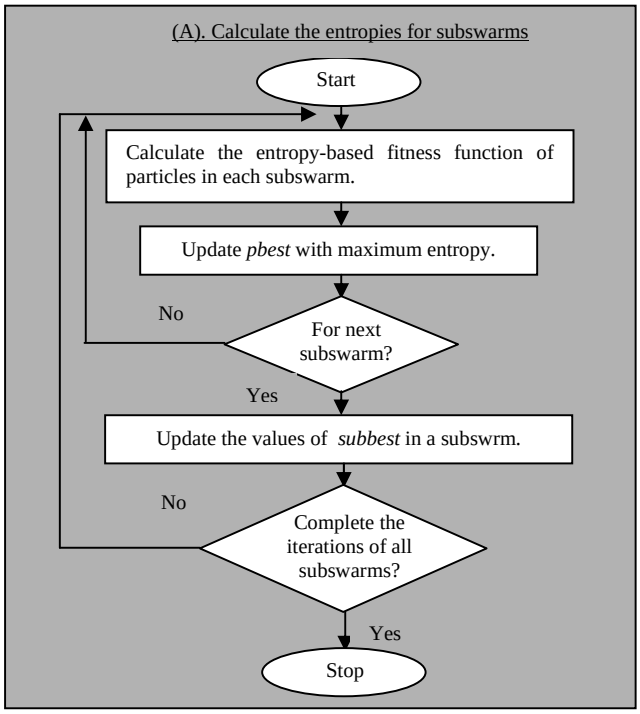

Figure 2. Flowchart of block (A) in Figure 1.

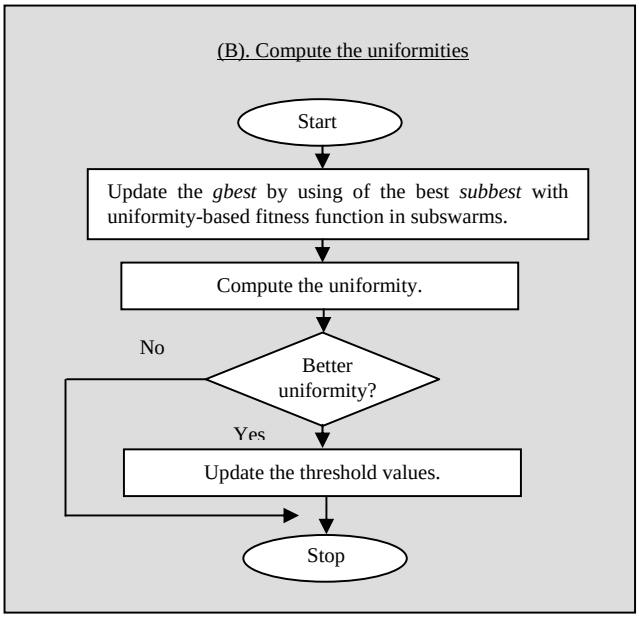

Figure 3. Flowchart of block (B) in Figure 1.

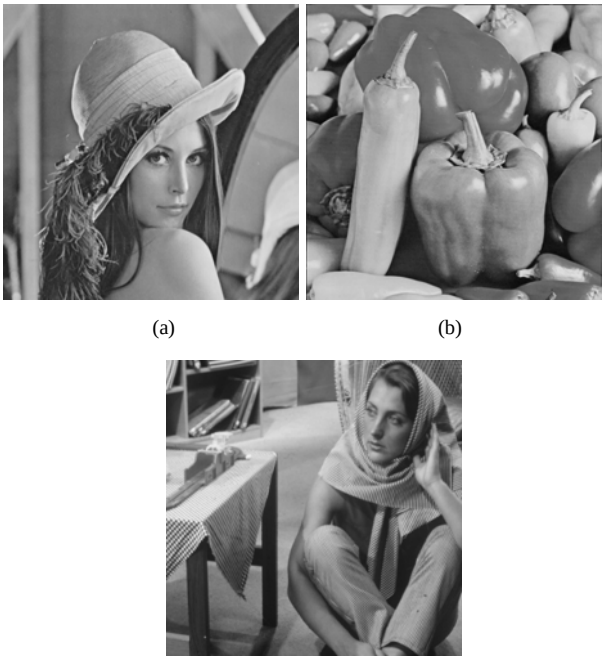

(a) (b)

(c)

Figure 4. Original 512x512 images; (a) Lena, (b) Pepper, and (c) Barbara.

IV. EXPERIMENTAL RESULTS

In order to show the performance, all simulations are executed with the interpreter language of MATLAB in a personal computer. The performance for the proposed MEUPSOS was compared with HCOCLPSO [11]. The original 512x512 test images (Lena, Pepper, and Barbara) are shown as in Figure 4. The segmented results with 6 clusters by the proposed MEUPSOS are shown as in Figure 5. A comparative study of uniformity for the proposed MEUPSOS and HCOCLPSO is shown as in Table I. From Table I, we can find that the uniformity by the proposed MEUPSOS is better that those got by the other algorithm HCOCLPSO.

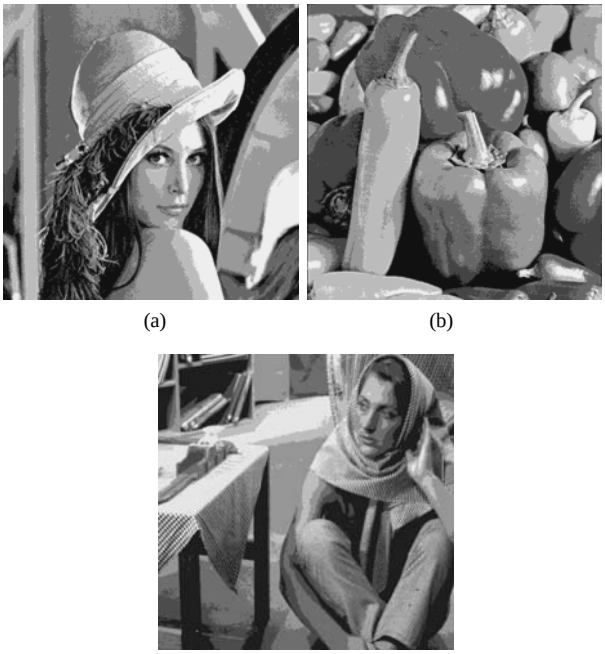

(a) (b)

(c)

Figure 5. Segmented results with 6 clusters by the proposed MEUPSOS.

TABLE I. A COMPARATIVE STUDY OF UNIFORMITY FOR THE PROPOSED MEUPSOS AND HCOCLPSO.

Image	k	Uniformity	
		Proposed MEUPPSO	HCOCLPSO
Lena	2	0.9889	0.9883
	3	0.9899	0.9886
	4	0.9904	0.9893
	5	0.9920	0.9903
Pepper	2	0.9878	0.9876
	3	0.9890	0.9875
	4	0.9918	0.9914
	5	0.9916	0.9914
barbara	2	0.9898	0.9893
	3	0.9911	0.9901
	4	0.9925	0.9911
	5	0.9921	0.9919

Although the object values obtained by the proposed MEUPSOS are smaller than those got by the HCOCLPSO with a small value about 0.05 ~ 0.55, the used particles in the proposed MEUPSOS are less than the HCOCLPSO. No matter what the number of threshold values is defined in advance by the proposed MEUPSOS, the number of particles is always fixed to *n*. If an image was segmented *k* clusters with *k*-1 threshold values, the number of particles is $n \times (k-1)$ in the

HCOCLPSO. Therefore, the computation performance in the proposed MEUPSOS is better than the HCOCLPSO.

TABLE II. A COMPARATIVE STUDY OF ENTROPY FOR THE PROPOSED MEUPSOS AND HCOCLPSO.

Image	k	Entropy			
		Proposed PSO		HCOCLPSO	
		Optimal thresholds	Object value	Optimal thresholds	Object value
Lena	2	88, 165	17.76	97, 164	17.8130
	3	72, 125, 179	22.0278	82, 126, 175	22.0993
	4	70, 117, 163, 197	25.8766	64, 97, 138, 179	25.9864
	5	53, 86, 123, 160, 207	29.1873	63, 94, 128, 163, 194	29.7348
Pepper	2	70, 146	18.0233	72, 144	18.0280
	3	56, 109, 164	22.4350	53, 102, 155	22.4694
	4	50, 98, 146, 196	26.3321	53, 98, 143, 191	26.5234
	5	35, 71, 106, 141, 191	30.3217	42, 74, 109, 149, 191	30.3483
barbara	2	90, 169	18.2646	98, 163	1832765
	3	72, 135, 187	22.6534	76, 127, 178	22.7182
	4	60, 111, 168, 208	26.6182	61, 100, 143, 187	26.7712
	5	66, 99, 135, 170, 208	30.5861	57, 92, 129, 166,199	30.6238

V. CONCLUSIONS

In this paper, we proposed a PSO algorithm with maximum entropy and uniformity with subswarm structure named MEUPSOS for image segmentation. In order to upgrade the computation performance, the number of particles was used with a fixed value no matter how the threshold values were changed. Although litter poor object values were obtained, the proposed MEUPSOS can get better uniformity and computation performance than those obtained by the HCOCLPSO for the segmented images.

ACKNOWLEDGMENT

This work was supported by the National Science Council, TAIWAN, under the Grants NSC100-2221-E-167-030 -

REFERENCES

[1] T. Pavlidis, and Y T Liow, "Integrating region growing and edge detection," IEEE Trans. on Pattern Anal. Mach. Intell., vol. 12, pp. 225-233, 1990.

[2] K. S. Fu, and J. K. Mu, "A survey on image sementation," Pattern Recognition, vol. 13, pp. 3-16, 1983.

[3] K. S. Cheng, J. S. Lin, and C. W. Mao, "The application of competitve Hopfield neural network on medical image segmentatin," IEEE Trans. on Medical Imaging, vol. 15, pp. 560-567, 1996.

[4] J. S. Lin "Segmentation of medical images through a penalized fuzzy Hopfield network with moments preservation," J. of the Chinese Institute of Eng., vol. 23, pp. 633-643, 2000.

[5] P. K. Sahoo, S. Soltani, A. K. C. Wong, and Y. C. Chen, "A survey of thresholding techniques," Comput. Vision, Graphic, and Imge Processing, vol. 41, pp. 233-260, 1988.

[6] M. Mairta, and A. Chatterjee "A hybrid cooperative-comprehensive learning based PSO algorithm for image segment using multilevel threshilding," Expert System with Applications, vol. 34, pp. 1341-1350, 2008.

[7] J. Kittler, J. Illingworth, "Minimum error threshold," Pattern Recognition, vol. 19, lssue 1,pp. 41-47,1986.

[8] D. Liu, J. Yu, "Otsu method and K-means," Hybrid Intelligent System," vol. 1, pp. 344-349, 2009.

[9] S. H. Liu, J. S. Lin, and Z. S. Lin, "An Annealed Ant System to the Shortest-path Network Problem," Int. J. of Electrical Engineering, vol. 13, pp. 209-217, 2006.

[10] H. Tang, C. Wu, L. Han, and X. Wang, "Image segment based on Improved PSO" Int. Conf. on Computer and Communication Technologies in Agriculture Engineering, pp. 191-194, 2010.

[11] D. Karaboga, B. Basturk, "Artificial bee colony (abc) optimization algorithm for solving constrained optimization problems," LNCS: Advances in Soft Computing: Foundations of Fuzzy Logic and Soft Computing, vol. 4529, Springer-Verlag, 2007, pp. 789-798,.

[12] D. Karaboga, B. Basturk, "A powerful and efficient algorithm for numerical function optimization: artificial bee colony (ABC) algorithm," J. of Global Optimization, vol. 39, pp. 459-171, 2007.

[13] M. Awad, K. Chehdi, and A. Nasri, "Multi-component image segmentation using a hybrid dynamic genetic algorithm and fuzzy C-means," Image Processing, IET, vol. 3, pp. 52-62, 2009.

[14] M. Hanmandlu, O. P. Verma, N. K. Kumar, and M. Kulkarni, "A novel optimal fuzzy system for color image enhancement using bacterial foraging," IEEE Trans. on Instrumentation and Mmeasurement, vol. 58, pp. 2867-2879, 2009.

[15] R. C. Eberhart and J. Kennedy, "A new optimizer using particle swarm theory," in Proc. 6th Symp. Micro Machine and Human Science, Nagoya, Japan, pp. 39-43, 1995.

[16] E. C. Laskari, K. E. Parsopoulos, and M. N. Vrahatis, "Particle swarm optimization for minimax problems," in Proc. IEEE 2002 Congr. Evolutionary Computation, Honolulu, pp. 1582-1587, 2002.

[17] E. C. Laskari, K. E. Parsopoulos, and M. N. Vrahatis, "Particle swarm optimization for integer programming," in Proc. IEEE 2002 Congr. Evolutionary Computation, Honolulu, pp. 1576-1581, 2002.

[18] K. E. Parsopoulos, and M. N. Vrahatis, "On the computation of all global minimizers through particle swarm optimization," IEEE Trans. on Evolutionary Computation, vol. 8, pp. 211-224, 2004.

[19] M. G. Omran and A. P. Engelbrecht, "A Color Image Quantization Algorithm Based on Particle Swarm Optimization," Informatica, vol. 29, pp. 261-269, 2005.

[20] M. A. Abido, "Optimal design of power system stabilizers using particle swarm optimization," IEEE Trans. Energy Conversion, vol. 17, pp. 406-413, 2002.

[21] E. T. Jaynes, "On the ratationale of maximum entropy methods," IEEE procedings, vol. 70, oo. 939-952, 1982.